DISSERTATION

SIGNALING COMPLEXES FORMED BY LUTEINIZING HORMONE RECEPTOR TRANS-ACTIVATION

Submitted by

Hanan Ali A.Shanta

Graduate Degree Program in Cell and Molecular Biology

In partial fulfillment of the requirements

For the Degree of Doctor of Philosophy

Colorado State University

Fort Collins, Colorado

Fall 2019

Doctoral Committee:

Advisor: B. George Barisas
Co-Advisor: Deborah A. Roess

Debbie C. Crans
Charles W. Miller

ABSTRACT

SIGNALING COMPLEXES FORMED BY LUTEINIZING HORMONE RECEPTOR TRANS-ACTIVATION

Signal transduction by luteinizing hormone (LH) receptors depends on hormone activation of these receptors, a process important for mammalian reproduction. The LH receptor, a member of the G protein-coupled receptor (GPCR) family, undergoes hormone-induced LH receptor dimerization and/or oligomerization and translocation into small membrane compartments where receptors are confined and exhibit slow lateral diffusion. However, the organization of the signaling complex confined within these structures is not clear. In this project, we used single particle tracking methods to evaluate the lateral motions of wild type receptor FLAG-LHR-YFP and mutant receptors defective in hormone binding ($LHR^{-hCG,\ +cAMP}$) or defective in signal transduction ($LHR^{+hCG,-cAMP}$) after exposure to human chorionic gonadotropin (hCG). These studies showed that, when wild type LH receptors and mutant receptors are coexpressed and treated with 100 nM hCG, there are decreases in receptor lateral diffusion, the number of receptor-occupied membrane microdomains and the size of receptor-containing membrane microdomains. These results suggest that wild type LH receptors are capable of both cis-activation of nearby wild type LH receptors and transactivation of $LHR^{-hCG,+cAMP}$, a receptor that is not able to bind hCG. We then investigated interactions between wild type LH receptors and mutant receptors using homo-transfer fluorescence resonance energy transfer (FRET) methods. We showed that LH receptors associate with one another and that the extent of self-association increases in response to increasing hCG concentrations. Using homo-transfer FRET methods, we showed that mutant LH receptors are

trans-activated by wild type receptors and undergo aggregation in response to 100 nM hCG despite being unable to bind hCG directly. Finally, we evaluated cAMP levels in cis-activated and trans-activated LH receptors using ICUE3, an EPAC-based reporter molecule for cAMP. We determined that increases in intracellular cAMP occur in cells expressing wild type receptors and exposed to increasing concentrations of hCG. Similarly, cells co-expressing mutant receptors exhibit increased cAMP when there is a 1:10 transfection ratio of $LHR^{+hCG,-cAMP}$ to $LHR^{-hCG,+cAMP}$ indicating that trans-activation is occurring. Disruption of membrane microdomains by pre-treatment of cells with 10 nM methyl-β-cyclodextrin for an hour has a negative effect on cAMP levels which indicates the importance of cholesterol-containing microdomains in signal transduction by LH receptors. Together these results demonstrate that trans-activated LH receptors can undergo receptor aggregation in response to hormone binding and can signal effectively despite the absence of a signal-transduction sequence in the mutant receptor.

ACKNOWLEDGEMENTS

I give deep thanks to my co-advisor, Dr. Deborah Roess, who supported and encouraged me. Her guidance helped me in conducting this research and preparing my dissertation. I could not imagine having a better advisor for my research. I am also so thankful to my advisor Dr. George Barisas for all his guidance in conducting the data analysis presented here. I would also like to thank my committee members, Dr. Crans and Dr. Miller. Each member of my committee has provided me with invaluable personal and professional guidance.

I would like especially to thank Dr. Aylin Hanyaloglub, Dr. Jonas Kim and Dr. IIpo T. Huhtaniemi for their assistance in providing us with vectors of LH mutant receptors used in this project. I would also like to thank Dr. Xiarong Li for her help in preparing the wild type LH type receptor.

I am deeply thankful for all my family who encouraged me and supported me while I pursued my studies here in the U.S. I would like to thank my parents, whose love and guidance are always with me. I would especially like to thank my sisters and brothers for all their encouragement and my husband and my three wonderful children, Jude, Ayhem and Jana, who provide unending inspiration. I thank my lab mates for all their help here in the U.S. and my friends in Tripoli University who have encouraged me at each step.

DEDICATION

To MY FAMILY Hanan. Sh

TABLE OF CONTENTS

LIST OF TABLES

LIST OF FIGURES

CHAPTER 1: BACKGROUND AND SIGNIFICANCE

1.1: Introduction

Human chorionic gonadotropin (hCG) is heterodimeric glycoprotein hormone acting on a G protein coupled receptor, the luteinizing hormone (LH) receptor, which is capable of binding either hCG and LH. The LH receptor, a member of the glycoprotein hormone receptor family, plays an important role in both normal and abnormal reproductive physiology in males and females (1-3). In males the LH receptor regulates the function and development of Leydig cells. In women LH receptors are important for ovulation, corpus luteum formation and progesterone secretion.

The LH receptor has become a target for drug discovery because of natural mutations in LH receptor where the receptor either cannot bind hormone or cannot initiate signal transduction and because of the relationship between these mutant receptors and human diseases such as Leydig cell hyperplasia. Much of this research has focused on the mechanism of activation of LH receptors which is still poorly understood.

LH receptor activation is generally accomplished through cis-activation of these glycoprotein hormone receptors. Cis-activation involves binding of cognate hormone to the receptor‘s exodomain followed by interactions between the receptor exodomain and the receptor transmembrane domains and extracellular loops (4,5). Trans-activation is believed to occur through interactions between a ligand-occupied exodomain on one receptor and the signaling domain of an adjoining receptor. It is assumed that the trans-activated receptor takes on an “active” conformation and signals similarly to a fully functional receptor that has bound and retained ligand or to a constitutively-active receptor that has never seen ligand but signals

continuously nonetheless. Whether LH receptor cis-activation and trans-activation includes protracted receptor-receptor interactions is examined in this research.

1.2: G protein-coupled receptors (GPCR)

G protein-coupled receptors (GPCRs) are the largest protein receptor family and are involved in signal transduction across membranes. Sensory perception uses members of the GPCR family. As examples, visual perception uses rhodopsin and sense of smell is accomplished using receptors of the olfactory epithelium which bind odorants. GPCRs have seven transmembrane domains (7TM) and undergo conformational changes after ligand binding, a process that transfers the signal through the cell membrane. Their name is based on their ability to activate G proteins to induce intracellular signaling (6). These receptors may also be called 7TM receptors based on their seven transmembrane helical segments, a name that is more accurate since GPCRs can interact with other signaling molecules that are not G proteins (7).

All GPCRs have seven transmembrane-spanning segments connected by intracellular and extracellular loops. The N-terminal of GPCRs has the amino terminus and the C-terminal has often contains serine or threonine residues (**Figure 1.1**). In mammals, many physiological processes are regulated by GPCRs and this makes them a target for pharmaceutical drugs (8). GPCRs are coupled to G proteins via their third transmembrane domain and cytoplasmic loop between transmembrane domains 2 and 3 as well as via the cytoplasmic tail in some receptors (6). The size of the GPCRs can vary and about 800 different human genes for this class of receptors have been demonstrated from the analysis of genome sequences (9).

The GPCR superfamily is further divided to three main classes of receptors. Class A is the largest class of GPCR and this class accounts for about 85% of the GPCR genes. Class A

GPCRs are also called rhodopsin-like receptors. All GPCRs have a common structure and mechanism for transducing signal, but they lack homology in their sequences. The first crystal structure of GPCRs was for bovine rhodopsin (10). In 2007, the structure of β_2-adrenergic receptor was described (11). Both β_2-adrenergic receptors and rhodopsin have similar orientations of their seven-transmembrane helices but with different conformations in the second extracellular loop. The structures of activated GPCRs have been also determined. This is the structure formed after the extracellular binding domain engages ligand and causes conformational changes in the cytoplasmic surface of the receptor (12).

Class B GPCRs, characterized by a large extracellular domain for ligand binding, are best exemplified by the parathyroid hormone receptor. The Class C GPCRs are a small group of receptors with a ligand binding domain located at the N-terminus tail. An example of a Class C GPCR is the heterodimeric $GABA_B$ receptor. These GPCRs are activated by an external signal, a ligand, which leads to activation of a G protein.

It is important to recognize that, although many GPCRs have similar structures in their seven transmembrane domains, the remainder of their structures can be very different. GPCR N-terminal domains are different in size and may contain the binding site for ligand. Their C-terminal domains may also vary in size.

1.3: Structure of LH and hCG

The glycoprotein hormone family includes human chorionic gonadotropin (hCG), luteinizing hormone (LH), follicle-stimulating hormone (FSH) and thyroid-stimulating hormone (TSH). LH and hCG, like other members of the glycoprotein hormone family, have a common

α-chain and hormone-specific β-chains. Their receptors are GPCRs with large extracellular domains that binds the glycoprotein ligands (13).

Both LH and hCG are heterodimers whose subunits are non-covalently associated (14). hCG is comprised of 237 amino acids with a β-subunit containing 145 residues, six disulfide bridges and two N-linked glycosylation sites (14). Its α-subunit contains 92 residues, five disulfide bridges, two N-linked glycosylation sites and four O-linked glycosylation sites. Glycoprotein hormones such as LH and hCG are glycosylated in the natural state and these carbohydrates have important roles in hormone stability and receptor signaling (15). Other than glycosylation patterns, LH and hCG have very similar amino acid sequences, structural properties, chemical composition and functions. hCG exhibits higher affinity binding to receptors than does LH, probably a consequence of its additional glycosylated sites.

In 1994, the structure of hCG was obtained at 2.6 Å resolution. This crystal structure, however, was missing the four N-linked and the four O-linked oligosaccharides and the β-subunit (16). In 2012, Cole added back these missing structures and predicted the final structure of hCG (17). The α and β subunits of hCG are associated to form a heterodimer which is essential for receptor binding. hCG forms a heterodimer by wrapping the β-subunit around the α-subunit and this wrapping is linked via a disulfide bond between Cys^{26}-Cys^{110} to form a "seat-belt region" which is important in the stability of the heterodimer (18). There are two sugar residues on the each one of the α-subunits and one sugar residue on the β-subunit. The carbohydrates of the α-subunit are attached to Asn^{52} on the double stranded loop and to Asn^{78} almost at the end of the β-hairpins.

1.4: LH receptors

LH receptors are members of the GPCR family (6) and are characterized by a large N-terminal extracellular domain containing the binding site for hCG and LH (19). The extracellular domain contains leucine-rich repeats and a short hinge region located between the leucine-rich repeat region and the first transmembrane helix (19). The hinge region is thought to act as a flexible region that allows the leucine-rich repeat domain to physically convey bound hCG or LH to the transmembrane domains (20). The leucine rich repeats are arranged in a horseshoe shape with parallel β strands and loops providing important binding sites for hormone (21).

The transmembrane domains of the LH receptor, TM1-TM7, span the plasma membrane seven times and are connected by three extracellular and three intracellular loops (**Figure 1.1**). The transmembrane domains of the receptor anchor the receptor in the membrane and transduce the signal initiated in the extracellular domain to G proteins (**Figure 1.1**). The three intracellular loops, especially loop 3, are important for interactions between the LH receptor and G proteins. The LH receptor also has six potential sites for N-linked glycosylation, all of which are located on the extracellular domain.

The human LH receptor contains 699 amino acids encoded by a single gene. The human and rat LH receptor genes are about 80 kb in size and have 11 exons and 10 introns, respectively (22,23). The cloning of complementary DNA for the human LH receptor was reported after the exon structure was identified (24). The mature LH receptor is 80 kDa with an additional 15 kDa contributed by multiple carbohydrate chains (25). The first and second extracellular loops of the receptor contain cysteine residues as do other receptors of the GPCR superfamily. These cysteine residues in rhodopsin receptor stabilize the seven-transmembrane helical by forming disulfide bridges (25). Cysteine residues Cys^{257} and Cys^{258} on exon 9 are important for LH

receptor expression on the plasma membrane; mutations of these cysteines lead to intracellular retention of the receptor without affecting ligand binding (25). Furthermore, mutation of cysteine residues in exon 1 ($Cys^{8,12,14,22}$) indicates that these residues are important for ligand binding to the receptor (1). Natural mutations of the LH receptor can lead to hormone-independent signaling which occurs in Ledyig cell hyperplasia (26). Shenker et al. (21) identified the first intrinsically active mutation of LH receptors in a patient with precious puberty.

1.5: Signal transduction by LH receptors

LH receptors have the ability to activate multiple G protein-dependent signaling pathways (27). Activated LH receptors interact with heterotrimeric G proteins which consist of three subunits (α, β and γ) leading to activation of adenylate cyclase (AC) and phospholipase C (PLC) (**Figures 1.6 and 1.7**). The LH receptor, like other GPCR family members, interacts mainly with Gs and, to a lesser extent with Gq and Gi. Like many GPCRs, receptor activation includes changes in the transmembrane domains and sometimes involves participation by the extracellular domains (28). The intracellular domains contact G proteins by interacting with the C-terminal domain of the receptor. More specifically, LH receptor coupling to G proteins is dependent on the C-terminus of the third loop and involves protein-protein interactions (29).

Signal transduction by the receptor through the membrane is not well understood. It is known that the receptor, in the absence of hormone, interacts with a G protein and that both are in an inactive state. Once ligand binds, the conformation of the receptor changes, the G protein is activated and dissociates from the receptor (**Figure 1.5**). The receptor now can activate another G protein or switch back to an inactive state.

A new mechanism for receptor activation of the glycoprotein hormone receptors, termed trans-activation, has been proposed as an alternative to the traditional mechanism known as cis-activation. (30). LH receptor-mediated signal transduction via cis-activation involves high affinity binding of either LH or hCG to the receptor's exodomain and interactions between the hormone-occupied exodomain and the receptor endodomain (**Figure 1.2** (4)). The receptor endodomain, as modeled by Fanelli and colleagues (31), is capable of interacting with G_s. LH receptors (30) and structurally-related FSH receptors (32) can also be activated by receptor trans-activation which involves at least two receptors (**Figure 1.4**). A functional LH receptor *exodomain* binds ligand and then interacts with an adjoining receptor that has not bound ligand. This leads to signal transduction by the second receptor's functional *endodomain* including activation of G proteins and adenylate cyclase. LH receptor trans-activation can be shown (30) using cells co-transfected with a functional LH receptor exodomain coupled to either a non-signaling LH receptor endodomain or to a protein or lipid membrane anchor (33) and with a second LH receptor containing one of several mutations in their exodomain that prevent binding of hormone. These cells produce cyclic AMP (cAMP) in response to hCG, presumably via signaling through the competent LH receptor endodomain. The demonstration of both cis- and trans-activation of LH receptors suggests that amplification of ligand signal may occur through sequential cis-activation of one receptor and by trans-activation of closely associated LH receptors. More recently, it has been shown that co-expressing mutant LH receptors deficient in binding or in signaling produces a hormone-induced signal in transgenic mice (34).

Signals by the LH receptor arise primarily through cAMP and protein kinase A (PKA). Following hormone binding, the LH receptor is activated, there is a conformational change in the transmembrane domain and binding of the intracellular domain with G proteins (**Figure 1.5**). G

proteins contain three distinct subunits α, β, and γ and, before ligand binding, are inactive. In the inactive state, the α subunit is bound to GDP while the β and γ subunits help to anchor the heterotrimer in the inner leaflet of the plasma membrane. When receptor is activated, GDP is released from the α-subunit resulting in the activation of G protein and dissociation from both the activated receptor and the β and γ subunits (19). Activation LH receptor leads to the activation of the G protein Gs. Following dissociation from β and γ, the α subunit activates adenylate cyclase. Activation of adenylate cyclase, in turn, converts adenosine triphosphate (ATP) to the second messenger molecule cAMP (**Figure 1.6**). cAMP binds to the regulating subunit of PKA and causes activation of its subunits. Upon receptor activation, phospholipase C (PLC) hydrolyzes the membrane lipid phosphatidylinositol 4,5-bisphosphate (PIP2), yielding inositol 1,4,5-triphosphate (IP3) and 1,2-diacylglycerol (DAG). IP3 leads to release of sequestered intracellular Ca^{+2} ions from endoplasmic reticulum. DAG increases the catalytic activity of protein kinase C (PKC) (**Figure 1.7**).

1.6: GPCR dimerization or oligomerization

For many years G protein-coupled receptors (GPCR) were thought to function as monomers but the concept that GPCRs can form dimers or oligomers has become widely accepted (35). The evidence for signal transduction by dimerization of GPCR was first demonstrated for $GABA_B$, metabotropic glutamate and calcium-sensing receptors (36). Oligomerization of GPCRs may be required for function as described for purified leukotriene B4 receptor (37). There is evidence of dimerization and oligomerization for some of GPCRs accompanying receptor activation. GPCR homodimers have been demonstrated for the β_2-adrenergic receptor, the δ-opioid receptor, and the dopamine D_1, D_2 and D_3 receptors (6).

GPCRs interact with components of the membrane bilayer such as lipids and with other GPCRs to form dimers or oligomers. These dimers and higher order-oligomers can affect ligand binding and signaling of GPCRs (38).

The serotonin$_{1A}$ receptor is a member of GPCR superfamily and serves as an important target for drugs. The oligomerization state of serotonin$_{1A}$ receptors has been observed using a homo-FRET measurements where fluorescence anisotropy increases with fluorophore photobleaching (39). In the glutamate receptor family of GPCRs, dimerization is important for receptor activation (40). For rhodopsin family members, dimerization may play a role in the receptor activation. However, the rhodopsin receptor could exist as a homodimers in the outer membrane as shown by microscopy images (41). Oligomerization of LH receptors has also been observed (42-44).

A number of methods have been used to demonstrate dimerization or oligomerization of GPCRs. A biochemical technique commonly used to identify the oligomerization state of GPCR is co-immunoprecipitation. In the co-immunoprecipitation technique, cells which express two epitope-tagged receptors are solubilized and the lysate is incubated with an antibody against one of the epitope tags (7). Then the complex is bound to a medium, electrophoresed, blotted and visualized using an antibody against the epitope tag on the second receptor of interest (7). Dimerization of GPCRs is induced by ligand binding to the receptor and this procedure is repeated. Dimerization of β_2-adrenergic receptor increases with the addition of its ligand isoproterenol (45). Ligand-induced receptor dimerization has been also demonstrated for CXCR2, CCR5 and CCR2 receptors (35). Dimers or oligomers of several GPCRs have been described during receptor desensitization or internalization either before, during, or after ligand binding (34).

1.7: The role of cholesterol in receptor function

Cholesterol is an amphiphilic sterol with a small –OH head group and four rigid rings that interact with plasma membrane phospholipids through their hydrophobic tails (46). Cholesterol is an important component of the plasma membrane and can play an important role in the function of membrane proteins (47) including a number of GPCRs. Cholesterol analogues and membrane fluidity measurements during receptor activity have been used to demonstrate direct and indirect cholesterol-receptor interactions (46). Direct interactions between cholesterol and membrane proteins have been demonstrated for some GPCRs including serotonin$_{1A}$ receptors (48). A specific binding site for cholesterol on the β_2-adrenergic receptor has been described (49).

There is evidence indicating that membrane cholesterol affects signal transduction by GPCRs. Cholesterol is important for formation of lipid microdomains (lipid rafts) (50) which are enriched in cholesterol and sphingolipids and thought to act as a signaling platforms for GPCRs. As an example, Smith et al. (51) have demonstrated that the LH receptors, upon hormone binding, become confined in small membrane microdomains which are essential for ligand-mediated receptor signaling.

How cholesterol functionally regulates GPCRs and how cells control cholesterol distribution is not understood. Nor is it clear whether these mechanisms are of pharmacological importance. However, cholesterol depletion using methyl-β-cyclodextrin leads to a decrease in the oligomerization of the serotonin receptors and decreased signal transduction in response to ligand (39). Decreasing cholesterol levels in membranes expressing μ-opioid receptors are accompanied by decreases in dimerization of the receptor and in receptor association with Gα, a result that reflects the importance of cholesterol in signaling transduction (52).

1.8: Single particle tracking

Single particle tracking (SPT) has become an important tool for studying the movement of molecules in live cells. The aim of SPT is to understand motion of individual molecules or particles in specific environments and to describe their lateral dynamics quantitatively (53). Single particle tracking permits measurement of the individual trajectory of a molecule on the cell surface (54). The trajectories obtained from SPT experiments provide the molecule's mean square displacement (MSD) which is the average square distance that a particle moves in a time period (55). The diffusion coefficient (D) can be calculated from the slope of a plot of MSD vs. time (56). Daumas et al. have calculated the diffusion coefficient from the first two points of the MSD plot (57).

1.9: Fluorescence resonance energy transfer (FRET)

FRET is a biophysical technique that can evaluate interactions between membrane receptors. FRET techniques include both hetero-transfer FRET and homo-transfer FRET. In FRET the energy is transferred from an excited donor to an acceptor when the donor and acceptor are less than about 10 nm apart (58). When a donor and acceptor fluorescent molecules are close, the emission spectrum of the donor overlaps the excitation spectrum of the acceptor, the donor emission is decreased and acceptor emission can be detected. FRET techniques have been used by researchers to study a variety of biological processes including receptor-receptor interactions that occur as part of oligomerization of GPCRs.

1.10: Hetero-FRET

Hetero-FRET is FRET between two different fluorescent proteins where one acts as a fluorescence donor and the other is a fluorescence acceptor. Commonly used FRET pairs

include CFP and YFP or CFP and GFP. Cyan fluorescent protein (CFP) and yellow fluorescent protein (YFP) are color variants of green fluorescent protein (GFP). Donor (CFP) excitation results in energy transfer to the acceptor (YFP) and emission by the acceptor when both donor and acceptor are at distances less than about 10 nm (58).

1.11: Homo-FRET

FRET usually refers to energy transfer between two different fluorophores, one acting as a donor and the other acting as an acceptor. However, in some biological conditions, researchers need to evaluate interactions between two copies of a single protein (59). In homo-transfer FRET both proteins will emit light with the same wavelengths but with differences in polarization between excitation and emission light of the fluorophores which can be detected (**Figure 1.4**). Thus energy is transferred between two identical donor and acceptor molecules (58). If the donor and acceptor molecules are sufficiently close for energy transfer, the emitted energy is polarized like the donor molecules, but less anisotropy is seen in FRET because the acceptor is oriented differently (**Figure 1.8** (60)). Decreased polarization reflects an increase in self-association and suggests that molecules of interest are in a dimeric or oligomeric structure.

Anisotropy is measured by collecting images using polarizers to obtain images of fluorescence emitted parallel ($I_{\parallel}$) and perpendicular ($I_{\perp}$) to the polarization of the exciting light. The following formula is used to calculate fluorescence anisotropy (r):

$$Anisotropy(r) = \frac{I_{\parallel} - I_{\perp}}{I_{\parallel} + 2I_{\perp}} \quad (1)$$

where $I_{\parallel}$ and $I_{\perp}$ are the intensities of the parallel and perpendicular polarized emission. Homo-transfer FRET can be used to examine protein-protein interaction on individual cells and it is widely used to evaluate the aggregation state in living cells (61).

1.12: EPAC-Based FRET Sensors

FRET-based sensors are ideal to measure the changes in intracellular concentrations of cAMP, a second messenger involved in GPCR signaling. cAMP is an important intermediate that regulates various cellular functions through protein kinase A (PKA) and Epac, an exchange protein directly activated by cAMP (62). Several Epac-based reporters called ICUE probes have been created using full length Epac1 or truncated forms of Epac2 sandwiched between ECFP and citrine. Similar to the biosensors formed from EPAC, ICUE3 was constructed by replacing citrine with a circularly permuted YFP. In FRET-based sensing, binding of cAMP to Epac induces an unfolding of CFP and YFP domains which increases the distance between CFP and YFP and increases the ratio of CFP emission to YFP sensitized emission (**Figure 1.9** (63)).

1.13: Hypothesis

Cis-activation of the glycoprotein hormone receptors, including receptors for luteinizing hormone (LH), involves binding of cognate hormone to these receptors' large exodomains followed by interactions between the receptor exodomain and the receptor transmembrane domain and extracellular loops (4,5). Intracellular signaling arising from these interactions is essential for development, regulation of metabolism and reproductive function. In addition to cis-activation, trans-activation of glycoprotein hormone receptors may amplify hormone signals. Trans-activation is believed to occur through interactions between a ligand-occupied exodomain on one receptor and the signaling domain of an adjoining receptor. It is assumed that the trans-activated receptors takes on an "active" conformation and signal similarly to a fully functional receptor that has bound and *retained* ligand or to a constitutively-active receptor that has never seen ligand but signals continuously nonetheless. **We hypothesize that hormone activation of**

LH receptors leads to formation of a signaling complex containing active receptors and that both cis- and trans-activated receptors are present in small membrane microdomains in which receptors motions are confined.

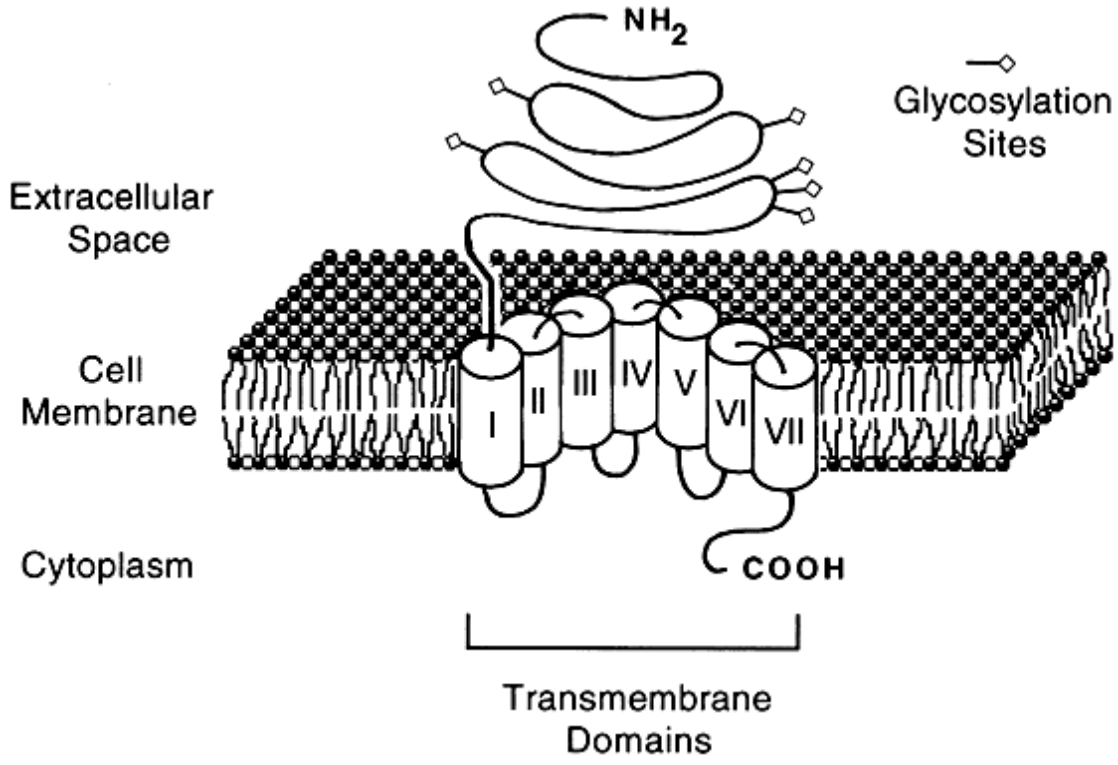

Figure 1.1: G protein-coupled hormone receptor. The luteinizing hormone (LH)/human chorionic gonadotropin (hCG) receptor is a representative of group II of the G protein-coupled receptors. The LH/hCG receptor is composed of seven highly conserved transmembrane domains (I through VII), a large extracellular domain with six potential glycosylation sites and a relatively short cytoplasmic domain. (Modified from Segaloff et al. (64)).

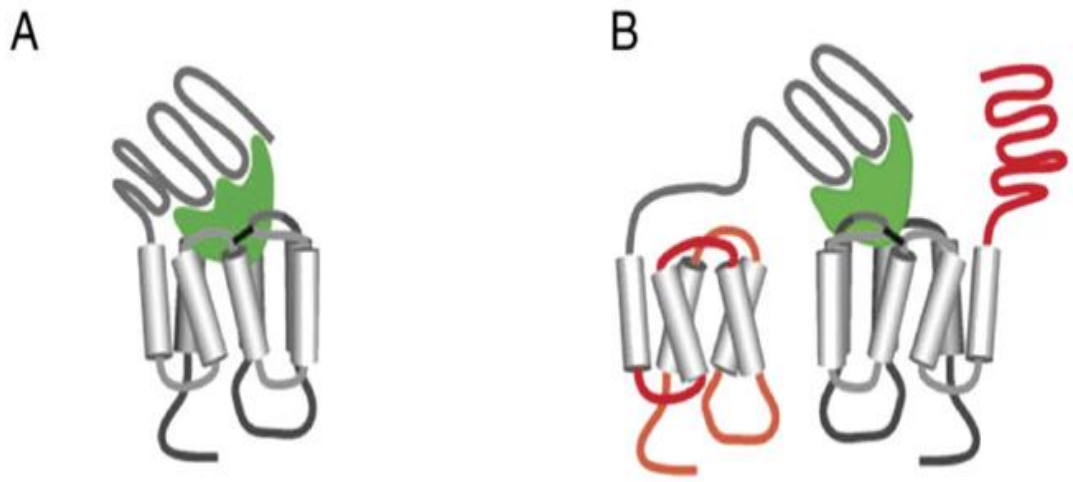

Figure 1.2: *A* and *B:* Schematic presentation of intramolecular (cis) and intermolecular (trans) activation of GPCRs. In cis-activation (A), the hormone-occupied exo-domain is capable of intramolecular activation of its cognate endo-domain. In trans-activation (B), the hormone-occupied exo-domain is capable of intramolecular activation of the endo-domain of the unliganded receptor. (Adapted from Rivero-Muller et al. (34)).

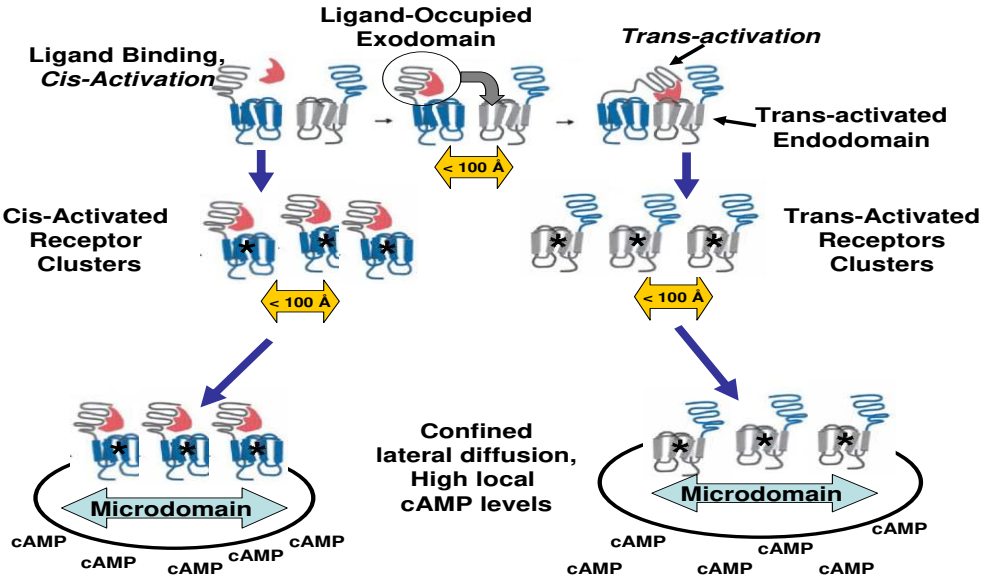

Figure 1.3: Schematic representation of *cis*-activation on the left and *trans*-activation on the right of LH receptors leading to receptor clustering, raft localization and increased intracellular cAMP.

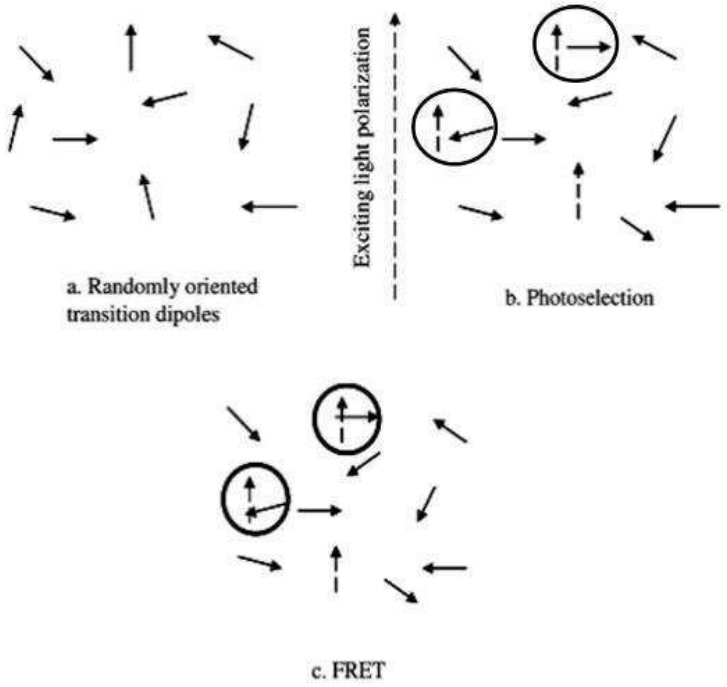

Figure 1.4: Polarization of fluorescence. (A) Fluorophore with randomly-oriented transition dipoles within an isotropic distribution. (B) When the isotropic distribution of fluorophors is excited with vertically polarized light, fluorophores oriented in parallel to the vertical polarization of exciting light are excited. (C) The excited fluorophores transfer energy to adjoining fluorophores resulting in randomly-oriented emitted fluorescence.

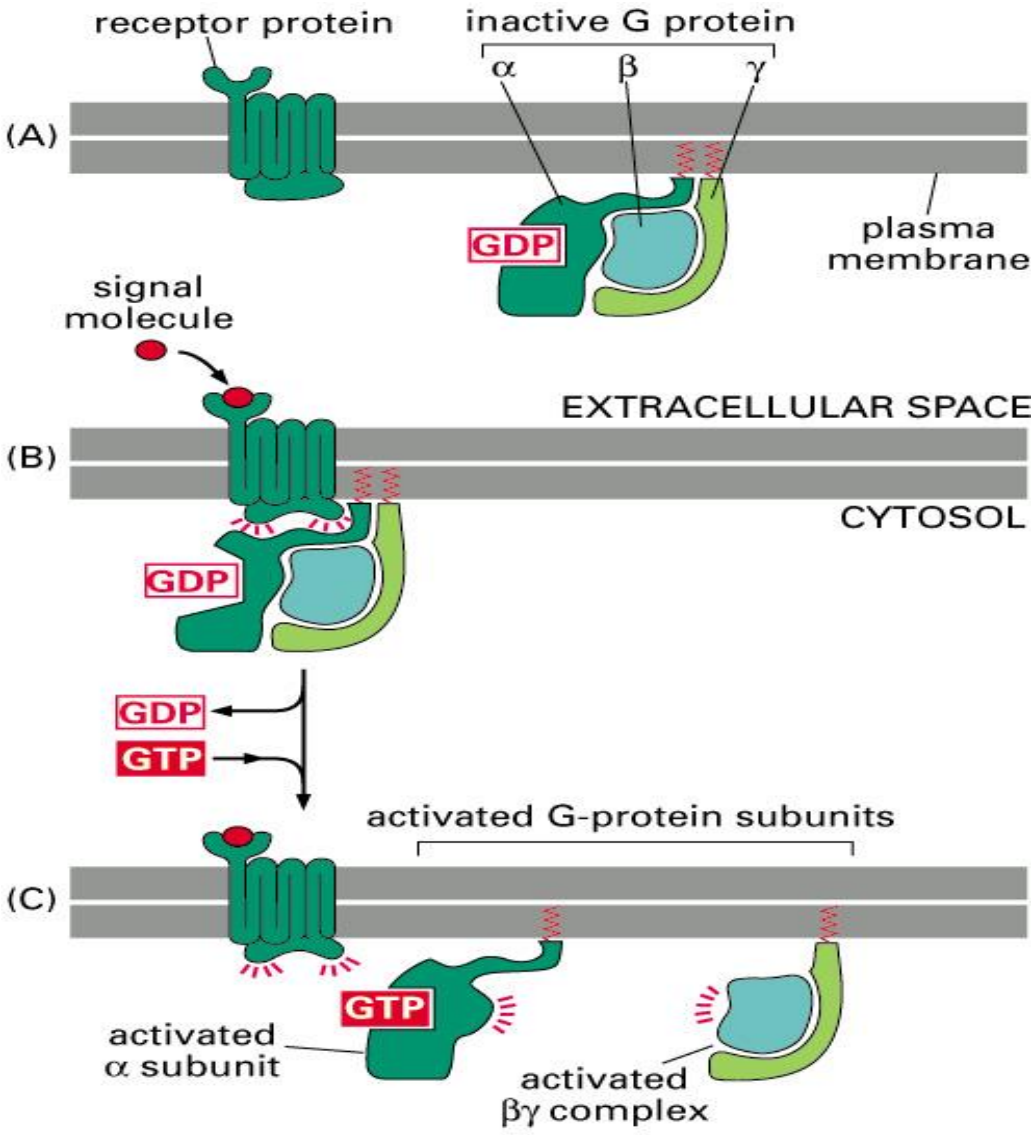

Figure 1.5: Activation of G-proteins (65).

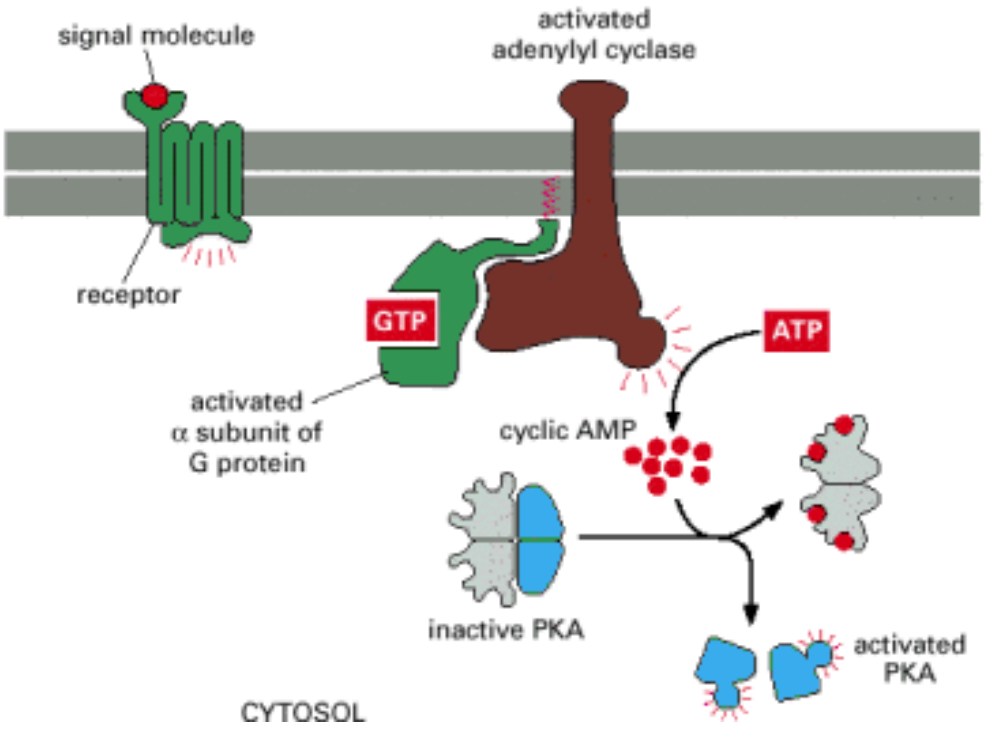

Figure 1.6: Activation of protein kinase A (65).

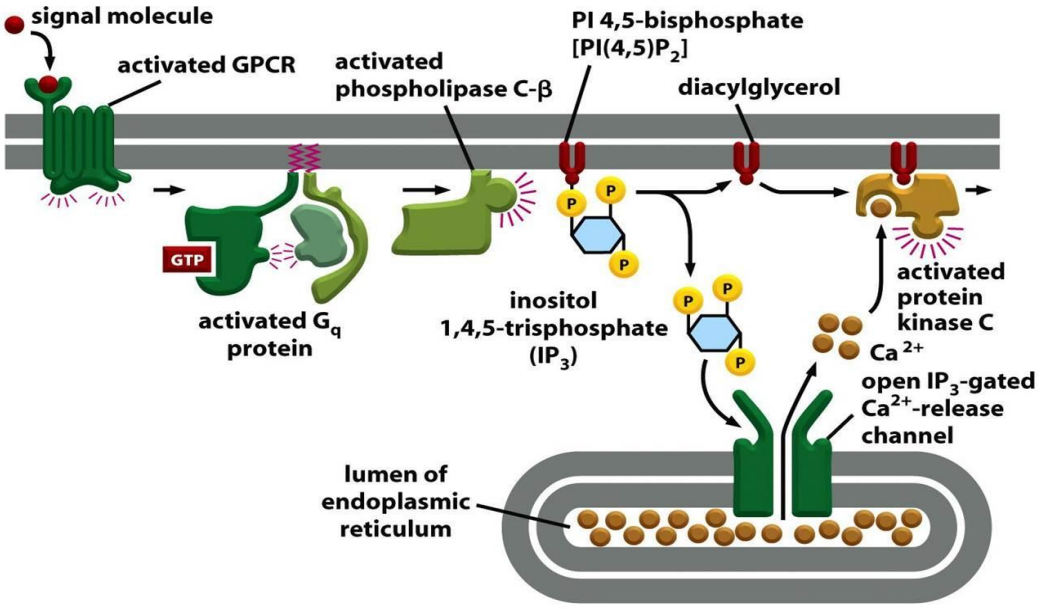

Figure 1.7: Activation of phospholipase C by activated G-protein (65).

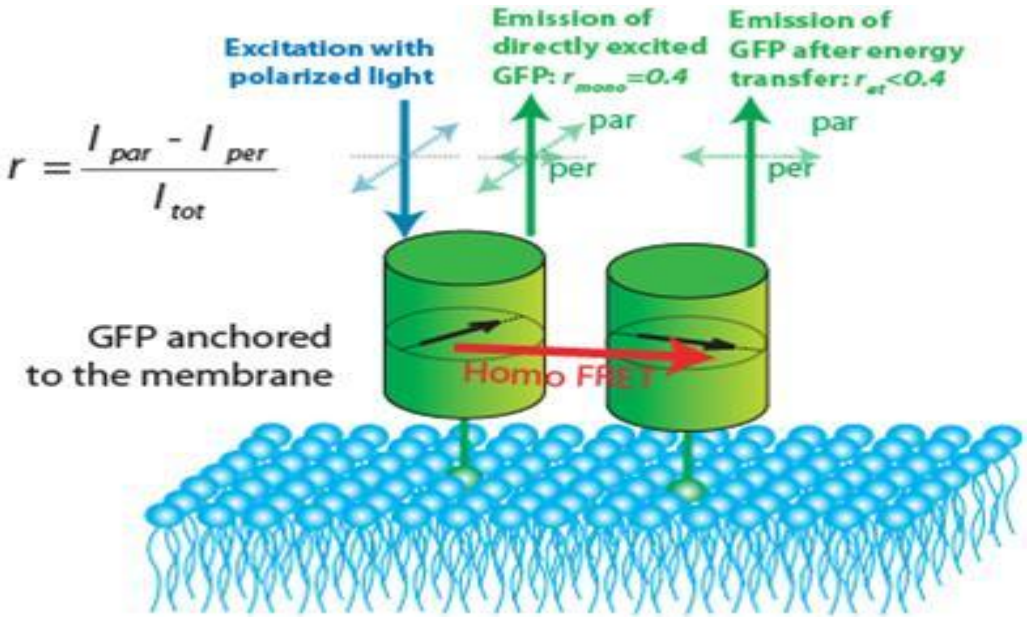

Figure 1.8: FRET results in depolarization of the fluorescence signal. The extent of such depolarization can be used to estimate the cluster size of proteins.

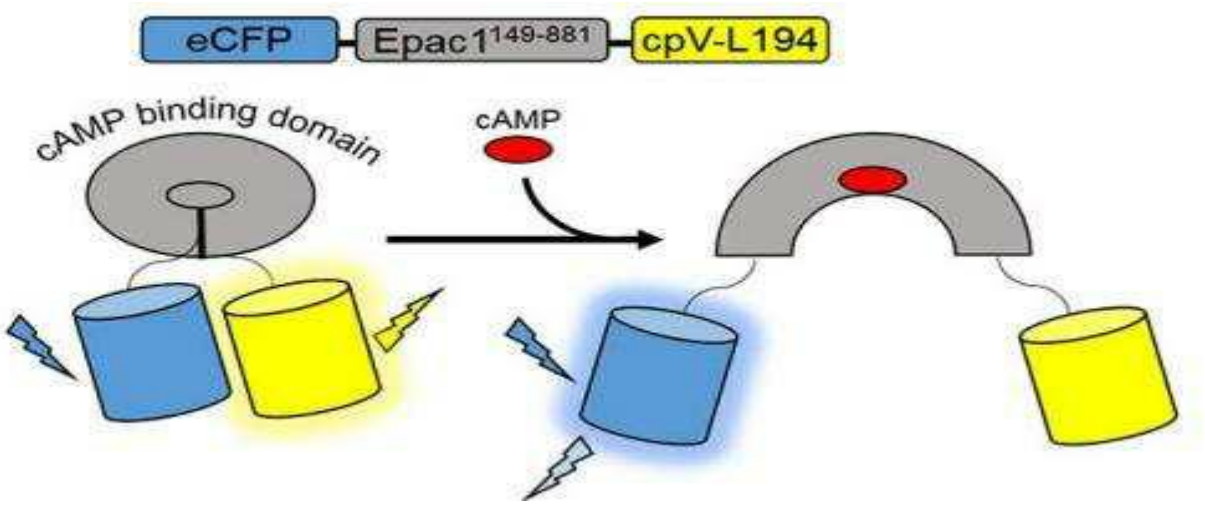

Figure 1.9: ICUE3 consists of an Epac1 149−881 sensing unit flanked by an ECFP donor and a cpV-L194 acceptor reporting unit. Upon binding cAMP, the sensor switches from a high FRET to a low FRET conformation. Adapted from Zhang et al., 2014 (66).

CHAPTER 2: MATERIALS AND METHODS

2.1: Introduction Single Particle Tracking (SPT)

Single particle tracking (SPT) is a biophysical technique that utilizes optical microscopy to provide important information about the diffusion of individual protein molecules on live cells (55). SPT also offers multiple advantages for evaluating protein diffusion when compared with other light microscope techniques (67). One of the important advantages of SPT is that it can give rates of diffusion for single molecules. In contrast, a related method, fluorescence recovery after photobleaching, provides diffusion coefficients for all molecules in an illuminated region of the cell surface, typically at least 50 proteins. Our lab previously examined the diffusion coefficient of LH receptors using colloidal gold particles and single particle tracking methods. In these earlier studies 40 nm gold particles were used as probes for labeling the LH receptors on the surface of living cells and the motion of these labeled receptors was imaged using light microscopy. In the present study, we use quantum dots (QDs) to examine the diffusion coefficient of LH receptors. QDs are inorganic semi-conducting nanoparticles that are 10-100 times brighter than organic dyes. QDs are attached to molecules of interest and imaged by light microscopy to obtain particle trajectories that are analyzed to obtain the mean square displacement of the particle and to distinguish between the different possible motions of the molecules.

2.2: Materials and cell culture

CHO (Chinese hamster ovary) cells were purchased from American Type Culture Collection (Manassas, VA). CHO cells were maintained in high glucose Dulbecco's Modification of Eagle's Medium (DMEM). DMEM medium was purchased from Corning

Cellgro (Visalia, CA) supplemented with 10% fetal bovine serum (FBS). FBS was purchased from Atlas Biologicals (Fort Collins, CO). Penicillin/streptomycin and L-glutamine solution were purchased from Gemini Bio-Products (West Sacramento, CA). 100x MEM non-essential amino acid solution and ethylenediamine tetraacetic acid (EDTA) were purchased from Sigma-Aldrich, Inc. (St.Louis, MO). Human chorionic gonadotropin (hCG) was purchased from Fitzgerald Industries (Acton, MA) and prepared in 1x PBS. Monoclonal anti-FLAG biotin antibody was purchased from Sigma-Aldrich, Inc. (St. Louis, MO). Qdot 605-streptavidin-conjugated quantum dots were purchased from Invitrogen (Carlsbad, CA). Lipofectamine 3000 regent and OPTI-MEM reduced serum medium were purchased from Life Technology (Carlsbad, CA). 35 mm diameter glass-bottom cell culture dishes with 14 mm diameter glass bottoms were purchased from Invitro Scientific (Sunnyvale, CA). CHO cells were grown in 5% CO_2 at 37°C in a humidified environment.

2.3: Amplification of FLAG-LHR-YFP in *E. coli* competent cells (DH5α)

2-5 µg of DNA plasmid (FLAG-LHR-YFP) was added to 50 µL of competent cells (DH5α) max efficiency. A mixture of *E. coli* (DH5α) with FLAG-LHR-YFP was heat shocked for 45 seconds at 42°C and then transferred to ice for 2 minutes. 950 µL LB liquid media was added to the mixture of *E .coli* cells with FLAG-LHR-YFP and were grown at 37°C with vigorous shaking at 225 rpm for one hour. *E. coli* cells with FLAG-LHR-YFP were plated together on LB-agar with antibiotic and cells were grown overnight at 37°C. A single colony was selected and incubated overnight with 3-5 mL of LB-broth media at 37°C with vigorous shaking at 250 rpm. Plasmid DNA was purified using a Qiagen mini-prep kit.

2.4: Amplification of FLAG-LHR$^{+hCG,-cAMP}$ and HA-LHR$^{-hCG,+cAMP}$ plasmids using *E. coli* cells (DH5α)

2-5 µg of DNA plasmid (FLAG-LHR$^{+hCG,-cAMP}$ or HA-LHR$^{-hCG,+cAMP}$) was added to 50 µL of competent cells (DH5α) max efficiency. A mixture of *E. coli* (DH5α) with FLAG-LHR$^{+hCG,-cAMP}$ or HA-LHR$^{-hCG,+cAMP}$ were heat shocked for 45 seconds at 42°C and then transferred to ice for 2 minutes. 950 µL LB liquid media was added to the mixture of *E. coli* cells with FLAG-LHR$^{+hCG,-cAMP}$ or HA-LHR$^{-hCG,+cAMP}$ and cells were grown at 37°C with vigorous shaking at 225 rpm for one hour. *E. coli* cells with FLAG-LHR$^{+hCG,-cAMP}$ or HA-LHR$^{-hCG,+cAMP}$ were plated on LB-agar with antibiotic and cells were grew overnight at 37°C. A single colony was selected and incubated overnight with 3-5 mL of LB-broth media at 37°C with vigorous shaking at 250 rpm. Plasmid DNA was purified using a Qiagen mini-prep kit.

2.5: Transfection of CHO cells with FLAG-LHR-YFP

CHO cells were grown in a 25 cm^2 culture flask in DMEM medium supplemented with 2 mM L-glutamine, 10% fetal bovine serum (FBS), 1% penicillin/streptomycin and 1% 1x MEM non-essential amino acid solution. Cells were grown in 5% CO_2 at 37°C in a humidified environment. CHO cells were transiently transfected with FLAG-LHR-YFP, kindly prepared by Dr. Xiaorong Li (Southwest University, Chongqing, China), using Lipofectamine 3000 in accordance with the Manufacturer's instructions. Two sterilized microcentrifuge tubes were needed, each one containing 125µL of OPTI-MEM medium. Tube one contained 5µL LP300 reagent and 0.4 µg of FLAG-LHR-YFP. Tube two contained 7.5µL of Lipofectamine 3000. Tube one was added drop wise to tube two and the mixture was incubated at room temperature for 5 to 15 min. The incubated mixture was added to the CHO cells. Cells were plated in a 35mm glass-bottom Petri dish and grown to approximately 80% confluence in 1mL OPTI-MEM

reduced serum medium. Cells were maintained in a humidified incubator in 5% CO_2 at 37°C. Transfection proceeded for at least 24 hours.

CHO cells were transiently co-transfected with 0.4 µg HA-LHR$^{-hCG,+cAMP}$ and FLAG-LHR$^{+hCG,-cAMP}$. These vectors were kindly provided by Dr. Aylin Hanyaloglub and Dr. Jonas Kim, members of Dr. Ilpo T. Huhtaniemi's research group at Imperial University, UK. Co-transfection procedures were similar to those used to transfect CHO cells with FLAG-LHR-YFP above.

2.6: Labeling with anti-FLAG-biotin antibody and QD 605-streptavidin:

CHO cells expressing either wild type FLAG-LHR-YFP or FLAG-LHR$^{+hCG,-cAMP}$ and HA-LHR$^{-hCG,+cAMP}$ were seeded onto sterile culture dishes and grown to 70% confluence. All labeling was performed in Tyrodes buffer containing 0.1% BSA. Cells were labeled first with anti-FLAG-biotin antibody at 0.2µg/mL for 30 min, washed three times for 1 min in 1 mL buffer, labeled with QD 605-streptavidin for 10 min and washed 6 times for 1 min in 1 mL of buffer. The QDs were then imaged. The binding specificity for FLAG-tagged receptors was tested by pre-incubating cells with excess of anti-FLAG antibody.

2.7: Single particle tracking of FLAG-LHR-YFP and FLAG-LHR$^{+hCG/-cAMP}$ co-expressed with HA-LHR$^{-hCG/+cAMP}$ on individual CHO cells

We examined the diffusion coefficient and confinement of LH receptors in plasma membrane microdomains by tracking the movement of individual receptors using single particle tracking methods as described by Kusumi and colleagues (68). CHO cells expressing FLAG-LHR-YFP alone or co-expressing FLAG-LHR$^{+hCG,-cAMP}$ with HA-LHR$^{-hCG,+cAMP}$ were seeded onto 35 mm^2 Petri dishes and grown to 50% confluence. All labeling was performed in

Tyrodes buffer containing 0.1% BSA. Cells were labeled first with anti-FLAG-biotin antibody at 0.2 μg/mL for 30-40 min, washed three times for 1 min in 1mL of buffer and labeled with quantum dot probe Qdot605-streptavidin conjugate at 100 pM for 10 min and then washed at least six times for 1 min in 1mL to remove unbound probe. In some experiments, cells were treated with 0.1, 1 or 100 nM hCG for 1 hour. Images were collected on a Zeiss Axiovert 200M microscope using a 63x 1.2 NA water objective and Qd605 filter set. Images were collected every 100 ms for up to 2 minutes at a final magnification of 315x onto a CCD camera with 16 x 16 μm pixels. Image acquisition was performed with MetaMorph 7.1.6. Determination of individual particle locations and the trajectories for individual particles were performed with Image J. The diffusion coefficient and the domain size were calculated using a program developed by Dr. George Barisas at Colorado State University.

2.8: Homo-Transfer FRET

After hormone treatment with either luteinizing hormone (LH) or human chorionic gonadotropin (hCG), LH receptors are self-associated into dimers/oligomers and translocated into small membrane compartment (lipid rafts) where receptor motions are confined. Polarization homo FRET is one of the FRET techniques that has been used to investigate self-association of LH receptors. The aggregation of LH receptors is related to hormone concentration as shown in a previous study using homo-FRET methods which show a decrease in anisotropy when CHO cells are incubated with 100 nM hCG (43). Homo-FRET is energy transfer between identical molecules, one acting as a donor and the other as an acceptor and this process can be assessed by imaging measurements of emission polarization. Decreasing anisotropy indicates increased self-association of the LH receptor. In this study, decreased anisotropy for wild type receptor after hormone treatment or mutant receptors defective in

hormone binding or signal transduction when co-expressed with wild type receptor was examined.

2.9: Materials and cell culture

CHO (Chinese hamster ovary) cells were purchased from American Type Culture Collection (Manassas, VA). CHO cells were maintained in high glucose Dulbecco's Modification of Eagle's Medium (DMEM). DMEM medium was purchased from Corning Cellgro (Visalia, CA) supplemented with 10% fetal bovine serum (FBS). FBS was purchased from Atlas Biologicals (Fort Collins, CO). Penicillin/streptomycin and L-glutamine solution were purchased from Gemini Bio-Products (West Sacramento, CA). 100x MEM non-essential amino acid solution and ethylenediamine tetraacetic acid (EDTA) were purchased from Sigma-Aldrich, Inc. (St. Louis, MO). Human chorionic gonadotropin (hCG) was purchased from Fitzgerald Industries (Acton, MA) and prepared in 1x PBS. Lipofectamine 3000 regent and OPTI-MEM reduced serum medium were purchased from Life Technology (Carlsbad, CA). Glass bottom cell culture dishes with 35 mm diameter and 14 mm diameter glass bottoms were purchased from Invitro Scientific (Sunnyvale, CA). CHO cells were grown in 5% CO_2 at 37°C in a humidified environment.

2.10: Transfection of CHO cells with FLAG-LHR-YFP

CHO cells were grown in a 25 cm^2 culture flask in DMEM medium supplemented with 2mM L-glutamine, 10% fetal bovine serum (FBS), 1% penicillin/streptomycin and 1% 1x MEM non-essential amino acid solution. Cells were grown in 5% CO_2 at 37°C in a humidified environment. CHO cells were transiently transfected with FLAG-LHR-YFP using Lipofectamine

3000 in accordance with the Manufacturer's instructions. Two sterilized microcentrifuge tubes were needed, each containing 125µL of OPTI-MEM medium. Tube one contained 5µL LP3000 reagent and 0.4µg of FLAG-LHR-YFP. Tube two contained 7.5µL of Lipofectamine 3000. Tube one was added drop wise to tube two and the mixture was incubated at room temperature for 5 to 15 min. The mixture was added to CHO cells. Cells were then plated in a 35mm glass-bottom Petri dish and grown to approximately 80% confluence in 1mL OPTI-MEM reduced serum medium. Cells were maintained in a humidified incubator in 5% CO_2 at 37°C. Transfection proceeded for at least 24 hours.

CHO cells were transiently co-transfected with 0.4 µg FLAG-LHR-YFP and excess of HA-LHR$^{-hCG,+cAMP}$ or 0.4µg FLAG-LHR-YFP and excess of FLAG-LHR$^{+hCG,-cAMP}$. Co-transfection procedures were similar to those used to transfect CHO cells with FLAG-LHR-YFP above.

2.11: Analysis of Polarization Homo-FRET

We investigated aggregation or self-association of LH receptors following hormone binding using polarized imaging microscopy to measure homo-FRET between receptors. CHO cells, after transient transfection with wild type receptor FLAG-LHR-YFP alone or co-expressing FLAG-LHR-YFP with excess of either HA-LHR$^{-hCG,+cAMP}$or FLAG-LHR$^{+hCG,-cAMP}$ were plated overnight in Willco 35 mm diameter #1.5 glass-bottom Petri dishes and grown to approximately 80-90 % confluence. Cells were washed twice with 1x phosphate buffered saline (PBS) pH 7.0. For untreated cells, the cells were incubated in 600 mL of PBS alone, while treated cells were incubated with different concentrations of hCG (0.1, 1 or 100 nM) at 37°C for one hour. Cells were imaged on a Zeiss Axiovert 200M inverted microscope using a 63x 1.2 NA water objective and YFP filter set. Images were acquired using an arc lamp for fluorescence

excitation with a polarized excitation filter. Homo-transfer FRET data are collected from two separate images obtained using an Andor Du897E EMCCD camera and a "Dual View" image dissector. This latter device provides simultaneous acquisition of separate images of fluorescence emission parallel to polarization of the excitation light and fluorescence perpendicular to excitation light, respectively. The cells were photobleached for 15 minutes and fluorescence emission was evaluated using MetaMorph 7.1.6. Each anisotropy measurement was taken with g-factor and background images, and image analysis was performed with Image J. Ten cells for each treatment were analyzed. The fluorescence polarization anisotropy (r) was calculated using the following formula: $r = (I_{\parallel} - g\ I_{\perp})/ (I_{\parallel} + 2g\ I_{\perp})$ where g is the g-factor, and $I_{\parallel}$, $I_{\perp}$ are the parallel and perpendicular polarized emission intensities generated by excitation with vertically polarized light.

2.12: EPAC-based FRET sensor

cAMP is a second messenger which regulates several cellular functions (69). The cAMP sensor is based on Epac, an exchange protein directly activated by cAMP. Several Epac-based probes, so-called ICUE probes, have used Epac1 and Epac2 as described by Zhang and colleagues (70). Epac based reporter molecules can be used to evaluate intracellular cAMP levels by sandwiching the full length Epac between cyan fluorescence protein (CFP) as a donor and yellow fluorescence protein (YFP) as an acceptor. Energy transfer FRET signals depend on the energy transferred from an excited donor to the FRET acceptor if both the donor and the acceptor are in close proximity. With energy transfer, fluorescence emission from the excited donor will be reduced and fluorescence emission from the acceptor will increase. In FRET-based sensors, binding of cAMP to Epac induces an unfolding of CFP and YFP domains which increases the distance between CFP and YFP. The ratio of CFP emission to sensitized

YFP emission also increases (63). In this study, we used ICUE3 to evaluate changes in cAMP in cells expressing LH receptors in response to hCG treatment.

2.13: Materials and cell culture

CHO (Chinese hamster ovary) cells were purchased from American Type Culture Collection (Manassas, VA). CHO cells were maintained in high glucose Dulbecco's Modification of Eagle's Medium (DMEM). DMEM medium was purchased from Corning Cellgro (Visalia, CA) supplemented with 10% fetal bovine serum (FBS). FBS was purchased from Atlas Biologicals (Fort Collins, CO). Penicillin/streptomycin and L-glutamine solution were purchased from Gemini Bio-Products (West Sacramento, CA) and methyl-β-cyclodextrin (MβCD) was purchased from Sigma-Aldrich, Inc (St. Louis, MO). 100x MEM non-essential amino acid solution and ethylenediamine tetraacetic acid (EDTA) were purchased from Sigma-Aldrich, Inc. (St. Louis, MO). Human chorionic gonadotropin (hCG) was purchased from Fitzgerald Industries (Acton, MA) and prepared in 1x PBS. Lipofectamine 3000 regent and OPTI-MEM reduced serum medium were purchased from Life Technology (Carlsbad, CA). 35 mm diameter glass-bottom cell culture dishes with 14 mm diameter glass-bottoms were purchased from Invitro Scientific (Sunnyvale, CA). CHO cells were grown in 5% CO_2 at 37°C in a humidified environment.

2.14: Transfection of CHO cells with FLAG-LHR-YFP and ICUE3

CHO cells were grown in a 25 cm^2 culture flask in DMEM medium supplemented with 2mM L-glutamine, 10% fetal bovine serum (FBS), 1% penicillin/streptomycin and 1% 1x MEM non-essential amino acid solution. Cells were grown in 5% CO_2 at 37°C in a humidified

environment. CHO cells were transiently co-transfected with FLAG-LHR-YFP and ICUE3 plasmid kindly provided by Dr. Jin Zhang (Johns Hopkins University, Baltimore, USA) using Lipofectamine 3000 in accordance with the Manufacturer's instructions. Two sterilized microcentrifuge tubes were needed, each one containing 125µL of OPTI-MEM medium. Tube one contained 5µL LP3000 (reagent) and 0.4µg of FLAG-LHR-YFP. Tube two contained 7.5µL of Lipofectamine 3000. Tube one was added drop wise to tube two and the mixture was incubated at room temperature for 5 to 15 min. Incubated mixture was added to the CHO cells, cells were plated in a 35mm glass-bottom Petri dish and grown to approximately 80% confluence in 1mL OPTI-MEM reduced serum medium. Cells were maintained in a humidified incubator in 5% CO_2 at 37°C. Transfection proceeded for at least 24 hours. CHO cells were transiently co-transfected with 0.4 µg ICUE3 and excess of HA-LHR$^{-hCG,+cAMP}$ and 0.4µg ICUE3 and excess of FLAG-LHR$^{+hCG,-cAMP}$. Co-transfection procedures were similar to those used to transfect CHO cells with FLAG-LHR-YFP and ICUE3 above.

2.15: FRET measurement using dual emission ratio imaging

After cells were transiently transfected with ICUE3, ICUE3 and FLAG-LHR-YFP, ICUE3 and excess HA-LHR$^{-hCG,+cAMP}$ or ICUE3 and excess FLAG-LHR$^{+hCG,-cAMP}$, medium was discarded from the Petri dish, cells were washed twice gently and maintained in 1x phosphate buffered saline (PBS) pH 7.4. Cells were then immediately imaged. Imaging data were collected using a 1.2 N.A. 63x water objective in a Zeiss Axiovert 200M inverted microscope with an EMCCD camera controlled by MetaFluor software. A 10% neutral density filter was used to reduce the intensity of the arc lamp and reduce fluorophore photobleaching. Emission ratios were obtained using a 436DF20 excitation filter, a 455 DRLP dichroic mirror, and two

emission filters, 480DF40 for CFP and 535DF30 for YFP. All filters used were from Chroma Technology. Images were taken at 60s intervals during acquisition and, for each experiment, a sequence of images were obtained. During experiments, data were collected from untreated cells or pretreated cells for 1 hour with 10mM MβCD for several minutes before the PBS solution was removed and replaced with PBS containing 0.1, 1, or 100 nM hCG and cells were incubated for 15 minutes at room temperature. The data were analyzed using Image J software. Emission ratios (CFP/YFP) were calculated from CFP emission intensity and FRET emission intensity after background correction of fluorescent images. These corrections were performed by subtracting the intensity of the background from the emission intensities of fluorescent cells expressing ICUE3.

2.16: Statistical analysis of data

Mean values ± S.E.M. or standard deviation are presented. Significance was evaluated using Student's t-test and p values are indicated ($p < 0.05$).

CHAPTER 3: RESULTS

3. 1: Introduction

The data presented here were obtained from CHO cells expressing either wild type receptor and/or mutant epitope-tagged receptors. We also examined the effect of treatment with hCG, a hormone which has been previously demonstrated to cause aggregation of wild type LHR (71), presumably through receptor cis-activation. The goal of these studies was to determine whether lateral motions or the aggregation state of wild type or mutant receptors provided evidence of LHR trans-activation and, similarly, whether there was increased intracellular cAMP when CHO cells expressed a pair of receptors (FLAG-LHR$^{+hCG,-cAMP}$ or HA-LH$^{-hCG,+cAMP}$) that could only function through receptor trans-activation.

3.2: Single particle tracking of wild type FLAG-LH receptors or FLAG-LHR$^{+hCG,-cAMP}$ co-expressed with HA-LHR$^{-hCG,+cAMP}$

To assess the diffusion coefficient of LH receptors, we used single particle tracking methods to track the movements of single LH receptors on the plasma membrane of CHO cells expressing FLAG-LHR-YFP wild type receptors or coexpressing FLAG- LHR$^{+hCG,-cAMP}$ and HA-LHR$^{-hCG,+cAMP}$. Trajectories used to create MSD plots were obtained from FLAG-tagged receptors using images were recorded for two minutes. A representative trace is shown in **Figure 3.1** and samples of data obtained are shown in **Table 3.1** and **3.2**. FLAG-LHR-YFP receptors before treatment with hCG had a microscopic diffusion coefficient ($D_{0,1}$) of $2.70 \times 10^{-10} \pm 1.05 \times 10^{-10}$ $cm^2 sec^{-1}$ (**Table 3.3**). The domain size and the number of domains occupied by wild type receptors were 0.40 ± 0.15 μm and 5, respectively (**Table 3.3**). The diffusion

coefficient $D_{0,1}$ and domain size of wild type receptors treated with 100 nM hCG were reduced to $1.51x10^{-10} \pm 1.20x10^{-10}$ cm^2sec^{-1} and 0.30 ± 0.20 µm, respectively. The number of domains accessed by the receptor decreased to 3 **(Table 3.3**).

The diffusion coefficient of mutant LH receptors FLAG-$LHR^{+hC,-cAMP}$ coexpressed with HA-$LHR^{-hCG,+AMP}$ before hormone hCG treatment was $8.76x10^{-10} \pm 3.97x10^{-10}$ cm^2sec^{-1}. The average domain size was 0.60 ± 0.43 µm and the number of domains was 5. After 100 nM hCG treatment, the diffusion coefficient decreased to $2.35x10^{-10} \pm 3.42x10^{-10}$ cm^2sec^{-1}. The domain size and the number of domains also decreased to 0.37 ± 0.24 µm and 3, respectively (**Table 3.3**). This results suggests that HA-$LHR^{-hCG,+AMP}$, a receptor which is unable to bind hCG, was nonetheless activated by FLAG-$LHR^{+hCG,-cAMP}$. In general, the diffusion coefficients measured, the size of domains occupied by receptors and the number of domains were reduced by treatment of cells with 100 nM hCG. SPT raw data are presented in Appendix I.

3.3: Effects of hCG treatment on aggregation of wild type FLAG-LHR-YFP, FLAG-LHR-YFP co-expressed with FLAG-$LHR^{+hCG,-cAMP}$ or FLAG-LHR-YFP co-expressed with HA- $LHR^{-hCG,+cAMP}$

To examine the aggregation state of LH receptors in response to cis-activation or trans-activation by hCG treatment, we performed homo-transfer FRET experiments using CHO cells expressing wild type receptor FLAG-LHR-YFP, FLAG-LHR-YFP co-expressed with FLAG-$LHR^{+hCG,-cAMP}$ or FLAG-LHR-YFP co-expressed with HA-$LHR^{-hCG,+cAMP}$**.** Homo-FRET was measured by imaging microscopy of polarized fluorescence from the YFP moiety attached to the C-terminus of FLAG-LHR-YFP. When YFP moieties are in close proximity, presumably

due to receptor aggregation, the acceptor YFP molecules are oriented differently than donor YFP molecules and anisotropy is subsequently decreased.

Hormone-treated LH receptors exhibited a higher degree of aggregation than did untreated LH receptors. As shown in **Table 3.4**, change on photobleaching in mean anisotropy of wild type FLAG-LHR-YFP following 100 nM hCG treatment was 0.060 ± 0.003, larger and significantly different from the change on photobleaching in mean anisotropy for untreated cells which was 0.010 ± 0.001. This suggests that receptor self-association accompanies cis-activation of wild type receptors in response to treatment of cells with increasing concentrations of hCG.

The change on photobleaching in mean anisotropy of CHO cells coexpressing wild type receptor FLAG-LHR-YFP and FLAG-LHR$^{+hCG,-AMP}$ with a transfection ratio of 1:1 following 100 nM hCG treatment was 0.100 ± 0.006 which was similar to the difference in mean anisotropy before hormone treatment, 0.100 ± 0.006. The difference in mean anisotropy for cells coexpressing FLAG-LHR-YFP and FLAG-LHR$^{+hCG,-AMP}$ with a transfection ratio of 1:2 was 0.090 ± 0.005 before 100 nM hCG treatment and 0.090 ± 0.006 after 100 nM hCG treatment. These values increased with a transfection ratio of 1:3 which resulted in a difference in mean anisotropy of 0.090 ± 0.007 before 100 nM hCG treatment and 0.120 ± 0.007 after cell treatment with 100 nM hCG.

The changes on photobleaching in mean anisotropy between wild type receptor FLAG-LHR-YFP and the mutant receptor, FLAG-LHR$^{+hCG,-AMP}$ which binds hormone but is unable to initiate signal were likely to be the result of trans-activation by the wild type receptor. As shown in **Table 3.4**, CHO cells coexpressing FLAG-LHR-YFP and HA-LHR$^{-hCG,+AMP}$, when the transfection ratio was 1:1, exhibited differences upon photobleaching in mean anisotropy of

0.070 ± 0.007 both before and after 100 nM hCG treatment. The photobleaching-induced differences in mean anisotropy between this same receptor pair, FLAG-LHR-YFP and HA-LHR$^{-hCG,+AMP}$ at a transfection ratio of 1:2 was 0.080 ± 0.004 after 100 nM hCG treatment, slightly larger than differences in mean anisotropy before hormone treatment of 0.070 ± 0.007. By increasing the transfection ratio for FLAG-LHR-YFP wt:HA-LHR$^{-hCG,+AMP}$ to 1:3, the photobleaching-induced difference in mean anisotropy following 100 nM hCG treatment was 0.110 ± 0.007, somewhat larger than the differences in mean anisotropy for untreated cells. Overall, photobleaching induced differences in mean anisotropies values increased with an increase in the transfection ratio use for CHO cells co-expressing FLAG-LHR-YFP and either FLAG-LHR$^{+hCG,-AMP}$ or HA-LHR$^{-hCG,+AMP}$ (**Table 3.4**). Examples of homo-FRET raw data are presented in Appendix II.

3.4: Effects of hCG treatment on intracellular cAMP levels in CHO cells expressing FLAG-LHR-YFP only or co-expressing FLAG-LHR$^{+hCG,-cAMP}$ and HA-LHR$^{-hCG,+cAMP}$.

LH receptor-mediated changes in intracellular cAMP levels were measured following hCG treatment. These studies used a live cell imaging technique to assess intramolecular hetero-FRET in ICUE3, a cAMP reporter molecule. As shown in **Table 3.5**, the emission ratio of FLAG-LHR-YFP before hCG treatment was 0.85 ± 0.01 which increased after 100 nM hCG treatment to 0.89 ± 0.02. This 1.05 fold increase in the ratio of CFP/YFPSE indicated cis-activation of wild type receptor by hCG.

In CHO cells coexpressing mutant receptors FLAG-LHR$^{+hCG,-AMP}$ and HA-LHR$^{-hCG,+AMP}$ using a 1:1 transfection ratio, the CFP/YFP emission ratio before hormone hCG treatment was 0.80 ± 0.01, a value that increased after 100 nM hCG treatment to 0.83 ± 0.01, a 1.03-fold

increase. CHO cells coexpressing FLAG-LHR$^{+hCG,-AMP}$ and HA-LHR$^{-hCG,+AMP}$, prepared using a transfection ratio of 1:10, had a CFP/YFP emission ratio before 100 nM hCG of 0.82 ± 0.01 and an emission ratio after 100 nM hCG treatment of 0.85 ± 0.01, a 1.04-fold change in the ratio of CFP to YFPSE emission. Thus, increasing the transfection ratio for CHO cells co-expressing FLAG-LHR$^{+hCG,-AMP}$ and HA-LHR$^{-hCG,+AMP}$ increased the CFP/YFPSE emission ratio CFP/YFPSE upon treatment with 100 nM hCG although the changes were small.

To assess effects of cholesterol depletion on intracellular cAMP levels in response to LH receptor mediated signaling, we pretreated CHO cells expressing FLAG-LHR-YFP or co-expressing FLAG-LHR$^{+hCG,-AMP}$ and HA-LHR$^{-hCG,+AMP}$ with MβCD as described in Chapter 2. As shown in **Table 3.5**, there was a significant decrease in the CFP/YFPSE emission ratio before and after 100 nM hCG treatment in cells expressing FLAG-LHR-YFP and pretreated with MβCD. Before hormone treatment, the CFP to YFPSE ratio was 0.84 ± 0.01. After hCG treatment, that ratio was 0.88 ± 0.02, a 1.04-fold increase. CHO cells co-expressing FLAG-LHR$^{+hCG,-AMP}$ and HA-LHR$^{-hCG,+AMP}$ with transfection ratio of 1:1 and pretreated with MβCD had an emission ratio before 100 nM hCG treatment of 0.79 ± 0.01 which is identical to the emission ratio observed after hormone treatment. The CFP to YFPSE emission ratio for CHO cells co-expressing both mutant receptors with transfection ratio of 1:10 and pre-treated with MβCD was 0.80 ± 0.01 before 100nM hCG treatment and 0.81 ± 0.01 after 100 nM hCG, a fold change of 1.01 (**Table 3.5**). **Figure 3.2** shows changes in the CFP to YFPSE ratio of CHO cells expressing FLAG-LHR-YFP untreated and treated with 100 nM hCG. Examples of cAMP raw data are presented in Appendix III.

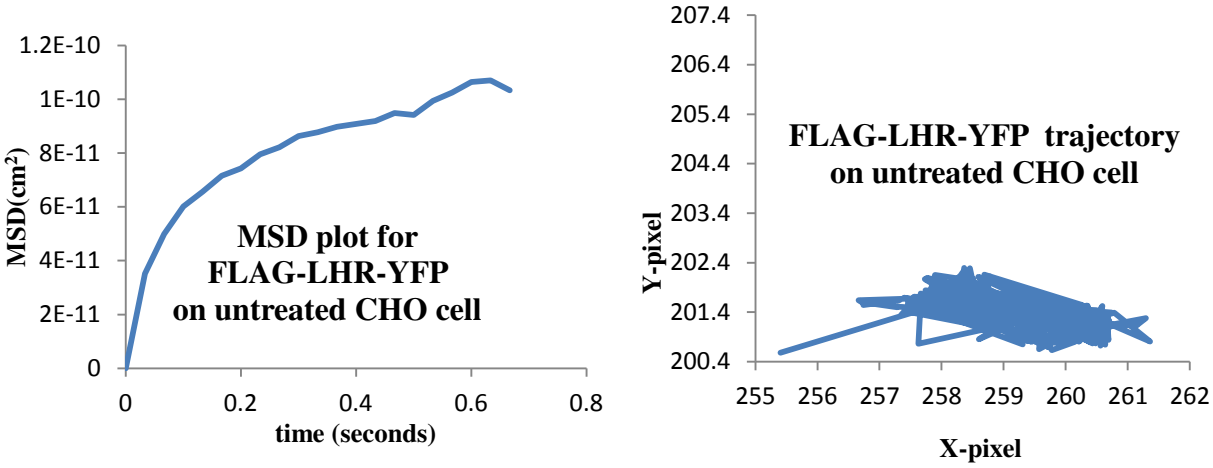

Figure 3.1: A representative trajectory (left panel) and MSD plot (right panel) for CHO cells expressing FLAG-LHR-YFP and otherwise untreated. The diffusion coefficient for this trajectory was 6.2×10^{-11} $cm^2 s^{-1}$, the number of domains was 5, and the domain size was 0.49 µm.

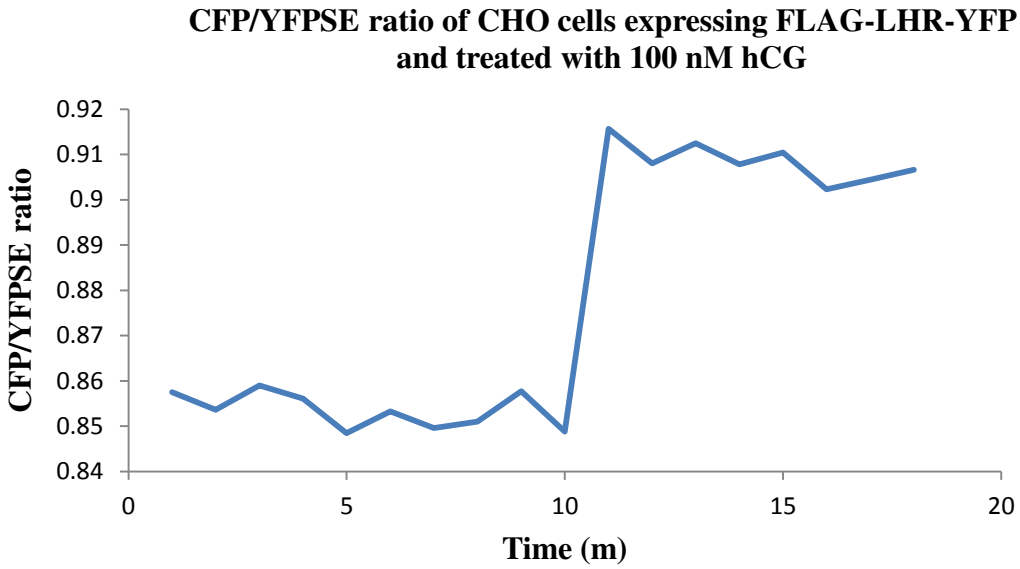

Figure 3.2: CFP/YFPSE ratio of CHO cells expressing FLAG-LHR-YFP and treated with 100 nM hCG after 9 minutes. Images were collected for an additional 10 minutes after hCG treatment.

Table 3.1: An example of a CSV file of a trajectory created from one image sequence. Only a portion of the file is shown here.

frame	y	x						
0	362.2074	103.6205	35	361.7089	103.3507	70	361.6321	103.3453
1	361.7675	103.5363	36	361.7371	103.4365	71	361.7239	103.2666
2	361.7477	103.48	37	361.7496	103.4086	72	361.6032	103.3174
3	361.7124	103.4647	38	362.2369	103.4233	73	361.6386	103.2722
4	362.2844	103.6019	39	361.6446	103.2604	74	361.6061	103.3162
5	361.7488	103.5112	40	361.5998	103.3562	75	361.5644	103.3303
6	361.7239	103.3871	41	361.7297	103.5121	76	361.5768	103.3217
7	361.6636	103.5022	42	361.7597	103.362	77	361.5991	103.3607
8	361.7643	103.4614	43	361.7054	103.3611	78	361.5637	103.366
9	361.7119	103.4779	44	361.6674	103.4123	79	361.6145	103.3901
10	361.7698	103.5175	45	361.7987	103.5439	80	361.4193	103.3601
11	362.2305	103.4263	46	361.6517	103.4339	81	361.7131	103.4154
12	362.226	103.4347	47	361.4847	103.2796	82	362.2495	103.479
13	361.7216	103.5122	48	361.6284	103.4079	83	362.2681	103.4893
14	361.658	103.4384	49	361.6579	103.5191	84	362.1398	103.5537
15	361.6832	103.4498	50	361.6483	103.3974	85		
16	362.3713	103.6831	51	361.6756	103.3978	86	361.58	103.3378
17	362.2883	103.6753	52	361.4899	103.2473	87	361.7633	103.5013
18	361.7733	103.6326	53	361.6345	103.3769	88	361.4713	103.3608
19	361.6608	103.4836	54	361.5051	103.2661	89	361.5767	103.4489
20	361.6614	103.355	55	361.6086	103.4446	90	361.7705	103.509
21	361.7368	103.4377	56	361.6755	103.444	91	361.6429	103.3094
22	361.6591	103.3342	57	361.7333	103.5169	92	361.2627	102.9066
23	361.63	103.4107	58	361.6823	103.452	93	361.506	103.2816
24	361.7461	103.4173	59	361.7072	103.525	94	361.6946	103.4288
25	361.8057	103.5106	60	361.7647	103.3981	95	361.6197	103.4413
26	361.6549	103.3493	61	361.756	103.4514	96	361.6233	103.3583
27	361.683	103.3722	62	362.3722	103.5696	97	361.6447	103.4498
28	361.5698	103.2961	63	361.6924	103.3799	98	361.6291	103.4127
29			64	362.3101	103.4804	99	361.6264	103.4456
30	362.4957	103.5051	65	361.6812	103.4843	100	361.6353	103.5436
31	362.1674	103.3978	66	361.7131	103.4792	101	361.6306	103.3703
32	361.7772	103.3153	67	362.2311	103.5243	102	361.636	103.4506
33	361.7458	103.3711	68	361.6142	103.3132	103	361.6092	103.3392
34	361.7426	103.3846	69	361.6623	103.3259	104	361.6209	103.397

Table 3.2: An example of the MSD file created from one image sequence. Only a portion of the file is shown here.

i	gx	gy	gr	gxCalc	gyCalc	grCalc
0	0	0	0	4.78E-03	4.78E-03	9.55E-03
1	0.292361	4.87E-02	0.341017	0.967169	0.967169	1.934339
2	0.425719	5.81E-02	0.48383	1.906026	1.906026	3.812051
3	0.515722	6.77E-02	0.583413	2.827262	2.827262	5.654523
4	0.565729	6.97E-02	0.635455	3.73404	3.73404	7.46808
5	0.620122	7.28E-02	0.692972	4.628308	4.628308	9.256615
6	0.642386	7.75E-02	0.719866	5.511398	5.511398	11.0228
7	0.689937	8.10E-02	0.770959	6.38429	6.38429	12.76858
8	0.716499	8.00E-02	0.796549	7.247747	7.247747	14.49549
9	0.755532	8.15E-02	0.836992	8.10238	8.10238	16.20476
10	0.772625	7.82E-02	0.850851	8.948695	8.948695	17.89739
11	0.790256	0.079241	0.869497	9.78712	9.78712	19.57424
12	0.798108	8.22E-02	0.880331	10.61802	10.61802	21.23605
13	0.808814	0.082326	0.89114	11.44173	11.44173	22.88345
14	0.83342	8.60E-02	0.919398	12.25851	12.25851	24.51702
15	0.826448	8.66E-02	0.913003	13.06863	13.06863	26.13726
16	0.873193	9.02E-02	0.96342	13.87231	13.87231	27.74462
17	0.899003	9.39E-02	0.992915	14.66975	14.66975	29.3395
18	0.935137	9.56E-02	1.030722	15.46115	15.46115	30.92229
19	0.941703	9.52E-02	1.036899	16.24666	16.24666	32.49333
20	0.908154	9.37E-02	1.001848	17.02646	17.02646	34.05292
21	0.899741	9.55E-02	0.995287	17.80068	17.80068	35.60136
22	0.898665	9.76E-02	0.996278	18.56946	18.56946	37.13891
23	0.893185	9.45E-02	0.987728	19.33292	19.33292	38.66584
24	0.876473	9.68E-02	0.973307	20.09118	20.09118	40.18236
25	0.882438	9.61E-02	0.978564	20.84435	20.84435	41.6887
26	0.881541	9.76E-02	0.979153	21.59254	21.59254	43.18507
27	0.865226	0.101343	0.966569	22.33583	22.33583	44.67166
28	0.8798	0.101781	0.981582	23.07432	23.07432	46.14865
29	0.898224	0.104611	1.002835	23.80811	23.80811	47.61621
30	0.903051	0.105444	1.008495	24.53726	24.53726	49.07452
31	0.916402	0.103461	1.019863	25.26186	25.26186	50.52371
32	0.944309	0.107579	1.051888	25.98198	25.98198	51.96396
33	0.947188	0.10876	1.055947	26.69769	26.69769	53.39538
34	0.935973	0.108833	1.044806	27.40906	27.40906	54.81812

Table 3.3: Effects of hCG on CHO cells expressed FLAG-LHR-YFP receptor or co-expressing FLAG-LHR$^{+hCG/-cAMP}$ and HA-LHR$^{-hCG/+cAMP}$ assessed by single particle tracking. Data shown are mean ± SD.

CHO Cell Line	n	[hCG] (nM)	D_{01}* (10^{-10} cm^2sec^{-1})	Domain size* (μm)	Domain Number
FLAG-LHR-YFP wt	10	None	2.70 ± 1.05[a]	0.40 ±0.15[d]	5 ± 2
FLAG-LHR-YFP wt	10	0.1	4.17 ± 2.02[a]	0.50 ±0.13[d]	5 ± 1
FLAG-LHR-YFP wt	10	1	1.89 ± 4.92[b]	0.50 ±0.31[e]	3 ± 1
FLAG-LHR-YFP wt	10	100	1.51 ± 1.20[b]	0.30 ±0.20[e]	2 ± 1
HA-LHR$^{-hCG/+cAMP}$, FLAG-LHR$^{+hCG/-cAMP}$	11	None	8.76 ± 3.97[c]	0.60 ±0.43[f]	5 ± 1
HA-LHR$^{-hCG/+cAMP}$, FLAG-LHR$^{+hCG/-cAMP}$	11	100	2.35 ± 3.42[c]	0.37 ±0.24[f]	3 ± 1

* Values with different superscripts (a,b,c,d,e,f) differ significantly ($p<0.05$).

Table 3.4: Homo-transfer FRET summary of wild type and mutant LH receptors expressed by CHO cells that were either untreated or treated with indicated concentrations of hCG. Data shown are mean ± S.E.M.

Receptor	Ratio of transfection	n	Treatment with hCG	Anisotropy		Differences (Final-Initial)*
				Initial anisotropy	Final anisotropy	
FLAG-LHR-YFP		6	-	0.28	0.29	$0.01 \pm 0.01^{a,b}$
		6	0.1 nM	0.27	0.30	0.03 ± 0.01^{a}
		8	1 nM	0.25	0.29	0.04 ± 0.01^{a}
		8	100 nM	0.22	0.28	0.06 ± 0.01^{a}
FLAG-LHR-YFP, FLAG-$LHR^{+hCG,-cAMP}$	1:1	10	-	0.20	0.30	0.10 ± 0.01^{b}
		10	100 nM	0.17	0.27	0.10 ± 0.01^{b}
	1:2	10	-	0.18	0.27	0.09 ± 0.01^{b}
		10	100 nM	0.16	0.25	0.09 ± 0.01^{b}
	1:3	10	-	0.17	0.26	0.09 ± 0.01^{b}
		10	100 nM	0.13	0.25	0.12 ± 0.01^{b}
FLAG-LHR-YFP, HA-$LHR^{-hCG,+cAMP}$	1:1	10	-	0.26	0.33	0.07 ± 0.01^{b}
		10	100 nM	0.22	0.29	0.07 ± 0.01^{b}
	1:2	10	-	0.22	0.29	0.07 ± 0.01^{b}
		10	100 nM	0.18	0.26	0.08 ± 0.01^{b}
	1:3	10	-	0.23	0.32	0.10 ± 0.01^{b}
		10	100 nM	0.21	0.32	0.11 ± 0.01^{b}

* Values with different superscripts (a,b) differ significantly ($p<0.05$)

Table 3.5: Effects of hCG treatment or MβCD pretreatment on CHO cells expressing wild type receptor FLAG-LHR-YFP or co-expressing $LHR^{+hCG, -cAMP}$ and $LHR^{-hCG,+cAMP}$. Data are shown are the mean ± SD.

Receptors	Transfec-tion Ratio	n	Pretreat-ment with MβCD	Treat-ment with 100 nM hCG	CFP/YFPSE emission ratio*		Ratio after/ before
					Before treatment	After treatment	
FLAG-LHR-YFP	1:1	10	-	+	0.85 ± 0.01^{b}	0.89 ± 0.02^{b}	1.05
		10	+	+	0.84 ± 0.01^{b}	0.88 ± 0.02^{b}	1.04
FLAG-$LHR^{+hCG,-cAMP}$ and HA-$LHR^{-hCG, +cAMP}$	1:1	10	-	+	0.80 ± 0.01^{a}	0.83 ± 0.01^{a}	1.03
	1:1	10	+	+	0.79 ± 0.01^{a}	0.79 ± 0.01^{a}	1.00
FLAG-$LHR^{+hCG, -cAMP}$ and HA-$LHR^{-hCG,+cAMP}$	1:10	10	-	+	0.82 ± 0.01^{a}	0.85 ± 0.01^{a}	1.04
	1:10	10	+	+	0.80 ± 0.01^{a}	0.81 ± 0.01^{a}	1.01

[a,b] Values with different superscripts differ significantly ($p<0.05$)

CHAPTER 4: DISCUSSION

Trans-activation of G protein-coupled receptors was described first for the epidermal growth factor receptor by Daub et al. (72). Subsequent *in vitro* studies by a number of investigators showed that the glycoprotein hormone receptors including LH receptors and FSH receptors could induce signaling via receptor trans-activation (30,32,73,74). Receptor trans-activation had the ability to rescue cAMP signaling despite deficiencies in the two receptors, one deficient in signaling and the other deficient in hormone binding, expressed in cells (30). In fact, Ji et al. (30) demonstrated that a hormone-occupied exodomain could trans-activate an unliganded endodomain on an adjoining receptor using the proposed mechanism shown in **Figure 4.1**. More recently, *in vitro* trans-activation of LH receptor has been demonstrated by Muller et al. (34). This was observed under conditions where a mutant LH receptor that could not initiate signal was co-expressed with an LH mutant receptor that could not bind hormone (75). Importantly, reproductive function in animals was conserved using this mechanism despite the lack of a fully functional LH receptor.

Our data presented here outline the use of biophysical methods, including single particle tracking, homo-transfer FRET and hetero-transfer FRET, by means of which we have evaluated molecular interactions occurring during cis- and trans-activation of luteinizing hormone/chorionic gonadotropin receptors. In this work, we specifically investigated whether cAMP signal increased in hormone-treated cells through cis-activation of wild type receptor and trans-activation of mutant receptors and whether signaling was accompanied by decreased diffusion of LH receptors and receptor aggregation. We found that 100 nM hCG treatment increased cAMP levels in cells expressing the wild type receptor FLAG-LHR-YFP in response

to cis-activation of LH receptor (**Table 3.5**). In addition, cAMP levels in cells expressing a pair of mutant receptors, FLAG-LHR$^{+hCG/-cAMP}$ and HA-LHR$^{-hCG/+cAMP}$, was similarly increased after 100 nM hCG treatment, a process that was dependent on the transfection ratio used to express the receptor pair (**Table 3.5**). Our results agree with previous studies of hormone enhancement of cAMP levels for wild type and mutant LH receptors by Ji and coworkers (30).

Tae Ji's initial description of LH receptor trans-activation used receptors pairs containing receptors with mutations in the leucine-rich repeat domains (LRRs) that introduced ligand binding defects coexpressed in the same cells were receptors containing mutations in exoloop 3 and transmembrane domain 7 that resulted in signaling defects. When co-expressed, these receptor pairs rescued cAMP production via trans-activation (30). The most straightforward explanation for the successful cAMP rescue is that the exodomain of the receptor binds hormone which results in a hormone-exodomain complex which activates the endodomain of a nearby mutant receptor to generate cAMP signal (76). Transgenic mice coexpressing mutant LH receptors where one receptor type was incapable of hormone binding and the other was incapable of inducing signal in the absence of wild type receptors exhibited rescued LH receptor function and induced cAMP signaling. When each mutant receptor was expressed individually in cells, there was no cAMP signal generation. Thus coexpressing two mutant receptors rescued cAMP signal by intermolecular activation, trans-activation, of the mutant receptors (75). Transactivation of a glycoprotein hormone receptor has also been demonstrated for the FSH receptor and, like LH receptors, involved co-expression of two different defective receptors, a non-binding mutant with intact signal generation, and another mutant that cannot generate signal but can bind hormone (32).

Studies of interactions between LH receptors tagged with fluorescent proteins as donor or acceptor showed evidence of inter-receptor interactions (42). Homo-FRET methods have been used to evaluate aggregation of LH receptor both by measuring absolute receptor anisotropies and by examining photobleaching-induced differences in emission anisotropy. Receptor hetero-dimerization has been invoked to explain trans-activation of the receptor from several studies (75). In one study, the Authors showed that activation occurs between a G-protein bound to the cytoplasmic tail of the inactive receptor and the intracellular domain of the active receptor, a process that could only be explained by dimerization of these receptors when one is active and the other is not (77).

Homo-FRET was used to evaluate interactions between either wild type FLAG-LHR-YFP receptors, between FLAG-LHR-YFP and FLAG-LHR$^{+hCG/-cAMP}$, or between FLAG-LHR-YFP and HA-LHR$^{-hCG/+cAMP}$ receptors (**Table 3.4**). We show that hormone-treated wild type receptors exhibit a high degree of aggregation in comparison with untreated LH receptors and that aggregation of wild type receptor when co-expressed with either mutant receptor increased in response to an increase in the ratio of receptor transfection. This observation means that trans-activation is dependent on the ratio of mutant receptors as indicated in cAMP results.

These data agree with a previous study showing increased aggregation of LH receptors following increases in hormone concentration (43). Earlier studies by electron microscopy showed small groups of LH receptors on the cell surface of luteal cells after exposure of cells to high concentrations of LH (78). Horvat et al. have measured FRET between FITC- and TrITC-derivatized hCG hormone bound to LH receptors (79). Bioluminescence resonance energy transfer, BRET, which is sensitive to the distance and orientation between the donor and

acceptor has been used to assess aggregation or dimerization of LH receptors (80). High order oligomers have been shown by homo-FRET for the GPCR serotonin 1A receptor. In this system the initial anisotropy was reduced following receptor stimulation by its ligand, serotonin, in comparison with untreated receptors (39).

Increased differences between receptor final and initial fluorescence anisotropy values (**Table 3.4**) were accompanied by decreases in the diffusion coefficient of LH receptor following hormone treatment of either wild type receptor FLAG-LHR-YFP or mutant receptors FLAG LHR$^{+hCG/-cAMP}$ and HA-LHR$^{-hCG/+cAMP}$. A previous study by Smith et al. has shown that binding of high concentrations of hCG to rat LH receptors leads to redistribution of LH receptors to cholesterol-rich membrane domains, that is, lipid rafts (51). Rat LH receptors became aggregated and raft-associated following treatment with LH or hCG (81).

Unlike methods used in previous studies, single particle tracking (SPT) techniques measure the diffusion coefficient of individual LH receptors rather than that of a large population of receptors. This allows us to analyze specific subpopulation of receptors that have specific diffusion properties (82). Our data (**Table 3.3**) show that the average receptor diffusion coefficient following 100 nM hCG treatment, a concentration sufficient to saturate available LH receptors, for wild type receptors expressed on CHO cells or wild type receptors coexpressed with mutant receptors was about $10^{-11}cm^2s^{-1}$. Following hormone treatment, the domain size and the number of domains were decreased for both FLAG-LHR-YFP wt and for mutant receptors FLAG-LHR$^{+hCG/-cAMP}$ and HA-LHR$^{-hCG/+cAMP}$. This agrees with previous studies of lateral diffusion of individual LH receptors where the average diffusion coefficient was reduced to about $10^{-12}cm^2s^{-1}$ following hormone treatment (82).

Using SPT, we also observed a decrease in the receptor diffusion coefficient in response to increasing hCG concentrations for both wild type and mutant receptors. This decrease in receptor lateral diffusion was accompanied by a corresponding increase in intracellular cAMP for hCG-treated wild type receptors and for mutant receptors when the transfection ratio was increased from 1:1 to 1:10. This suggests that trans-activation between $LHR^{+hCG/-cAMP}$ and $LHR^{-hCG/+cAMP}$ receptors depends on the expression ratio of these receptors. A single hormone-binding mutant needs access to multiple copies of the hormone-binding, signaling-deficient mutant for successful interactions and signaling. This agrees with previous measurements of diffusion coefficients of LH receptors on M17 neuroblastoma cells and levels of intracellular cAMP following hormone treatment when the activation of LH receptors resulted in decreased diffusion coefficients and increased levels of cAMP signal (82).

A variety of techniques have been used to examine the relationship between functional LH receptor and the environment of LH receptors membrane during cell signaling. One of these methods required isolation of membrane microdomains that "float" in sucrose gradients. Receptors such as epidermal growth factor receptor, a plasma membrane receptor, are found in membrane rafts during signal transduction (83) and these membrane rafts have high concentrations of proteins necessary for signal transduction such as G-proteins (84). In this work we used ICUE3 as an indicator of cAMP levels and measured cAMP levels following depletion of membrane cholesterol using MβCD for CHO cells expressing wild type receptor FLAG-LHR-YFP and co-expressing mutant receptors FLAG-$LHR^{+hCG/-cAMP}$ and HA-$LHR^{-hCG/+cAMP}$ with transfection ratios of 1:1 and 1:10. These experiments were designed to assess the importance of membrane cholesterol in signal transduction (**Table 3.5**). We found that there is a decrease in cAMP levels in cells expressing wild type receptors after pretreatment

with MβCD and exposure to 100 nM hCG. When cells expressed mutant receptors arising from a transfection ratio of 1:1, the cAMP level was slightly decreased. Increasing the transfection ratio to 1:10 for mutant receptors and pre-treating with MβCD caused further decreases in intracellular cAMP.

The mechanism for this effect is not known. Preincubation of LH receptor with MβCD to extract cholesterol from the plasma membrane is presumed to disrupt membrane rafts which work as signalplatforms and thus reduce cell signaling by the receptor in response to hormone treatment, Interestingly, direct interaction with cholesterol and protein α-helices has been shown for β_2-adrenergic receptor. One possible role of cholesterol could be to force receptors to specific membrane regions where interactions with signaling components occurs (85). The luteinizing hormone receptor (LH) has been shown to assemble in small membrane microdomains which are rich in cholesterol when the receptor is active, i.e. has bound ligand, which increases the molecular weight of the complex (79). The disruption of these lipid rafts using MβCD decreases the signal produced by liganded receptors (86). Diffusion coefficients for the LH receptor also decrease with hCG treatment (86) which agrees with our results for wild type receptors and mutant receptors where diffusion coefficient decrease and cAMP levels increased following hormone treatment. These observations suggest that inducing cAMP signaling requires functional LH receptors that are located in membrane rafts as dimers or high oligomers.

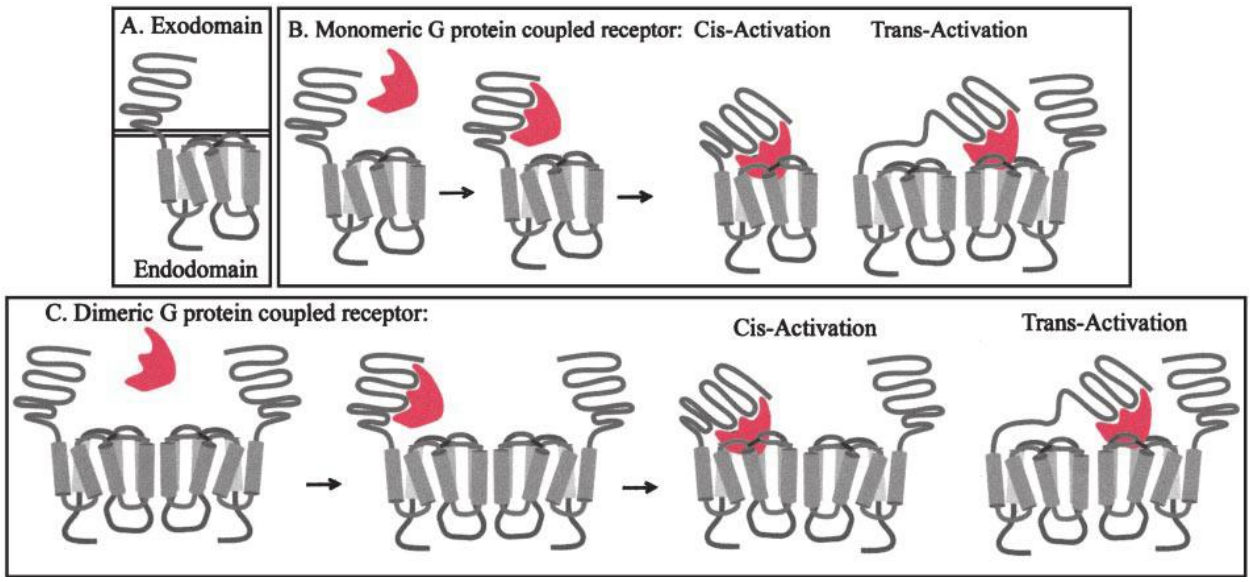

Figure. 4.1. Proposed models of monomeric and dimeric cis-activation and trans-activation. Panel A shows the domain structure of LHR, including an exo-domain where the ligand binds and an endo-domain where the hormone signal is generated. Panel B shows cis- and trans-activation of monomeric LHRs. The ligand is shown in red. Panel C shows cis- and trans-activation of dimeric LHRs. In trans-activation, the receptor dimer is formed by a hormone-occupied receptor which interacts with an unliganded receptor to initiate signal transduction (32).

CHAPTER 5: CONCLUSIONS AND FUTURE DIRECTIONS

Functional LH receptors play an important role in reproductive function in females by enhancing ovulation and follicle maturation. In this study, we demonstrated evidence of dimerization and/or oligomerization of LH receptors involved in trans-activation. Our results suggest that, in addition to cis-activation of wild type receptor, trans-activation also occurs for mutant receptors where a receptor that cannot bind hormone is able to initiate signal when co-expressed with wild type receptors or mutant receptors that can bind hormone but cannot generate signal. Our single particle tracking study shows a hormone-induced decrease in lateral diffusion of individual wild type receptors involved in cis-activation and of mutant receptors activated via trans-activation.

Further study of trans-activating LH receptor pairs could include an examination of HA-LHR$^{-hCG/+cAMP}$ lateral dynamics before and after hormone treatment when expressed together with FLAG-LHR$^{+hCG/-cAMP}$. These studies would be performed by single particle tracking of LH receptors on CHO cells co-expressing FLAG-LHR$^{+hCG/-cAMP}$ and HA-LHR$^{-hCG/+cAMP}$, treated with hCG and labeled with anti-HA-biotin antibody for 30 min, washed and labeled with QD 605-streptavidin. Images would be collected on a Zeiss Axiovert 200M fluorescence microscopy using a 63x 1.2 NA water objective and Qd605 filter set. We would expect to see decreased receptor diffusion coefficients, domain size and the number of domains occupied by HA-LHR$^{-hCG/+cAMP}$ if trans-activation by FLAG-LHR$^{+hCG/-cAMP}$ occurs.

We are also interested in the role of the cytoskeleton in transactivation of LH receptors. A previous study of the lateral diffusion of LH receptor indicates that intact actin filaments may be needed for decreasing lateral motions of LH receptors in response to hormone (43). It would be of interest to image actin filaments using fluorophore-tagged actin, for the same cell population,

and evaluate single particle tracking of cis- and trans-activated LH receptors. CHO cells expressing either wild type LH or trans-activating LH receptor pairs would be treated with cytochalasin D to disrupt the actin filaments prior to hCG treatment. We would expect to see an increase in the diffusion coefficient, domain size and number of domains for cis-activated wild type receptors. It would be of interest to know whether one or both members of the trans-activating receptor pair behave similarly to wild type LH receptors when microfilament structures are disrupted.

Previous studies have shown that LH receptors can exist as monomers as well as forming dimers or high order oligomers. Our FRET study of wild type LH receptors demonstrates self-association or aggregation of LH receptors in response to cis-activation following hormone treatment. The demonstration of LH mutant receptor dimerization/oligomerization resulting from the interaction between receptors suggests that the LH receptor can aggregate in the course of receptor trans-activation. A future experiment would be using acceptor photobleaching FRET (hetero-FRET) to evaluate whether binding of hormone hCG to wild type FLAG-LHR-YFP or FLAG-LHR$^{+hCG/-cAMP}$ is accompanied by interactions with HA-LHR$^{-hCG/+cAMP}$. This experiment would evaluate FRET between receptors with a fluorescence donor such as CFP or a fluorescence acceptor such as YFP by measuring the intensity of the fluorescence donor in the presence and absence of a fluorescence acceptor. CHO cells co-expressing FLAG-LHR-YFP and FLAG-LHR$^{+hCG/-cAMP}$-CFP or FLAG-LHR-YFP and HA-LHR$^{-hCG/+cAMP}$-CFP would be examined using an as described previously. CFP and YFP would be imaged separately and YFP would then be irreversibly photobleached for five minutes. After photobleaching, CFP and YFP would be imaged again. The intensity of CFP signal after (I_{after}) and before YFP photobleaching (I_{before}) would then used to evaluate energy transfer efficiency (%E). Energy transfer efficiency

could be calculated as $(1-I_{before}/I_{after})x100$. We would expect to see an increase in hetero-FRET efficiency resulting from receptor-receptor interactions between trans-activating receptor pairs and between wild type receptors if HA-LHR$^{-hCG/+cAMP}$ is trans-activated following binding of hCG to wild type receptors LHR$^{+hCG/+cAMP}$. We would then use ICUE3 to determine whether LH receptor trans-activation has produced increased cell signaling. These experiments would need to take into account our observation in this project that trans-activation of mutant LH receptors is dependent on the ratio of mutant receptors and requires an excess of the "hormone binding, non-signaling" receptor.

Lastly, cholesterol depletion of LH receptor resulted in a decrease in hormone-induced cAMP levels. Hence we conclude that cholesterol is important for signal transduction by LH receptor. We could perform single particle tracking studies as a future experiment for CHO cells expressing FLAG-LHR-YFP wt or co-expressing HA-LHR$^{-hCG/+cAMP}$ and FLAG- LHR$^{+hCG/-cAMP}$ after cholesterol depletion using 10 mM MβCD at 37°C for 1 hour to evaluate the interactions between receptors and confinement in small membrane microdomains in cholesterol-depleted cell membranes. We would expect to see faster receptor diffusion and disruption of membrane microdomains with cholesterol depletion.

In conclusion, these experiments have provided a better understanding of cis- and trans-activation of the LH receptor in response to hCG. Such understanding of the mechanisms involved in signaling by functional LH receptors or, more generally GPCR, will be helpful in designing drug treatments for diseases where modulation of receptor-mediated signal generation is required.

REFERENCES

1. Dufau ML. The luteinizing hormone receptor. Annual Review of Physiology 1998; 60:461-496

2. Misrahi M, Beau I, Meduri G, Bouvattier C, Atger M, Loosfelt H, Ghinea N, Hai MV, Bougneres PF, Milgrom E. Gonadotropin receptors and the control of gonadal steroidogenesis: physiology and pathology. Baillieres Clin Endocrinol Metab 1998; 12:35-66

3. Segaloff DL, Ascoli M. The lutropin/choriogonadotropin receptor...4 years later. Endocrine Reviews 1993; 14:324-347

4. Karges B, Gidenne S, Chantal A, Haddad F, Kelly P, Milgrom E, N dR. Zero-length cross-linking reveals that tight interactions between the extracellular and transmembrane domains of the luteinizing hormone receptor persist during receptor activation. Molecular Endocrinology 2005; 19:2086-2098

5. Vassart G, Pardo L, Costagliola S. A molecular dissection of the glycoprotein hormone receptors. TRENDS in Biochemical Sciences 2004; 29:119-126

6. Gether U. Uncovering molecular mechanisms involved in activation of G protein-coupled receptors. Endocrine Reviews 2000; 21:90-113

7. Szidonya L, Cserző M, Hunyady L. Dimerization and oligomerization of G-protein-coupled receptors: debated structures with established and emerging functions. Journal of Endocrinology 2008; 196:435-453

8. Shoichet BK, Kobilka BK. Structure-based drug screening for G-protein-coupled receptors. Trends in Pharmacological Sciences 2012; 33:268-272

9. Bjarnadóttir TK, Gloriam DE, Hellstrand SH, Kristiansson H, Fredriksson R, Schiöth HB. Comprehensive repertoire and phylogenetic analysis of the G protein-coupled receptors in human and mouse. Genomics 2006; 88:263-273

10. Palczewski K, Kumasaka T, Hori T, Behnke CA, Motoshima H, Fox BA, Le Trong I, Teller DC, Okada T, Stenkamp RE. Crystal structure of rhodopsin: AG protein-coupled receptor. science 2000; 289:739-745

11. Rosenbaum DM, Cherezov V, Hanson MA, Rasmussen SG, Thian FS, Kobilka TS, Choi H-J, Yao X-J, Weis WI, Stevens RC. GPCR engineering yields high-resolution structural insights into β2-adrenergic receptor function. science 2007; 318:1266-1273

12. Xu F, Wu H, Katritch V, Han GW, Jacobson KA, Gao Z-G, Cherezov V, Stevens RC. Structure of an agonist-bound human A2A adenosine receptor. Science 2011; 332:322-327

13. McFarland K, Sprengel R, Phillips HS, Kohler M, Rosemblit N, Nikolics K, Segaloff DL, Seeburg PH. Lutropin-choriogonadotropin receptor: an unusual member of the G protein-coupled receptor family. Science 1989; 245:494-499

14. Pierce JG, Parsons TF. Glycoprotein hormones: structure and function. Annual review of biochemistry 1981; 50:465-495

15. Bousfield GR, Butnev VY, Gotschall RR, Baker VL, Moore WT. Structural features of mammalian gonadotropins. Molecular and Cellular Endocrinology 1996; 125:3-19

16. Wu H, Lustbader JW, Liu Y, Canfield RE, Hendrickson WA. Structure of human chorionic gonadotropin at 2.6 Å resolution from MAD analysis of the selenomethionyl protein. Structure 1994; 2:545-558

17. Cole LA. hCG, five independent molecules. Clinica chimica acta 2012; 413:48-65

18. Lapthorn A, Harris D, Littlejohn A, Lustbader J, Canfield R, Machin K, Morgan F, Isaacs N. Crystal structure of human chorionic gonadotropin. Nature 1994; 369:455

19. Ascoli M, Fanelli F, Segaloff D. The lutropin/choriogonadotropin receptor, a 2002 perspective. Endocrine Reviews 2002; 23:141-174

20. Moyle W, Lin W, Myers R, Cao D, Kerrigan J, Bernard M. Models of glycoprotein hormone receptor interaction. Endocrine 2005; 26:189-206

21. Shenker A, Laue L, Kosugi S, Merendino Jr JJ, Minegishi T, Cutler Jr GB. Aconstitutively activating mutation of the luteinizing hormone receptor in familial male precocious puberty. Nature 1993; 365:652-654

22. Ji I, Tae JH. Exons 1-10 of the rat lh receptor encode a hidh affinity hormone binding site and exon 11 encodes G-protein modulation and a potential binding site. Endocrinology 1991; 128:2648-2650

23. Tsai-Morris CH, Buczko E, Wang W, Xie S-Z, Dufau ML. Structural organization of the rat luteinizing hormone (LH) receptor gene. Journal of Biological Chemistry 1991; 266:11355-11359

24. Minegish T, Nakamura K, Takakura Y, Miyamoto K, Hasegawa Y, Ibuki Y, Igarashi M. Cloning and sequencing of human LHhCG receptor cDNA. Biochemical and biophysical research communications 1990; 172:1049-1054

25. Dufau M, Minegishi T, Buczko E, Delgado C, Zhang R. Characterization and structure of ovarian and testicular LH/hCG receptors. Journal of Steroid Biochemistry 1989; 33:715-720

26. Shenker A. Activating mutations of the lutropin choriogonadotropin receptor in precocious puberty. Receptors and Channels 2002; 8:3-18

27. Gudermann T, Birnbaumer M, Birnbaumer L. Evidence for dual coupling of the murine luteinizing hormone receptor to adenylyl cyclase and phophoinositide breakdown and Ca^{2+} mobilization. Journal of Biological Chemistry 1992; 267:4479-4488

28. Sánchez-Yagüe J, Hipkin RW, Ascoli M. Biochemical properties of the agonist-induced desensitization of the follicle-stimulating hormone and luteinizing hormone/chorionic gonadotropin-responsive adenylyl cyclase in cells expressing the recombinant gonadotropin receptors. Endocrinology 1993; 132:1007-1016

29. Strader CD, Fong TM, Tota MR, Underwood D, Dixon RA. Structure and function of G protein-coupled receptors. Annual review of biochemistry 1994; 63:101-132

30. Ji I, Lee C, Song Y, Conn P, Ji T. *Cis*- and *trans*-activation of hormone receptors: the LH receptor. Molecular Endocrinology 2002; 16:1299-1308

31. Puett D, Li Y, DeMars G, Angelova K, Fanelli F. A functional transmembrane complex: The luteinizing hormone receptor with bound ligand and G protein. Molecular and Cellular Endocrinology 2007; 260-262:126-136

32. Ji I, Lee C, Jeoung M, Koo Y, Sievert GA, Ji TH. Trans-activation of mutant follicle-stimulating hormone receptors selectively generates only one of two hormone signals. Molecular Endocrinology 2004; 18:968-978.

33. Osuga Y, Kudo M, Kaipia A, Kobilka B, Hsueh A. Derivation of Functional Antagonists Using N - Terminal Extracellular Domain of Gonadotropin and Thyrotropin Receptors. Molecular Endocrinology 1997; 11:1659 - 1668

34. Rivero-Muller A, Chou Y-Y, Ji I, Lajic S, Hanyaloglu AC, Jonas K, Rahman N, Ji TH, Huhtaniemi I. Rescue of defective G protein-coupled receptor function in vivo by

intermolecular cooperation. Proceedings of the National Academy of Sciences 2010; 107:2319-2324

35. Ferre S, Casado V, Devi A, Filizola M, Jockers R, Lohse MJ, Milligan G, Pin J-P, Guitart X. G protein-coupled receptor oligomerization revisited: functional and Pharmacological perspectives. Pharmacological Reviews 2014; 66:413-434

36. Kaupmann K, Malitschek B, Schuler V, Heid J, Froestl W, Beck P, Mosbacher J, Bischoff S, Kulik A, Shigemoto R. GABA B-receptor subtypes assemble into functional heteromeric complexes. Nature 1998; 396:683

37. Banères J-L, Parello J. Structure-based analysis of GPCR function: evidence for a novel pentameric assembly between the dimeric leukotriene B4 receptor BLT1 and the G-protein. Journal of molecular biology 2003; 329:815-829

38. Goddard AD, Watts A. Contributions of fluorescence techniques to understanding G protein-coupled receptor dimerisation. Biophysical reviews 2012; 4:291-298

39. Ganguly S, Clayton AHA, Chattopadhyay A. Organization of Higher-Order Oligomers of the Serotonin1A Receptor Explored Utilizing Homo-FRET in Live Cells. Biophysical Journal 2011; 100:361-368

40. El Moustaine D, Granier S, Doumazane E, Scholler P, Rahmeh R, Bron P, Mouillac B, Banères J-L, Rondard P, Pin J-P. Distinct roles of metabotropic glutamate receptor dimerization in agonist activation and G-protein coupling. Proceedings of the National Academy of Sciences 2012:201205838

41. Liang Y, Fotiadis D, Filipek S, Saperstein DA, Palczewski K, Engel A. Organization of the G protein-coupled receptors rhodopsin and opsin in native membranes. Journal of Biological Chemistry 2003; 278:21655-21662

42. Wolf-Ringwall A, Winter P, Roess D, Barisas B.G. Luteinizing Hormone Receptors are Confined in Mesoscale Plasma Membrane Microdomains Throughout Recovery from Receptor Desensitization. Cell Biochemistry and Biophysics 2014; 68:561-569

43. Wolf-Ringwall AL, Winter PW, Liu J, Van Orden AK, Roess DA, Barisas BG. Restricted lateral diffusion of luteinizing hormone receptors in membrane microdomains. Journal of Biological Chemistry 2011; 286:29818-29827

44. Lei Y, Hagen G, Smith S, Liu J, Barisas BG, Roess D. Constitutively-active human LH receptors are self-associated and localized in rafts. Molecular and Cellular Endocrinology 2007; 260-262:65-72

45. Angers S, Salahpour A, Joly E, Hilairet S, Chelsky D, Dennis M, Bouvier M. Detection of ß$_2$-adrenergic receptor dimerization in living cells using bioluminescence resonance energy transfer (BRET). Proc Natl Acad Sci USA 2000; 97, no. 7:3684-3689

46. Oates J, Watts A. Uncovering the intimate relationship between lipids, cholesterol and GPCR activation. Current opinion in structural biology 2011; 21:802-807

47. Burger K, Gimpl G, Fahrenholz F. Regulation of receptor function by cholesterol. Cellular and Molecular Life Sciences CMLS 2000; 57:1577-1592

48. Singh P, Paila YD, Chattopadhyay A. Differential effects of cholesterol and 7-dehydrocholesterol on the ligand binding activity of the hippocampal serotonin1A receptor: Implications in SLOS. Biochemical and Biophysical Research Communications 2007; 358:495-499

49. Hanson MA, Cherezov V, Griffith MT, Roth CB, Jaakola V-P, Chien EY, Velasquez J, Kuhn P, Stevens RC. A specific cholesterol binding site is established by the 2.8 Å structure of the human β2-adrenergic receptor. Structure 2008; 16:897-905

50. Simons K, Ikonen E. Functional rafts in cell membranes. nature 1997; 387:569

51. Smith SML, Lei Y, Liu J, Cahill ME, Hagen GM, Barisas BG, Roess DA. Luteinizing hormone receptors translocate to plasma membrane microdomains after binding of human chorionic gonadotropin. Endocrinology 2006; 147:1789-1795

52. Zheng H, Pearsall EA, Hurst DP, Zhang Y, Chu J, Zhou Y, Reggio PH, Loh HH, Law P-Y. Palmitoylation and membrane cholesterol stabilize μ-opioid receptor homodimerization and G protein coupling. BMC cell biology 2012; 13:6

53. Shen H, Tauzin LJ, Baiyasi R, Wang W, Moringo N, Shuang B, Landes CF. Single Particle Tracking: From Theory to Biophysical Applications. Chemical Reviews 2017; 117:7331-7376

54. Jacobson K, Sheets ED, Simson R. Revisiting the Fluid Mosaic Model of Membranes. Science 1995; 268:1441-1442

55. Bates IR, Hébert B, Luo Y, Liao J, Bachir AI, Kolin DL, Wiseman PW, Hanrahan JW. Membrane Lateral Diffusion and Capture of CFTR within Transient Confinement Zones. Biophysical Journal 2006; 91:1046-1058

56. Saxton MJ. Single-particle tracking: the distribution of diffusion coefficients. Biophysical Journal 1997; 72:1744-1753

57. Daumas F, Destainville N, Millot C, Lopez A, Dean D, Salomé L. Confined diffusion without fences of a G protein coupled receptor as revealed by single particle tracking. Biophysical Journal 2003; 84:356-366

58. Patterson GH, Piston DW, Barisas BG. Förster distances between green fluorescent protein pairs. Analytical Biochemistry 2000; 284:438-440

59. Bader AN, Hofman EG, Voortman J, van Bergen en Henegouwen PMP, Gerritsen HC. Homo-FRET Imaging Enables Quantification of Protein Cluster Sizes with Subcellular Resolution. Biophysical Journal 2009; 97:2613-2622

60. Lidke D, Nagy P, Barisas B, Heintzmann R, Post J, Lidke K, Clayton A, Arndt-Jovin D, Jovin T. Imaging molecular interactions in cells by dynamic and static fluorescence anisotropy (rFLIM and emFRET). Biochemical Society Transactions 2003; 31:1020-1027

61. Rees EJ, Erdelyi M, Schierle GSK, Knight A, Kaminski CF. Elements of image processing in localization microscopy. Journal of Optics 2013; 15:094012

62. DiPilato LM, Zhang J. Fluorescent protein-based biosensors: resolving spatiotemporal dynamics of signaling. Current Opinion in Chemical Biology 2010; 14:37-42

63. Paramonov VM, Mamaeva V, Sahlgren C, Rivero-Müller A. Genetically-encoded tools for cAMP probing and modulation in living systems. Frontiers in Pharmacology 2015; 6:196

64. Segaloff DL, Sprengel R, Nikolics K, Ascoli M. Structure of the lutropin/choriogonadotropin receptor. Recent Progress in Hormone Research 1990; 46:261-303

65. Alberts B, Bray D, Lewis J, Raff M, Roberts K, Watson JD. Molecular biology of the cell. second ed. New York and London: Garland Publishing, Inc.

66. Aye-Han N-N, Zhang J. A Multiparameter Live Cell Imaging Approach to Monitor Cyclic AMP and Protein Kinase A Dynamics in Parallel. In: Zhang J, Ni Q, Newman RHD, eds. Fluorescent Protein-Based Biosensors, Humana Press 2014:207-215.

67. Saxton MJ, Jacobsen K. Single particle tracking: applications to membrane dynamics. 1996;

68. Kusumi A, Sako Y, Yamamoto M. Confined lateral diffusion of membrane receptors as studied by single particle tracking (nanovid microscopy). Effects of calcium-induced differentiation in cultured epithelial cells. Biophysical Journal 1993; 65:2021-2040

69. Chin KV, Yang WL, Ravatn R, Kita T, Reitman E, Vettori D, Cvijic ME, Shin M, Iacono L. Reinventing the wheel of cyclic AMP. Annals of the New York Academy of Sciences 2002; 968:49-64

70. DiPilato L, Cheng X, Zhang J. Fluorescent indicators of cAMP and Epac activation reveal differential dynamics of cAMP signaling within discrete subcellular compartments. PNAS 2004; 101:16513-16518

71. Roess DA, Smith SML. Self-association and raft localization of functional luteinizing hormone receptors. Biology of Reproduction 2003; 69:1765-1770

72. Daub H, Weiss FU, Wallasch C, Ullrich A. Role of transactivation of the EGF receptor in signalling by G-protein-coupled receptors. Nature 1996; 379:557

73. Guan R, Feng X, Wu X, Zhang M, Zhang X, Hebert T, Segaloff D. Bioluminescence resonance energy transfer studies reveal constitutive dimerization of the human lutropin receptor and a lack of correlation between receptor activation and propensity for dimerization. J Biol Chem 2009; 284:7483-7494

74. Urizar E, Montanelli L, Loy T, Bonomi M, Swillens S, Gales C, Bouvier M, Smits G, Vassart G, Costagliola S. Glycoprotein hormone receptors: link between receptor homodimerization and negative cooperativity. The EMBO Journal 2005; 24:1954-1964

75. Rivero-Müller A, Jonas KC, Hanyaloglu AC, Huhtaniemi I. Di/oligomerization of GPCRs—mechanisms and functional significance. Progress in Molecular Biology and Translational Science. Vol 117: Elsevier; 2013:163-185.

76. Lee C, Ji I, Ji TH. Distinct mechanisms of cAMP induction by constitutively activating LH receptor and wild-type LH receptor activated by hCG. Endocrine 2004; 25:111-115

77. Carrillo JJ, Pediani J, Milligan G. Dimers of class AG protein-coupled receptors function via agonist-mediated trans-activation of associated G proteins. Journal of Biological Chemistry 2003; 278:42578-42587

78. Luborsky JL, Slater WT, Behrman HR. Luteinizing hormone (LH) receptor aggregation: Modification of ferritin-LH binding and aggregation by prostaglandin F_{2a} and ferritin-LH. Endocrinology 1984; 115:2217-2226

79. Horvat RD, Barisas BG, Roess DA. Luteinizing hormone receptors are self-associated in slowly diffusing complexes during receptor desensitization. Molecular Endocrinology 2001; 15:534-542

80. Overton MC, Blumer KJ. G-protein-coupled receptors function as oligomers in vivo. Current Biology 2000; 10, no. 6:341-344

81. Horvat RD, Nelson S, Clay CM, Barisas BG, Roess DA. Intrinsically fluorescent luteinizing hormone receptor demonstrates hormone-driven aggregation. Biochem Biophys Res Comm 1999; 255:382-385

82. Wolf Ringwall A, Winter P, Liu J, Van Orden A, Roess D, Barisas BG. Restricted lateral diffusion of luteinizing hormone receptors in membrane microdomains. Journal of Biological Chemistry 2011; 286:29818-29827

83. Harder T, Scheiffele P, Verkade P, Simons K. Lipid domain structure of the plasma membrane revealed by patching of membrane components. Journal of Cell Biology 1998; 141:929-942

84. Harder T, Simons K. Caveolae, DIGs, and the dynamics of sphingolipid-cholesterol microdomains. Current Opinion in Cell Biology 1997; 9, no. 4:534-542

85. Oates J, Watts A. Uncovering the intimate relationship between lipids, cholesterol and GPCR activation. Current Opinion in Structural Biology Proteins/Catalysis and regulation 2011; 21:802-807

86. Smith SM, Lei Y, Liu J, Cahill ME, Hagen GM, Barisas BG, Roess DA. Luteinizing hormone receptors translocate to plasma membrane microdomains after binding of human chorionic gonadotropin. Endocrinology 2006; 147:1789-1795.

APPENDIX I: Data Analysis for Single Particle Tracking

Table A1: Diffusion coefficient of untreated CHO cells expressed FLAG-LHR-YFP (p1)

param	value
g Column=	D
iDim=	2
nPts=	323
iFirstRow=	1
iLastRow=	500
sumWts=	52003.0000
sumWtdResid=	4893.28
chiSq=	0.094096127
SD=	0.306750921
w (pix)=	1.65E+00
D (pix^2/frame)=	2.745011789
m(pix^2/frame)	6.02804754E-04
um per pixel=	16
mag (obj*Extender)=	63
sec per frame=	0.12
w(um)=	0.4190
D01(cm^2/sec)=	3.13E-10
Dhop(cm^2/sec)=	3.24E-12

FUNCTION AkiDisp(w,t,D)
multi-expon approx to 1D diff confined in region of width w
re-derived and checked against early Kusumi paper
accurate to 1:1000 @ t=0
w is width of domain (n cells orig)
t is time (i jumps orig)
D is diffusion coeff
IF D=0 THEN 'diffusion for t steps of length 1 with <r2>in steps^2
Tau=(2*w^2)/(pi^2)
ELSE
Tau=w^2/(pi^2*D)'continuous diffusion for a time t with <r2> in cm2

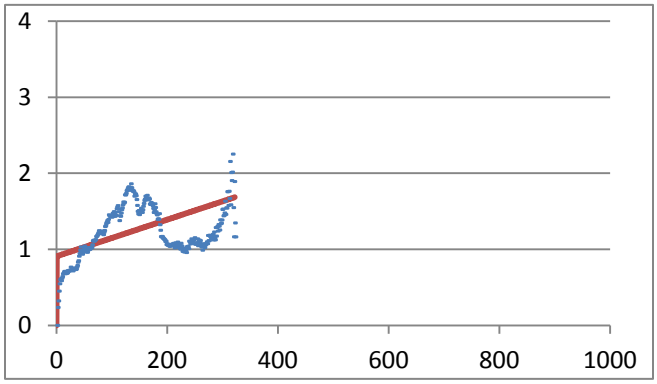

Table A2: Diffusion coefficient of untreated CHO cells expressed FLAG-LHR-YFP (p2)

param	value
g Column=	D
iDim=	2
nPts=	595
iFirstRow=	1
iLastRow=	500
sumWts=	172059.0000
sumWtdResid=	3760.25
chiSq=	0.021854447
SD=	0.147832495
w (pix)=	2.01E+00
D (pix^2/frame)=	0.001848142
m(pix^2/frame)	4.14918404E-05
um per pixel=	16
mag (obj*Extender)=	63
sec per frame=	0.12
w(um)=	0.5093
D01(cm^2/sec)=	2.74E-10
Dhop(cm^2/sec)=	2.23E-13

FUNCTION
AkiDisp(w,t,D)
multi-expon approx to 1D diff confined in region of width w
re-derived and checked against early Kusumi paper
accurate to 1:1000 @ t=0
w is width of domain (n cells orig)
t is time (i jumps orig)
D is diffusion coeff
IF D=0 THEN 'diffusion for t steps of length 1 with <r2>in steps^2
Tau=(2*w^2)/(pi^2)
ELSE
Tau=w^2/(pi^2*D)'continuous diffusion for a time t with <r2> in cm2

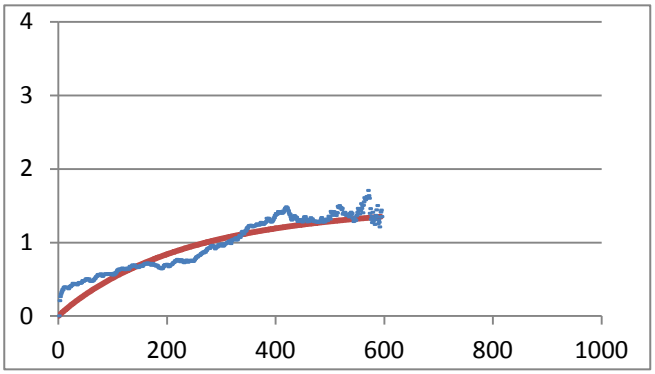

Table A3: Diffusion coefficient of untreated CHO cells expressed FLAG-LHR-YFP (p3)

param	value
g Column=	D
iDim=	2
nPts=	1000
iFirstRow=	1
iLastRow=	500
sumWts=	373749.0000
sumWtdResid=	9798.35
chiSq=	0.026216391
SD=	0.161914764
w (pix)=	1.97E+00
D (pix^2/frame)=	0.008747263
m(pix^2/frame)	2.17977990E-03
um per pixel=	16
mag (obj*Extender)=	63
sec per frame=	0.12
w(um)=	0.4998
D01(cm^2/sec)=	3.50E-10
Dhop(cm^2/sec)=	1.17E-11

FUNCTION
AkiDisp(w,t,D)
multi-expon approx to 1D diff confined in region of width w
re-derived and checked against early Kusumi paper
accurate to 1:1000 @ t=0
w is width of domain (n cells orig)
t is time (i jumps orig)
D is diffusion coeff
IF D=0 THEN 'diffusion for t steps of length 1 with <r2>in steps^2
Tau=(2*w^2)/(pi^2)
ELSE
Tau=w^2/(pi^2*D)'continuous diffusion for a time t with <r2> in cm2

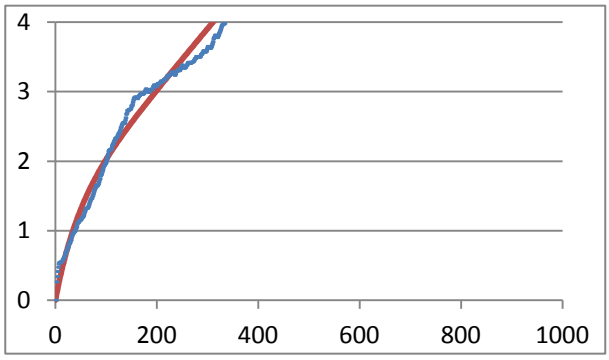

Table A4: Diffusion coefficient of untreated CHO cells expressed FLAG-LHR-YFP (p4)

param	value
g Column=	D
iDim=	2
nPts=	559
iFirstRow=	1
iLastRow=	500
sumWts=	154131.0000
sumWtdResid=	331076.70
chiSq=	2.14802146
SD=	1.465612998
w (pix)=	1.80E+00
D (pix^2/frame)=	7.27914E-07
m(pix^2/frame)	6.77938731E-03
um per pixel=	16
mag (obj*Extender)=	63
sec per frame=	0.12
w(um)=	0.4568
D01(cm^2/sec)=	4.33E-10
Dhop(cm^2/sec)=	3.64E-11

FUNCTION AkiDisp(w,t,D)
multi-expon approx to 1D diff confined in region of width w
re-derived and checked against early Kusumi paper
accurate to 1:1000 @ t=0
w is width of domain (n cells orig)
t is time (i jumps orig)
D is diffusion coeff
IF D=0 THEN 'diffusion for t steps of length 1 with <r2>in steps^2
Tau=(2*w^2)/(pi^2)
ELSE
Tau=w^2/(pi^2*D)'continuous diffusion for a time t with <r2> in cm2

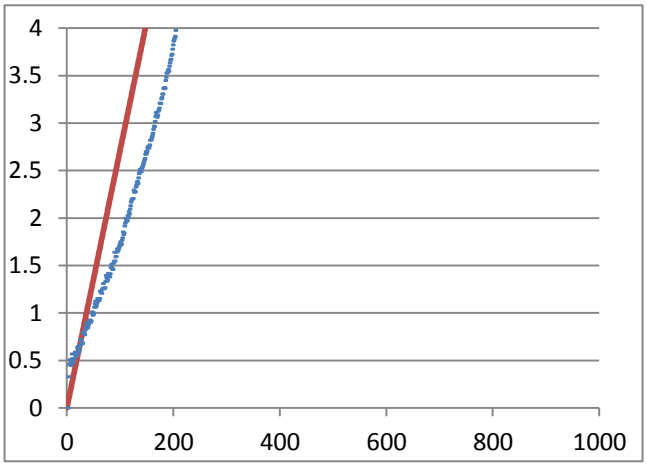

Table A5: Diffusion coefficient of untreated CHO cells expressed FLAG-LHR-YFP (p5)

param	value
g Column=	D
iDim=	2
nPts=	417
iFirstRow=	1
iLastRow=	500
sumWts=	86736.0000
sumWtdResid=	992.06
chiSq=	0.011437651
SD=	0.106946956
w (pix)=	1.35E+00
D (pix^2/frame)=	0.070474342
m(pix^2/frame)	6.18111733E-04
um per pixel=	16
mag (obj*Extender)=	63
sec per frame=	0.0333
w(um)=	0.3421
D01(cm^2/sec)=	3.11E-10
Dhop(cm^2/sec)=	1.20E-11

FUNCTION AkiDisp(w,t,D)
multi-expon approx to 1D diff confined in region of width w
re-derived and checked against early Kusumi paper
accurate to 1:1000 @ t=0
w is width of domain (n cells orig)
t is time (i jumps orig)
D is diffusion coeff
IF D=0 THEN 'diffusion for t steps of length 1 with <r2>in steps^2
Tau=(2*w^2)/(pi^2)
ELSE
Tau=w^2/(pi^2*D)'continuous diffusion for a time t with <r2> in cm2

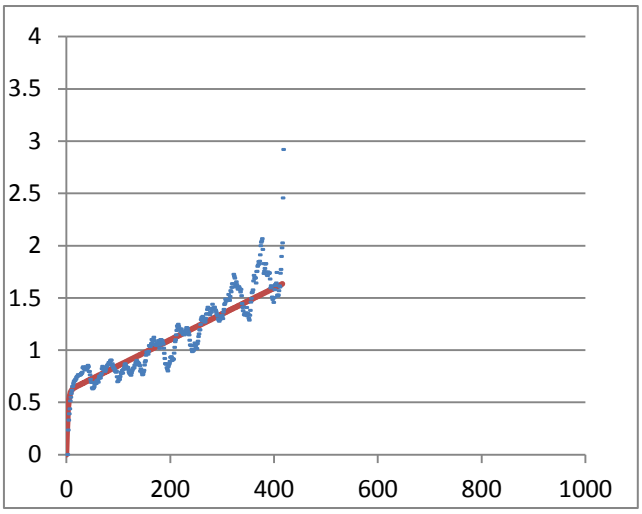

Table A6: Diffusion coefficient of untreated CHO cells expressed FLAG-LHR-YFP (p6)

param	value
g Column=	D
iDim=	2
nPts=	1000
iFirstRow=	1
iLastRow=	500
sumWts=	373749.0000
sumWtdResid=	217.03
chiSq=	0.000580674
SD=	0.024097181
w (pix)=	7.17E-01
D (pix^2/frame)=	0.001808873
m(pix^2/frame)	2.46416691E-04
um per pixel=	16
mag (obj*Extender)=	63
sec per frame=	0.0333
w(um)=	0.1821
D01(cm^2/sec)=	6.89E-11
Dhop(cm^2/sec)=	4.77E-12

FUNCTION AkiDisp(w,t,D)
multi-expon approx to 1D diff confined in region of width w
re-derived and checked against early Kusumi paper
accurate to 1:1000 @ t=0
w is width of domain (n cells orig)
t is time (i jumps orig)
D is diffusion coeff
IF D=0 THEN 'diffusion for t steps of length 1 with <r2>in steps^2
Tau=(2*w^2)/(pi^2)
ELSE
Tau=w^2/(pi^2*D)'continuous diffusion for a time t with <r2> in cm2

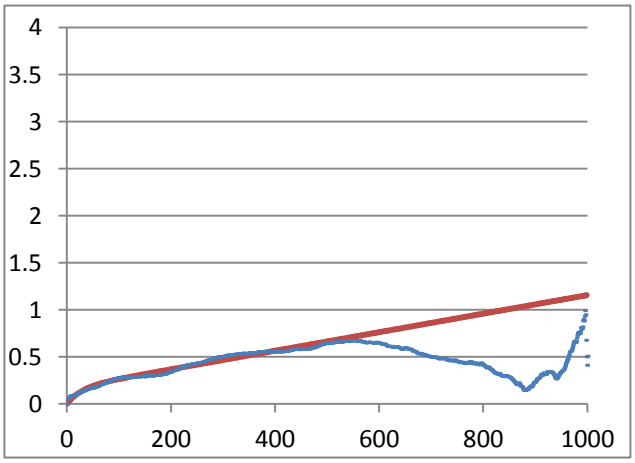

Table A7: Diffusion coefficient of untreated CHO cells expressed FLAG-LHR-YFP (p7)

param	value
g Column=	D
iDim=	2
nPts=	964
iFirstRow=	1
iLastRow=	500
sumWts=	355821.0000
sumWtdResid=	467.98
chiSq=	0.001315205
SD=	0.036265758
w (pix)=	1.08E+00
D (pix^2/frame)=	0.034210944
m(pix^2/frame)	1.28682509E-04
um per pixel=	16
mag (obj*Extender)=	63
sec per frame=	0.0333
w(um)=	0.2749
D01(cm^2/sec)=	2.98E-10
Dhop(cm^2/sec)=	2.49E-12

FUNCTION AkiDisp(w,t,D)
multi-expon approx to 1D diff confined in region of width w
re-derived and checked against early Kusumi paper
accurate to 1:1000 @ t=0
w is width of domain (n cells orig)
t is time (i jumps orig)
D is diffusion coeff
IF D=0 THEN 'diffusion for t steps of length 1 with <r2>in steps^2
Tau=(2*w^2)/(pi^2)
ELSE
Tau=w^2/(pi^2*D)'continuous diffusion for a time t with <r2> in cm2

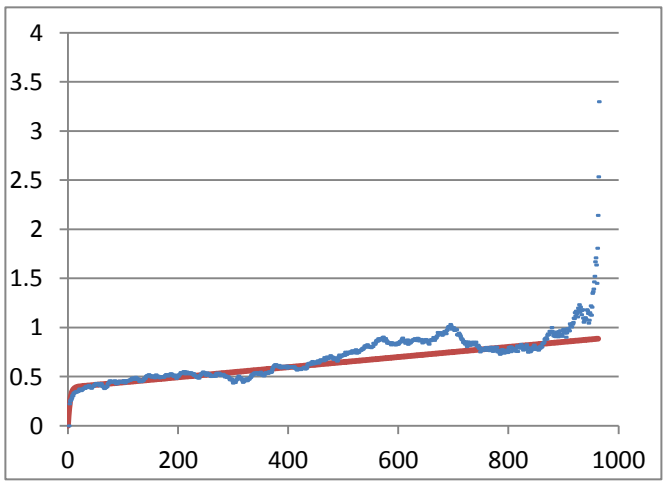

Table A8: Diffusion coefficient of CHO cells expressed FLAG-LHR-YFP and treated with 1nM hCG (p1)

param	value
g Column=	D
iDim=	2
nPts=	750
iFirstRow=	1
iLastRow=	500
sumWts=	249249.0000
sumWtdResid=	105812.69
chiSq=	0.424526031
SD=	0.651556621
w (pix)=	3.70E+00
D (pix^2/frame)=	0.004014622
m(pix^2/frame)	7.18298774E-07
um per pixel=	16
mag (obj*Extender)=	63
sec per frame=	0.12
w(um)=	0.6797
D01(cm^2/sec)=	7.57E-11
Dhop(cm^2/sec)=	3.86E-15

FUNCTION AkiDisp(w,t,D)
multi-expon approx to 1D diff confined in region of width w
re-derived and checked against early Kusumi paper
accurate to 1:1000 @ t=0
w is width of domain (n cells orig)
t is time (i jumps orig)
D is diffusion coeff
IF D=0 THEN 'diffusion for t steps of length 1 with <r2>in steps^2
Tau=(2*w^2)/(pi^2)
ELSE
Tau=w^2/(pi^2*D)'continuous diffusion for a time t with <r2> in cm2

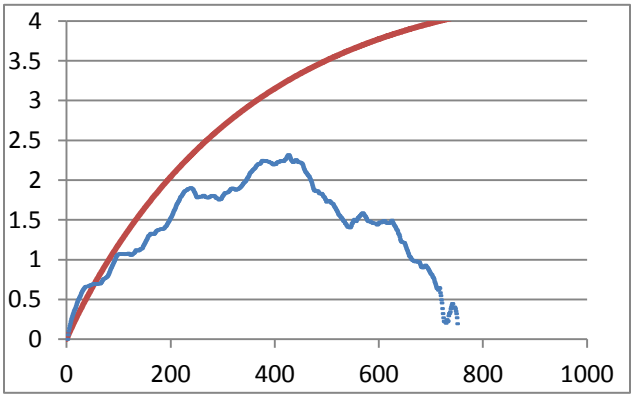

Table A9: Diffusion coefficient of CHO cells expressed FLAG-LHR-YFP and treated with 1nM hCG (p2)

param	value
g Column=	D
iDim=	2
nPts=	750
iFirstRow=	1
iLastRow=	500
sumWts=	249249.0000
sumWtdResid=	210.70
chiSq=	0.000845323
SD=	0.029074434
w (pix)=	3.00E+00
D (pix^2/frame)=	7.18089E-05
m(pix^2/frame)	3.81569709E-05
um per pixel=	16
mag (obj*Extender)=	63
sec per frame=	0.12
w(um)=	0.7619
D01(cm^2/sec)=	2.77E-12
Dhop(cm^2/sec)=	2.05E-13

FUNCTION
AkiDisp(w,t,D)
multi-expon approx to 1D diff confined in region of width w
re-derived and checked against early Kusumi paper
accurate to 1:1000 @ t=0
w is width of domain (n cells orig)
t is time (i jumps orig)
D is diffusion coeff
IF D=0 THEN 'diffusion for t steps of length 1 with <r2>in steps^2
Tau=(2*w^2)/(pi^2)
ELSE
Tau=w^2/(pi^2*D)'continuous diffusion for a time t with <r2> in cm2

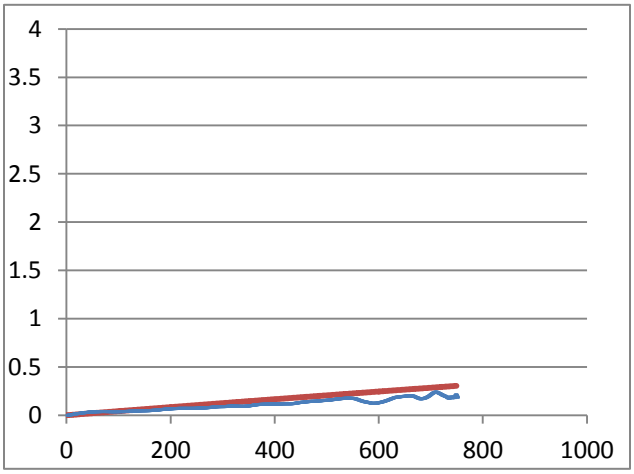

Table A10: Diffusion coefficient of CHO cells expressed FLAG-LHR-YFP and treated with 1nM hCG (p3)

param	value
g Column=	D
iDim=	2
nPts=	750
iFirstRow=	1
iLastRow=	500
sumWts=	249249.0000
sumWtdResid=	10.70
chiSq=	4.29365E-05
SD=	0.006552596
w (pix)=	5.00E-01
D (pix^2/frame)=	0.000343875
m(pix^2/frame)	1.29676594E-05
um per pixel=	16
mag (obj*Extender)=	63
sec per frame=	0.12
w(um)=	0.1270
D01(cm^2/sec)=	7.60E-12
Dhop(cm^2/sec)=	6.97E-14

FUNCTION AkiDisp(w,t,D)
multi-expon approx to 1D diff confined in region of width w
re-derived and checked against early Kusumi paper
accurate to 1:1000 @ t=0
w is width of domain (n cells orig)
t is time (i jumps orig)
D is diffusion coeff
IF D=0 THEN 'diffusion for t steps of length 1 with <r2>in steps^2
Tau=(2*w^2)/(pi^2)
ELSE
Tau=w^2/(pi^2*D)'continuous diffusion for a time t with <r2> in cm2

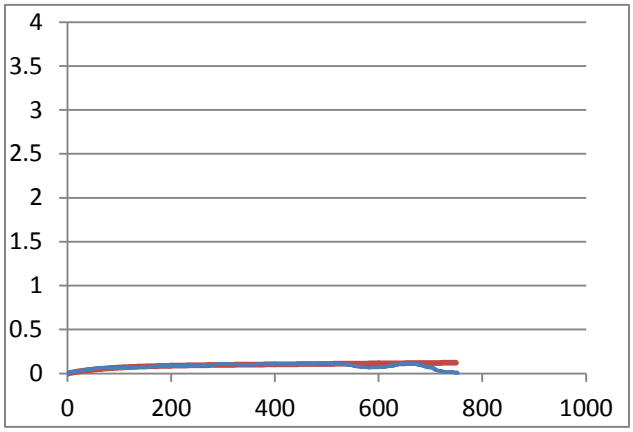

Table A11: Diffusion coefficient of CHO cells expressed FLAG-LHR-YFP and treated with 1nM hCG (p4)

param	value
g Column=	D
iDim=	2
nPts=	120
iFirstRow=	1
iLastRow=	500
sumWts=	52620.0000
sumWtdResid=	2.61
chiSq=	4.96213E-05
SD=	0.007044235
w (pix)=	1.00E+00
D (pix^2/frame)=	0.000376393
m(pix^2/frame)	6.38576225E-05
um per pixel=	16
mag (obj*Extender)=	63
sec per frame=	0.12
w(um)=	0.2540
D01(cm^2/sec)=	1.20E-11
Dhop(cm^2/sec)=	3.43E-13

FUNCTION AkiDisp(w,t,D)
multi-expon approx to 1D diff confined in region of width w
re-derived and checked against early Kusumi paper
accurate to 1:1000 @ t=0
w is width of domain (n cells orig)
t is time (i jumps orig)
D is diffusion coeff
IF D=0 THEN 'diffusion for t steps of length 1 with <r2>in steps^2
Tau=(2*w^2)/(pi^2)
ELSE
Tau=w^2/(pi^2*D)'continuous diffusion for a time t with <r2> in cm2

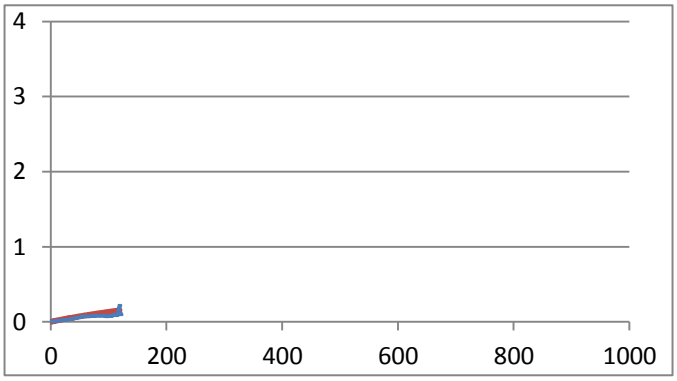

Table A12: Diffusion coefficient of CHO cells expressed FLAG-LHR-YFP and treated with 1nM hCG (p5)

param	value
g Column=	D
iDim=	2
nPts=	145
iFirstRow=	1
iLastRow=	500
sumWts=	10440.0000
sumWtdResid=	15.53
chiSq=	0.001487421
SD=	0.038567092
w (pix)=	4.48E-01
D (pix^2/frame)=	0.047585985
m(pix^2/frame)	3.75191232E-04
um per pixel=	16
mag (obj*Extender)=	63
sec per frame=	0.0333
w(um)=	0.1137
D01(cm^2/sec)=	8.27E-11
Dhop(cm^2/sec)=	7.27E-12

FUNCTION AkiDisp(w,t,D)
multi-expon approx to 1D diff confined in region of width w
re-derived and checked against early Kusumi paper
accurate to 1:1000 @ t=0
w is width of domain (n cells orig)
t is time (i jumps orig)
D is diffusion coeff
IF D=0 THEN 'diffusion for t steps of length 1 with <r2>in steps^2
Tau=(2*w^2)/(pi^2)
ELSE
Tau=w^2/(pi^2*D)'continuous diffusion for a time t with <r2> in cm2

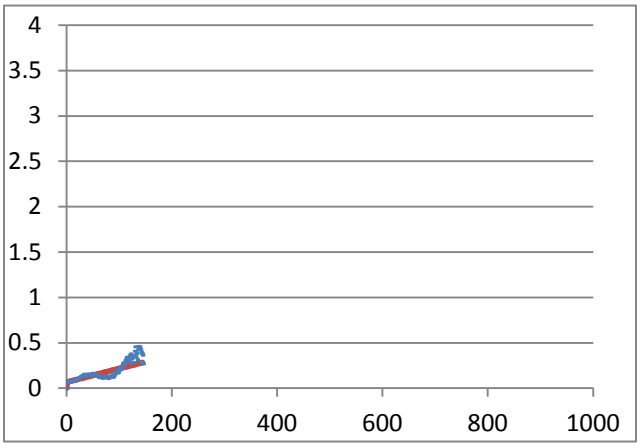

Table A13: Diffusion coefficient of CHO cells expressed FLAG-LHR-YFP and treated with 1nM hCG (p6)

param	value
g Column=	D
iDim=	2
nPts=	138
iFirstRow=	1
iLastRow=	500
sumWts=	9453.0000
sumWtdResid=	1674.03
chiSq=	0.177089349
SD=	0.420819853
w (pix)=	2.88E+00
D (pix^2/frame)=	1.111206291
m(pix^2/frame)	1.02861292E-03
um per pixel=	16
mag (obj*Extender)=	63
sec per frame=	0.12
w(um)=	0.7323
D01(cm^2/sec)=	2.74E-09
Dhop(cm^2/sec)=	5.53E-12

FUNCTION AkiDisp(w,t,D)
multi-expon approx to 1D diff confined in region of width w
re-derived and checked against early Kusumi paper
accurate to 1:1000 @ t=0
w is width of domain (n cells orig)
t is time (i jumps orig)
D is diffusion coeff
IF D=0 THEN 'diffusion for t steps of length 1 with <r2>in steps^2
Tau=(2*w^2)/(pi^2)
ELSE
Tau=w^2/(pi^2*D)'continuous diffusion for a time t with <r2> in cm2

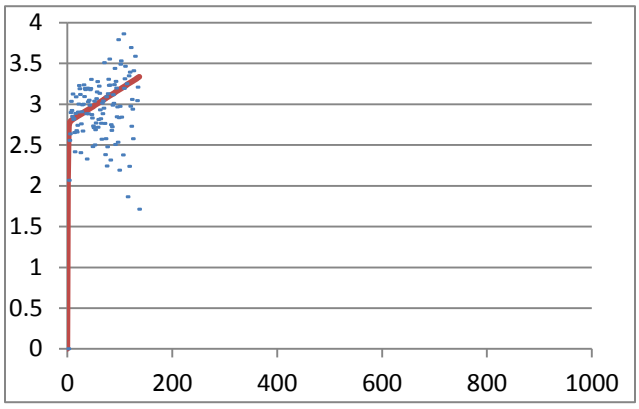

Table A14: Diffusion coefficient of CHO cells expressed FLAG-LHR-YFP and treated with 1nM hCG (p7)

param	value
g Column=	D
iDim=	2
nPts=	750
iFirstRow=	1
iLastRow=	500
sumWts=	249249.0000
sumWtdResid=	4801.58
chiSq=	0.019264205
SD=	0.13879555
w (pix)=	3.00E+00
D (pix^2/frame)=	0.00027471
m(pix^2/frame)	5.46220432E-07
um per pixel=	16
mag (obj*Extender)=	63
sec per frame=	0.12
w(um)=	0.1619
D01(cm^2/sec)=	1.11E-11
Dhop(cm^2/sec)=	2.94E-15

FUNCTION AkiDisp(w,t,D)
multi-expon approx to 1D diff confined in region of width w
re-derived and checked against early Kusumi paper
accurate to 1:1000 @ t=0
w is width of domain (n cells orig)
t is time (i jumps orig)
D is diffusion coeff
IF D=0 THEN 'diffusion for t steps of length 1 with <r2>in steps^2
Tau=(2*w^2)/(pi^2)
ELSE
Tau=w^2/(pi^2*D)'continuous diffusion for a time t with <r2> in cm2

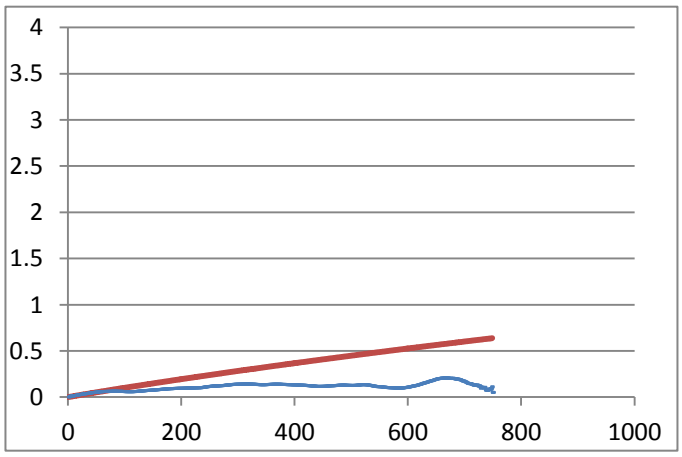

Table A15: Diffusion coefficient of CHO cells expressed FLAG-LHR-YFP and treated with 0.1nM hCG (p1)

param	value
g Column=	D
iDim=	2
nPts=	418
iFirstRow=	1
iLastRow=	500
sumWts=	87153.0000
sumWtdResid=	6888.47
chiSq=	0.079038871
SD=	0.281138527
w (pix)=	1.35E+00
D (pix^2/frame)=	5.76964E-07
m(pix^2/frame)	3.24127888E-03
um per pixel=	16
mag (obj*Extender)=	63
sec per frame=	0.12
w(um)=	0.3437
D01(cm^2/sec)=	2.20E-10
Dhop(cm^2/sec)=	1.74E-11

FUNCTION AkiDisp(w,t,D)
multi-expon approx to 1D diff confined in region of width w
re-derived and checked against early Kusumi paper
accurate to 1:1000 @ t=0
w is width of domain (n cells orig)
t is time (i jumps orig)
D is diffusion coeff
IF D=0 THEN 'diffusion for t steps of length 1 with <r2>in steps^2
Tau=(2*w^2)/(pi^2)
ELSE
Tau=w^2/(pi^2*D)'continuous diffusion for a time t with <r2> in cm2

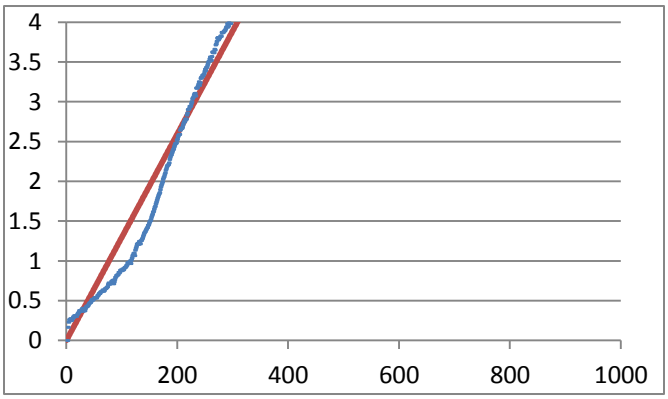

Table A16: Diffusion coefficient of CHO cells expressed FLAG-LHR-YFP and treated with 0.1nM hCG (p2)

param	value
g Column=	D
iDim=	2
nPts=	183
iFirstRow=	1
iLastRow=	500
sumWts=	16653.0000
sumWtdResid=	726.88
chiSq=	0.043648649
SD=	0.208922592
w (pix)=	1.30E+00
D (pix^2/frame)=	0.095737255
m(pix^2/frame)	2.60947081E-03
um per pixel=	16
mag (obj*Extender)=	63
sec per frame=	0.12
w(um)=	0.3302
D01(cm^2/sec)=	3.08E-10
Dhop(cm^2/sec)=	1.40E-11

FUNCTION AkiDisp(w,t,D)
multi-expon approx to 1D diff confined in region of width w
re-derived and checked against early Kusumi paper
accurate to 1:1000 @ t=0
w is width of domain (n cells orig)
t is time (i jumps orig)
D is diffusion coeff
IF D=0 THEN 'diffusion for t steps of length 1 with <r2>in steps^2
Tau=(2*w^2)/(pi^2)
ELSE
Tau=w^2/(pi^2*D)'continuous diffusion for a time t with <r2> in cm2

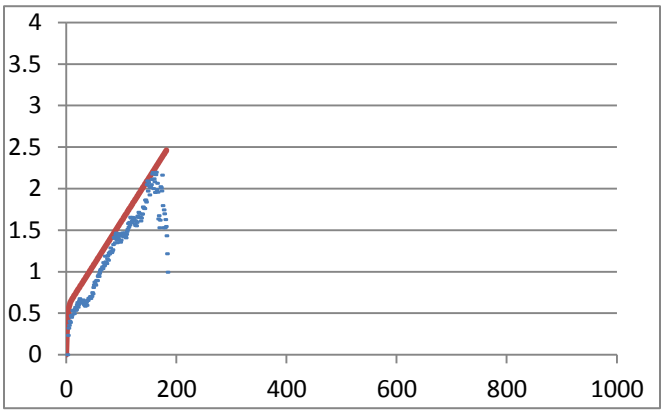

Table A17: Diffusion coefficient of CHO cells expressed FLAG-LHR-YFP and treated with 0.1nM hCG (p3)

param	value
g Column=	D
iDim=	2
nPts=	210
iFirstRow=	1
iLastRow=	500
sumWts=	21945.0000
sumWtdResid=	1340.83
chiSq=	0.061099749
SD=	0.247183635
w (pix)=	1.50E+00
D (pix^2/frame)=	0.407616657
m(pix^2/frame)	8.47554682E-04
um per pixel=	16
mag (obj*Extender)=	63
sec per frame=	0.0333
w(um)=	0.3810
D01(cm^2/sec)=	6.59E-10
Dhop(cm^2/sec)=	1.64E-11

FUNCTION
AkiDisp(w,t,D)
multi-expon approx to 1D diff confined in region of width w
re-derived and checked against early Kusumi paper
accurate to 1:1000 @ t=0
w is width of domain (n cells orig)
t is time (i jumps orig)
D is diffusion coeff
IF D=0 THEN 'diffusion for t steps of length 1 with <r2>in steps^2
Tau=(2*w^2)/(pi^2)
ELSE
Tau=w^2/(pi^2*D)'continuous diffusion for a time t with <r2> in cm2

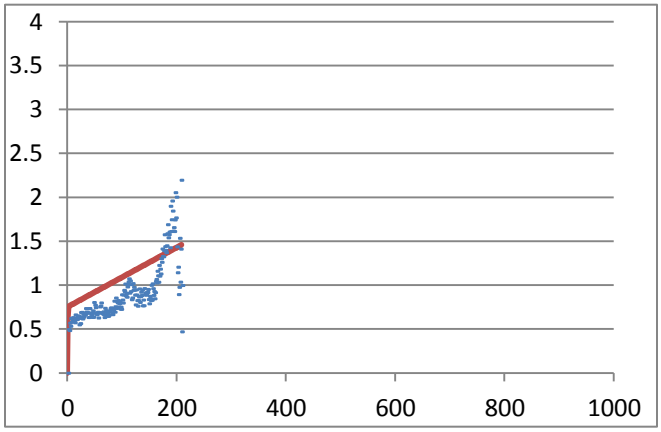

Table A18: Diffusion coefficient of CHO cells expressed FLAG-LHR-YFP and treated with 0.1nM hCG (p4)

param	value
g Column=	D
iDim=	2
nPts=	903
iFirstRow=	1
iLastRow=	500
sumWts=	325443.0000
sumWtdResid=	5718.53
chiSq=	0.017571528
SD=	0.132557641
w (pix)=	1.93E+00
D (pix^2/frame)=	0.00530133
m(pix^2/frame)	1.01467117E-04
um per pixel=	16
mag (obj*Extender)=	63
sec per frame=	0.12
w(um)=	0.4895
D01(cm^2/sec)=	7.79E-10
Dhop(cm^2/sec)=	5.45E-13

FUNCTION
AkiDisp(w,t,D)
multi-expon approx to 1D diff confined in region of width w
re-derived and checked against early Kusumi paper
accurate to 1:1000 @ t=0
w is width of domain (n cells orig)
t is time (i jumps orig)
D is diffusion coeff
IF D=0 THEN 'diffusion for t steps of length 1 with <r2>in steps^2
Tau=(2*w^2)/(pi^2)
ELSE
Tau=w^2/(pi^2*D)'continuous diffusion for a time t with <r2> in cm2

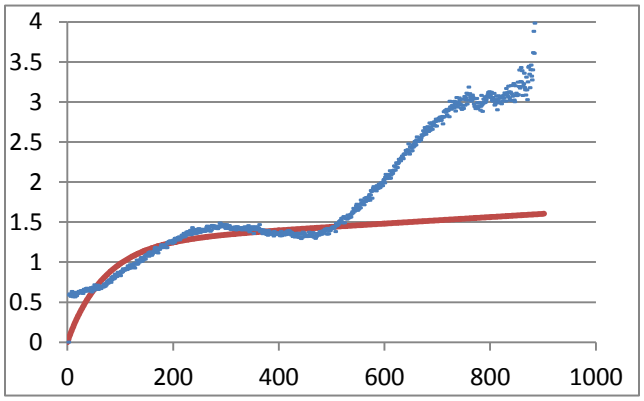

Table A19: Diffusion coefficient of CHO cells expressed FLAG-LHR-YFP and treated with 0.1nM hCG (p5)

param	value
g Column=	D
iDim=	2
nPts=	750
iFirstRow=	1
iLastRow=	500
sumWts=	249249.0000
sumWtdResid=	1023.89
chiSq=	0.004107898
SD=	0.064092884
w (pix)=	3.00E+00
D (pix^2/frame)=	0.000283191
m(pix^2/frame)	1.33444733E-04
um per pixel=	16
mag (obj*Extender)=	63
sec per frame=	0.12
w(um)=	0.7619
D01(cm^2/sec)=	3.63E-11
Dhop(cm^2/sec)=	7.17E-13

FUNCTION AkiDisp(w,t,D)
multi-expon approx to 1D diff confined in region of width w
re-derived and checked against early Kusumi paper
accurate to 1:1000 @ t=0
w is width of domain (n cells orig)
t is time (i jumps orig)
D is diffusion coeff
IF D=0 THEN 'diffusion for t steps of length 1 with <r2>in steps^2
Tau=(2*w^2)/(pi^2)
ELSE
Tau=w^2/(pi^2*D)'continuous diffusion for a time t with <r2> in cm2

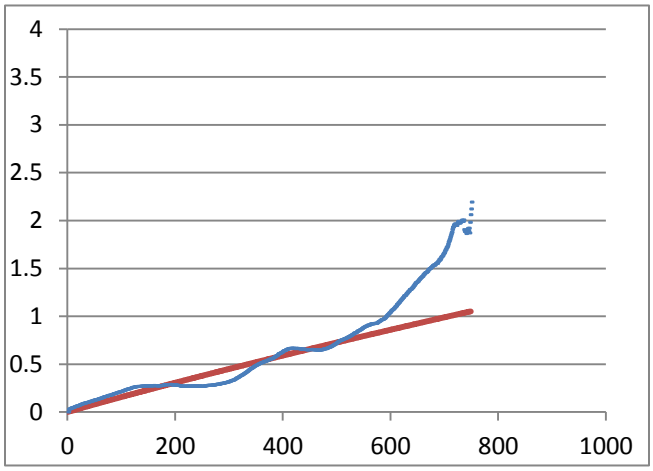

Table A20: Diffusion coefficient of CHO cells expressed FLAG-LHR-YFP and treated with 0.1nM hCG (p6)

param	value
g Column=	D
iDim=	2
nPts=	367
iFirstRow=	1
iLastRow=	500
sumWts=	67161.0000
sumWtdResid=	11310.30
chiSq=	0.168405747
SD=	0.410372692
w (pix)=	2.00E+00
D (pix^2/frame)=	0.018243018
m(pix^2/frame)	1.77447436E-07
um per pixel=	16
mag (obj*Extender)=	63
sec per frame=	0.12
w(um)=	0.5079
D01(cm^2/sec)=	2.52E-10
Dhop(cm^2/sec)=	9.54E-16

FUNCTION AkiDisp(w,t,D)
multi-expon approx to 1D diff confined in region of width w
re-derived and checked against early Kusumi paper
accurate to 1:1000 @ t=0
w is width of domain (n cells orig)
t is time (i jumps orig)
D is diffusion coeff
IF D=0 THEN 'diffusion for t steps of length 1 with <r2>in steps^2
Tau=(2*w^2)/(pi^2)
ELSE
Tau=w^2/(pi^2*D)'continuous diffusion for a time t with <r2> in cm2

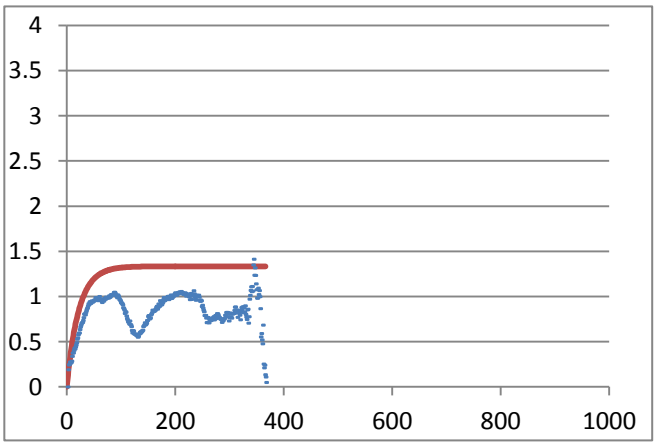

Table A21: Diffusion coefficient of CHO cells expressed FLAG-LHR-YFP and treated with 0.1nM hCG (p7)

param	value
g Column=	D
iDim=	2
nPts=	850
iFirstRow=	1
iLastRow=	500
sumWts=	299049.0000
sumWtdResid=	4874.94
chiSq=	0.016301489
SD=	0.127677286
w (pix)=	2.13E+00
D (pix^2/frame)=	0.02404313
m(pix^2/frame)	8.36658587E-05
um per pixel=	16
mag (obj*Extender)=	63
sec per frame=	0.12
w(um)=	0.5413
D01(cm^2/sec)=	4.64E-10
Dhop(cm^2/sec)=	4.50E-13

FUNCTION AkiDisp(w,t,D)
multi-expon approx to 1D diff confined in region of width w
re-derived and checked against early Kusumi paper
accurate to 1:1000 @ t=0
w is width of domain (n cells orig)
t is time (i jumps orig)
D is diffusion coeff
IF D=0 THEN 'diffusion for t steps of length 1 with <r2>in steps^2
Tau=(2*w^2)/(pi^2)
ELSE
Tau=w^2/(pi^2*D)'continuous diffusion for a time t with <r2> in cm2

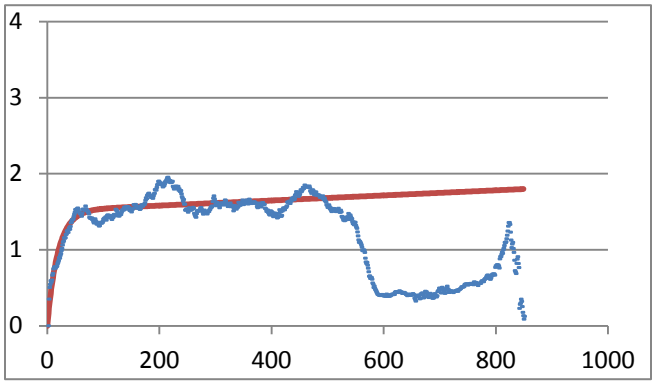

Table A22: Diffusion coefficient of CHO cells expressed FLAG-LHR-YFP and treated with 100 nM hCG (p1)

param	value
g Column=	D
iDim=	2
nPts=	925
iFirstRow=	1
iLastRow=	500
sumWts=	336399.0000
sumWtdResid=	5496.97
chiSq=	0.016340615
SD=	0.127830416
w (pix)=	1.20E+00
D (pix^2/frame)=	0.07800169
m(pix^2/frame)	1.28397312E-03
um per pixel=	16
mag (obj*Extender)=	63
sec per frame=	0.12
w(um)=	0.3048
D01(cm^2/sec)=	4.25E-10
Dhop(cm^2/sec)=	6.90E-12

FUNCTION AkiDisp(w,t,D)
multi-expon approx to 1D diff confined in region of width w
re-derived and checked against early Kusumi paper
accurate to 1:1000 @ t=0
w is width of domain (n cells orig)
t is time (i jumps orig)
D is diffusion coeff
IF D=0 THEN 'diffusion for t steps of length 1 with <r2>in steps^2
Tau=(2*w^2)/(pi^2)
ELSE
Tau=w^2/(pi^2*D)'continuous diffusion for a time t with <r2> in cm2

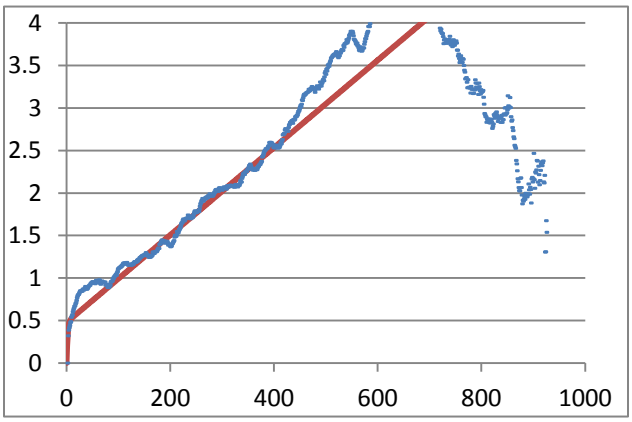

Table A23: Diffusion coefficient of CHO cells expressed FLAG-LHR-YFP and treated with 100 nM hCG (p2)

param	value
g Column=	D
iDim=	2
nPts=	919
iFirstRow=	1
iLastRow=	500
sumWts=	333411.0000
sumWtdResid=	1532.26
chiSq=	0.004595703
SD=	0.067791615
w (pix)=	2.19E+00
D (pix^2/frame)=	0.001522389
m(pix^2/frame)	6.66937031E-07
um per pixel=	16
mag (obj*Extender)=	63
sec per frame=	0.12
w(um)=	0.5559
D01(cm^2/sec)=	1.84E-10
Dhop(cm^2/sec)=	3.58E-15

FUNCTION AkiDisp(w,t,D)
multi-expon approx to 1D diff confined in region of width w
re-derived and checked against early Kusumi paper
accurate to 1:1000 @ t=0
w is width of domain (n cells orig)
t is time (i jumps orig)
D is diffusion coeff
IF D=0 THEN 'diffusion for t steps of length 1 with <r2>in steps^2
Tau=(2*w^2)/(pi^2)
ELSE
Tau=w^2/(pi^2*D)'continuous diffusion for a time t with <r2> in cm2

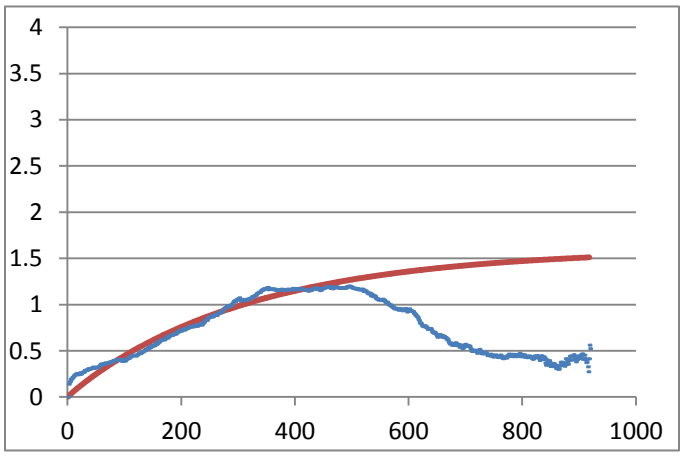

Table A24: Diffusion coefficient of CHO cells expressed FLAG-LHR-YFP and treated with 100 nM hCG (p3)

param	value
g Column=	D
iDim=	2
nPts=	1000
iFirstRow=	1
iLastRow=	500
sumWts=	373749.0000
sumWtdResid=	1024.46
chiSq=	0.002741039
SD=	0.052354931
w (pix)=	6.00E-01
D (pix^2/frame)=	0.001812308
m(pix^2/frame)	2.46731711E-04
um per pixel=	16
mag (obj*Extender)=	63
sec per frame=	0.12
w(um)=	0.1524
D01(cm^2/sec)=	6.98E-11
Dhop(cm^2/sec)=	1.33E-12

FUNCTION AkiDisp(w,t,D)
multi-expon approx to 1D diff confined in region of width w
re-derived and checked against early Kusumi paper
accurate to 1:1000 @ t=0
w is width of domain (n cells orig)
t is time (i jumps orig)
D is diffusion coeff
IF D=0 THEN 'diffusion for t steps of length 1 with <r2>in steps^2
Tau=(2*w^2)/(pi^2)
ELSE
Tau=w^2/(pi^2*D)'continuous diffusion for a time t with <r2> in cm2

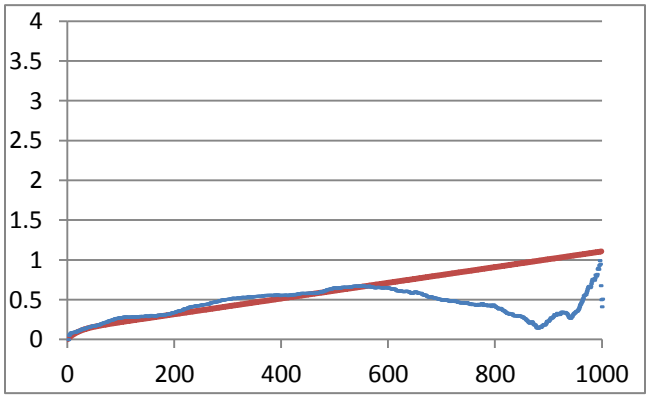

Table A25: Diffusion coefficient of CHO cells expressed FLAG-LHR-YFP and treated with 100 nM hCG (p4)

param	value
g Column=	D
iDim=	2
nPts=	346
iFirstRow=	1
iLastRow=	500
sumWts=	59685.0000
sumWtdResid=	19969.66
chiSq=	0.33458424
SD=	0.578432572
w (pix)=	5.00E-01
D (pix^2/frame)=	11.87915042
m(pix^2/frame)	5.99516731E-04
um per pixel=	16
mag (obj*Extender)=	63
sec per frame=	0.12
w(um)=	0.1270
D01(cm^2/sec)=	1.15E-10
Dhop(cm^2/sec)=	3.22E-12

FUNCTION AkiDisp(w,t,D)
multi-expon approx to 1D diff confined in region of width w
re-derived and checked against early Kusumi paper
accurate to 1:1000 @ t=0
w is width of domain (n cells orig)
t is time (i jumps orig)
D is diffusion coeff
IF D=0 THEN 'diffusion for t steps of length 1 with <r2>in steps^2
Tau=(2*w^2)/(pi^2)
ELSE
Tau=w^2/(pi^2*D)'continuous diffusion for a time t with <r2> in cm2

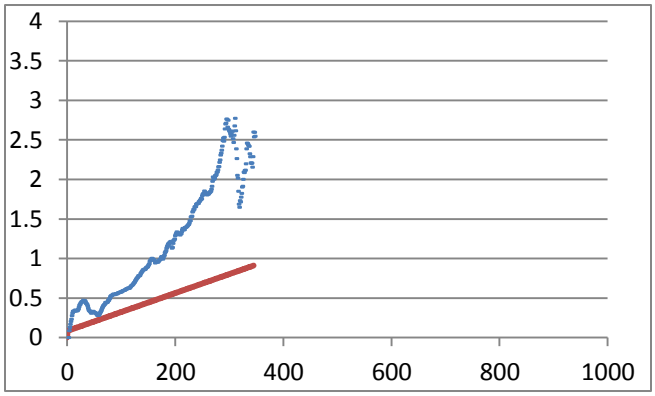

Table A26: Diffusion coefficient of CHO cells expressed FLAG-LHR-YFP and treated with 100 nM hCG (p5)

param	value
g Column=	D
iDim=	2
nPts=	101
iFirstRow=	1
iLastRow=	500
sumWts=	5050.0000
sumWtdResid=	80.97
chiSq=	0.016034031
SD=	0.126625556
w (pix)=	1.57E+00
D (pix^2/frame)=	0.004543118
m(pix^2/frame)	6.18349081E-04
um per pixel=	16
mag (obj*Extender)=	63
sec per frame=	0.12
w(um)=	0.3982
D01(cm^2/sec)=	2.71E-10
Dhop(cm^2/sec)=	3.32E-12

FUNCTION AkiDisp(w,t,D)
multi-expon approx to 1D diff confined in region of width w
re-derived and checked against early Kusumi paper
accurate to 1:1000 @ t=0
w is width of domain (n cells orig)
t is time (i jumps orig)
D is diffusion coeff
IF D=0 THEN 'diffusion for t steps of length 1 with <r2>in steps^2
Tau=(2*w^2)/(pi^2)
ELSE
Tau=w^2/(pi^2*D)'continuous diffusion for a time t with <r2> in cm2

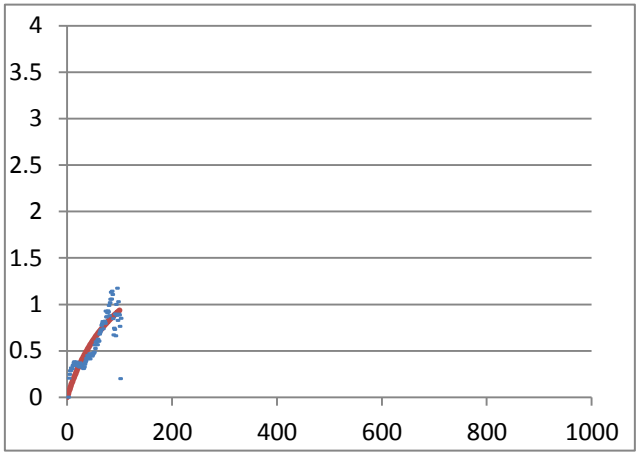

Table A27: Diffusion coefficient of CHO cells expressed FLAG-LHR-YFP and treated with 100 nM hCG (p6)

param	value
g Column=	D
iDim=	2
nPts=	702
iFirstRow=	1
iLastRow=	500
sumWts=	225345.0000
sumWtdResid=	20866.56
chiSq=	0.092598287
SD=	0.304299666
w (pix)=	1.70E+00
D (pix^2/frame)=	0.002037065
m(pix^2/frame)	2.21349152E-04
um per pixel=	16
mag (obj*Extender)=	63
sec per frame=	0.12
w(um)=	0.4317
D01(cm^2/sec)=	1.47E-10
Dhop(cm^2/sec)=	1.19E-12

FUNCTION
AkiDisp(w,t,D)
multi-expon approx to 1D diff confined in region of width w
re-derived and checked against early Kusumi paper
accurate to 1:1000 @ t=0
w is width of domain (n cells orig)
t is time (i jumps orig)
D is diffusion coeff
IF D=0 THEN 'diffusion for t steps of length 1 with <r2>in steps^2
Tau=(2*w^2)/(pi^2)
ELSE
Tau=w^2/(pi^2*D)'continuous diffusion for a time t with <r2> in cm2

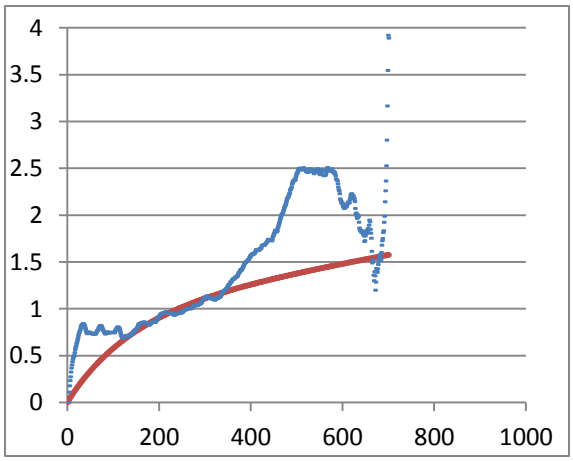

Table A28: Diffusion coefficient of CHO cells expressed FLAG-LHR-YFP and treated with 100 nM hCG (p7)

param	value
g Column=	D
iDim=	2
nPts=	1000
iFirstRow=	1
iLastRow=	500
sumWts=	373749.0000
sumWtdResid=	2014.68
chiSq=	0.005390468
SD=	0.073419804
w (pix)=	1.97E+00
D (pix^2/frame)=	0.002712664
m(pix^2/frame)	1.98532253E-07
um per pixel=	16
mag (obj*Extender)=	63
sec per frame=	0.0333
w(um)=	0.5011
D01(cm^2/sec)=	1.22E-10
Dhop(cm^2/sec)=	3.85E-15

FUNCTION
AkiDisp(w,t,D)
multi-expon approx to 1D diff confined in region of width w
re-derived and checked against early Kusumi paper
accurate to 1:1000 @
t=0
w is width of domain (n cells orig)
t is time (i jumps orig)
D is diffusion coeff
IF D=0 THEN 'diffusion for t steps of length 1 with <r2>in steps^2
Tau=(2*w^2)/(pi^2)
ELSE
Tau=w^2/(pi^2*D)'continuous diffusion for a time t with <r2> in cm2

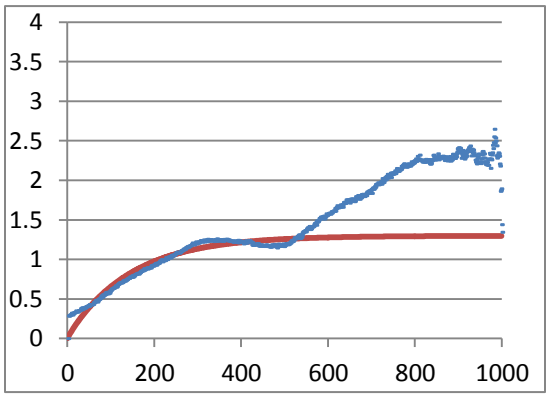

Table A29: Diffusion coefficient of untreated CHO cells coexpressed mutant receptors of FLAG-LHR$^{+hCG/-cAMP}$ and HA-LHR$^{-hCG/+cAMP}$ (p1)

param	value
g Column=	D
iDim=	2
nPts=	194
iFirstRow=	1
iLastRow=	500
sumWts=	18721.0000
sumWtdResid=	48.55
chiSq=	0.00259346
SD=	0.050926029
w (pix)=	1.00E+00
D (pix^2/frame)=	0.906092354
m(pix^2/frame)	7.17258340E-04
um per pixel=	16
mag (obj*Extender)=	63
sec per frame=	0.0333
w(um)=	0.2540
D01(cm^2/sec)=	1.80E-10
Dhop(cm^2/sec)=	1.39E-11

FUNCTION
AkiDisp(w,t,D)
multi-expon approx to 1D diff confined in region of width w
re-derived and checked against early Kusumi paper
accurate to 1:1000 @ t=0
w is width of domain (n cells orig)
t is time (i jumps orig)
D is diffusion coeff
IF D=0 THEN 'diffusion for t steps of length 1 with <r2>in steps^2
Tau=(2*w^2)/(pi^2)
ELSE
Tau=w^2/(pi^2*D)'continuous diffusion for a time t with <r2> in cm2

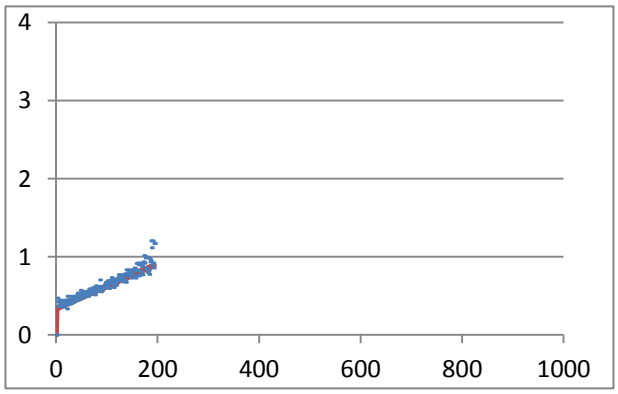

Table A30: Diffusion coefficient of untreated CHO cells coexpressed mutant receptors of FLAG-LHR$^{+hCG/-cAMP}$ and HA-LHR$^{-hCG/+cAMP}$ (p2)

param	value
g Column=	D
iDim=	2
nPts=	225
iFirstRow=	1
iLastRow=	500
sumWts=	25200.0000
sumWtdResid=	6838.56
chiSq=	0.271371443
SD=	0.520933242
w (pix)=	1.05E+00
D (pix^2/frame)=	1.642650126
m(pix^2/frame)	7.18404383E-03
um per pixel=	16
mag (obj*Extender)=	63
sec per frame=	0.0333
w(um)=	0.3667
D01(cm^2/sec)=	6.09E-10
Dhop(cm^2/sec)=	1.39E-10

FUNCTION AkiDisp(w,t,D)
multi-expon approx to 1D diff confined in region of width w
re-derived and checked against early Kusumi paper
accurate to 1:1000 @ t=0
w is width of domain (n cells orig)
t is time (i jumps orig)
D is diffusion coeff
IF D=0 THEN 'diffusion for t steps of length 1 with <r2>in steps^2
Tau=(2*w^2)/(pi^2)
ELSE
Tau=w^2/(pi^2*D)'continuous diffusion for a time t with <r2> in cm2

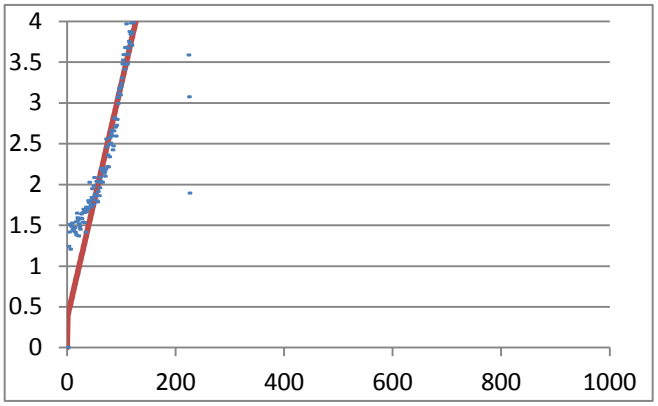

Table A31: Diffusion coefficient of untreated CHO cells coexpressed mutant receptors of FLAG-LHR$^{+hCG/-cAMP}$ and HA-LHR$^{-hCG/+cAMP}$ (p3)

param	value
g Column=	D
iDim=	2
nPts=	153
iFirstRow=	1
iLastRow=	500
sumWts=	11628.0000
sumWtdResid=	903.61
chiSq=	0.077710243
SD=	0.278765569
w (pix)=	2.63E+00
D (pix^2/frame)=	0.929512055
m(pix^2/frame)	4.00797978E-04
um per pixel=	16
mag (obj*Extender)=	63
sec per frame=	0.0333
w(um)=	0.6686
D01(cm^2/sec)=	8.56E-10
Dhop(cm^2/sec)=	7.76E-12

FUNCTION AkiDisp(w,t,D)
multi-expon approx to 1D diff confined in region of width w
re-derived and checked against early Kusumi paper
accurate to 1:1000 @ t=0
w is width of domain (n cells orig)
t is time (i jumps orig)
D is diffusion coeff
IF D=0 THEN 'diffusion for t steps of length 1 with <r2>in steps^2
Tau=(2*w^2)/(pi^2)
ELSE
Tau=w^2/(pi^2*D)'continuous diffusion for a time t with <r2> in cm2

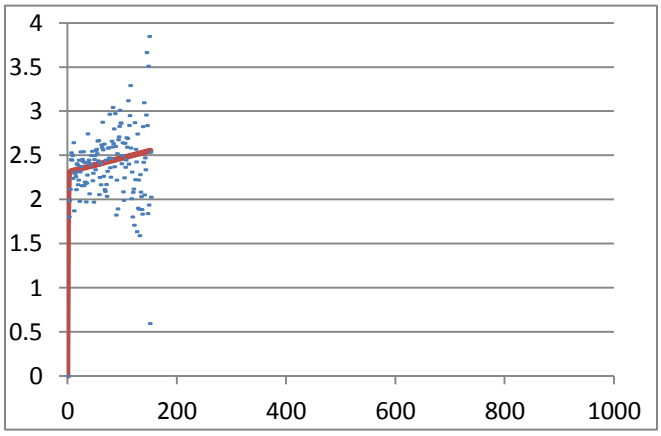

Table A32: Diffusion coefficient of untreated CHO cell coexpressed mutant receptors of FLAG-LHR$^{+hCG/-cAMP}$ and HA-LHR$^{-hCG/+cAMP}$ (p4)

param	value
g Column=	D
iDim=	2
nPts=	118
iFirstRow=	1
iLastRow=	500
sumWts=	6903.0000
sumWtdResid=	1341.99
chiSq=	0.194407355
SD=	0.440916494
w (pix)=	1.80E+00
D (pix^2/frame)=	1.198744834
m(pix^2/frame)	3.68662280E-04
um per pixel=	16
mag (obj*Extender)=	63
sec per frame=	0.0333
w(um)=	0.4571
D01(cm^2/sec)=	6.02E-10
Dhop(cm^2/sec)=	7.14E-12

FUNCTION AkiDisp(w,t,D)
multi-expon approx to 1D diff confined in region of width w
re-derived and checked against early Kusumi paper
accurate to 1:1000 @ t=0
w is width of domain (n cells orig)
t is time (i jumps orig)
D is diffusion coeff
IF D=0 THEN 'diffusion for t steps of length 1 with <r2>in steps^2
Tau=(2*w^2)/(pi^2)
ELSE
Tau=w^2/(pi^2*D)'continuous diffusion for a time t with <r2> in cm2

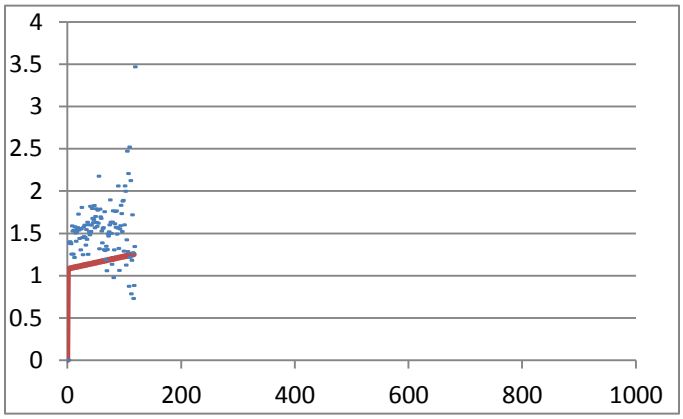

Table A33: Diffusion coefficient of untreated CHO cell coexpressed mutant receptors of FLAG-LHR$^{+hCG/-cAMP}$ and HA-LHR$^{-hCG/+cAMP}$ (p5)

param	value
g Column=	D
iDim=	2
nPts=	367
iFirstRow=	1
iLastRow=	500
sumWts=	67161.0000
sumWtdResid=	43272.22
chiSq=	0.644305807
SD=	0.802686618
w (pix)=	3.44E+00
D (pix^2/frame)=	1.03472486
m(pix^2/frame)	1.71220312E-03
um per pixel=	16
mag (obj*Extender)=	63
sec per frame=	0.0333
w(um)=	0.7124
D01(cm^2/sec)=	1.41E-09
Dhop(cm^2/sec)=	3.32E-11

FUNCTION AkiDisp(w,t,D)
multi-expon approx to 1D diff confined in region of width w
re-derived and checked against early Kusumi paper
accurate to 1:1000 @ t=0
w is width of domain (n cells orig)
t is time (i jumps orig)
D is diffusion coeff
IF D=0 THEN 'diffusion for t steps of length 1 with <r2>in steps^2
Tau=(2*w^2)/(pi^2)
ELSE
Tau=w^2/(pi^2*D)'continuous diffusion for a time t with <r2> in cm2

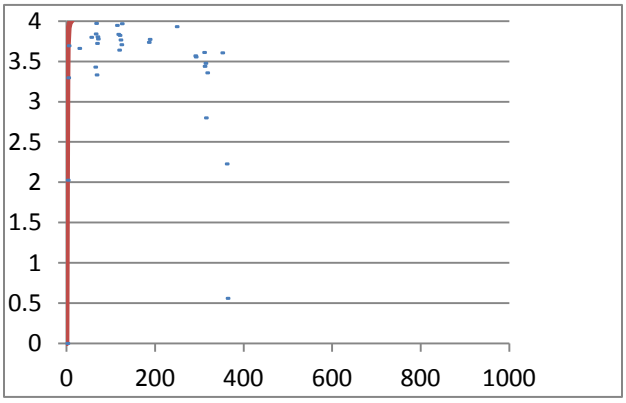

Table A34: Diffusion coefficient of untreated CHO cell coexpressed mutant receptors of FLAG-LHR$^{+hCG/-cAMP}$ and HA-LHR$^{-hCG/+cAMP}$ (p6)

param	value
g Column=	D
iDim=	2
nPts=	185
iFirstRow=	1
iLastRow=	500
sumWts=	17020.0000
sumWtdResid=	3505.36
chiSq=	0.20595547
SD=	0.453823171
w (pix)=	2.25E+00
D (pix^2/frame)=	1.305288786
m(pix^2/frame)	2.16840124E-03
um per pixel=	16
mag (obj*Extender)=	63
sec per frame=	0.0333
w(um)=	0.5718
D01(cm^2/sec)=	8.21E-10
Dhop(cm^2/sec)=	4.20E-11

FUNCTION AkiDisp(w,t,D)
multi-expon approx to 1D diff confined in region of width w
re-derived and checked against early Kusumi paper
accurate to 1:1000 @ t=0
w is width of domain (n cells orig)
t is time (i jumps orig)
D is diffusion coeff
IF D=0 THEN 'diffusion for t steps of length 1 with <r2>in steps^2
Tau=(2*w^2)/(pi^2)
ELSE
Tau=w^2/(pi^2*D)'continuous diffusion for a time t with <r2> in cm2

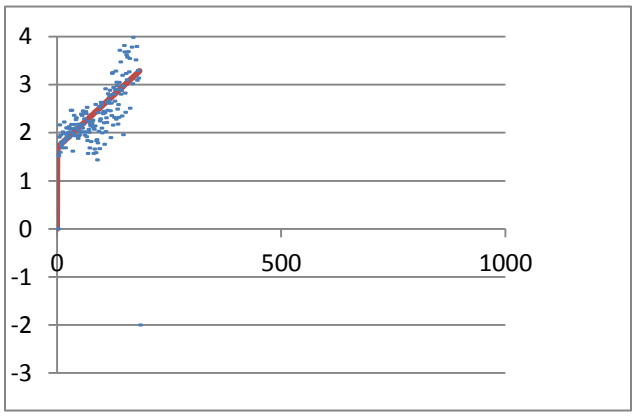

Table A35: Diffusion coefficient of untreated CHO cell coexpressed mutant receptors of FLAG-LHR$^{+hCG/-cAMP}$ and HA-LHR$^{-hCG/+cAMP}$ (p7)

param	value
g Column=	D
iDim=	2
nPts=	182
iFirstRow=	1
iLastRow=	500
sumWts=	16471.0000
sumWtdResid=	722.23
chiSq=	0.0438486
SD=	0.209400574
w (pix)=	2.31E+00
D (pix^2/frame)=	1.088064527
m(pix^2/frame)	1.13258958E-04
um per pixel=	16
mag (obj*Extender)=	63
sec per frame=	0.0333
w(um)=	0.5879
D01(cm^2/sec)=	8.06E-10
Dhop(cm^2/sec)=	2.19E-12

FUNCTION AkiDisp(w,t,D)
multi-expon approx to 1D diff confined in region of width w
re-derived and checked against early Kusumi paper
accurate to 1:1000 @ t=0
w is width of domain (n cells orig)
t is time (i jumps orig)
D is diffusion coeff
IF D=0 THEN 'diffusion for t steps of length 1 with <r2>in steps^2
Tau=(2*w^2)/(pi^2)
ELSE
Tau=w^2/(pi^2*D)'continuous diffusion for a time t with <r2> in cm2

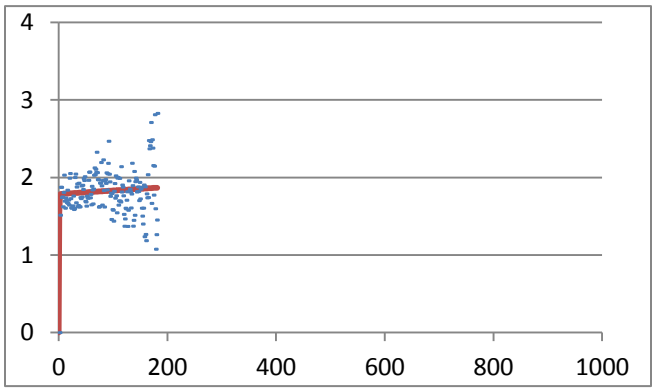

Table A36: Diffusion coefficient of CHO cell coexpressed mutant receptors of FLAG-LHR$^{+hCG/-cAMP}$ and HA-LHR$^{-hCG/+cAMP}$ and treated with 100 nM hCG (p1)

param	value
g Column=	D
iDim=	2
nPts=	111
iFirstRow=	1
iLastRow=	500
sumWts=	6105.0000
sumWtdResid=	3.96
chiSq=	0.000648199
SD=	0.025459749
w (pix)=	8.65E-01
D (pix^2/frame)=	0.266354025
m(pix^2/frame)	1.91578482E-04
um per pixel=	16
mag (obj*Extender)=	63
sec per frame=	0.0333
w(um)=	0.2196
D01(cm^2/sec)=	2.06E-10
Dhop(cm^2/sec)=	3.71E-1

FUNCTION AkiDisp(w,t,D)
multi-expon approx to 1D diff confined in region of width w
re-derived and checked against early Kusumi paper
accurate to 1:1000 @ t=0
w is width of domain (n cells orig)
t is time (i jumps orig)
D is diffusion coeff
IF D=0 THEN 'diffusion for t steps of length 1 with <r2>in steps^2
Tau=(2*w^2)/(pi^2)
ELSE
Tau=w^2/(pi^2*D)'continuous diffusion for a time t with <r2> in cm2

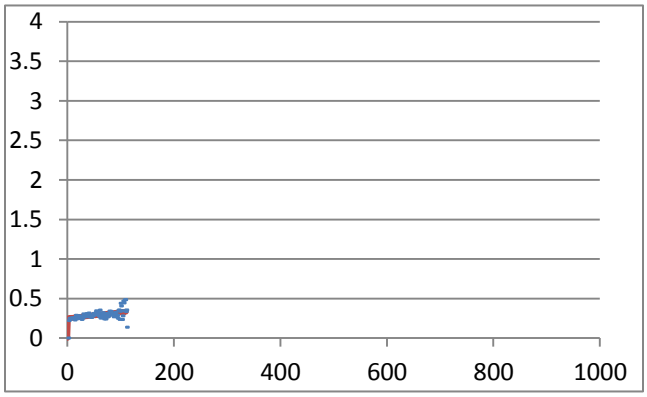

Table A37: Diffusion coefficient of CHO cell coexpressed mutant receptors of FLAG-LHR$^{+hCG/-cAMP}$ and HA-LHR$^{-hCG/+cAMP}$ and treated with 100 nM hCG (p2)

param	value
g Column=	D
iDim=	2
nPts=	582
iFirstRow=	1
iLastRow=	500
sumWts=	165585.0000
sumWtdResid=	714.93
chiSq=	0.004317624
SD=	0.065708631
w (pix)=	6.25E-01
D (pix^2/frame)=	0.306715771
m(pix^2/frame)	6.81926764E-04
um per pixel=	16
mag (obj*Extender)=	63
sec per frame=	0.0333
w(um)=	0.1588
D01(cm^2/sec)=	8.99E-11
Dhop(cm^2/sec)=	1.32E-11

FUNCTION AkiDisp(w,t,D)
multi-expon approx to 1D diff confined in region of width w
re-derived and checked against early Kusumi paper
accurate to 1:1000 @ t=0
w is width of domain (n cells orig)
t is time (i jumps orig)
D is diffusion coeff
IF D=0 THEN 'diffusion for t steps of length 1 with <r2>in steps^2
Tau=(2*w^2)/(pi^2)
ELSE
Tau=w^2/(pi^2*D)'continuous diffusion for a time t with <r2> in cm2

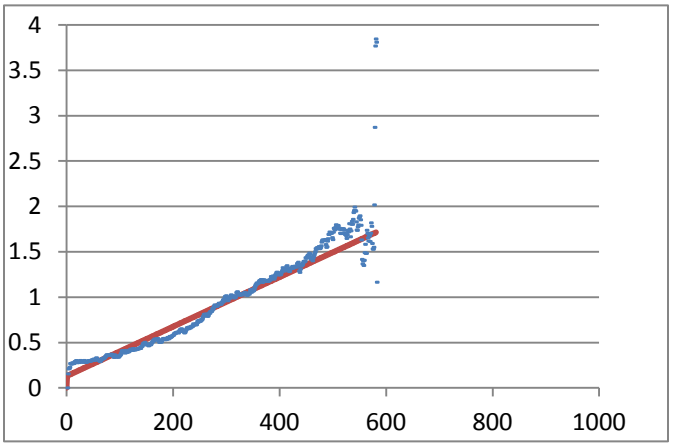

Table A38: Diffusion coefficient of CHO cell coexpressed mutant receptors of FLAG-LHR$^{+hCG/-cAMP}$ and HA-LHR$^{-hCG/+cAMP}$ and treated with 100 nM hCG (p3)

param	value
g Column=	D
iDim=	2
nPts=	206
iFirstRow=	1
iLastRow=	500
sumWts=	81473.0000
sumWtdResid=	4.68
chiSq=	5.74046E-05
SD=	0.007576581
w (pix)=	4.90E-01
D (pix^2/frame)=	0.056586347
m(pix^2/frame)	3.52607706E-05
um per pixel=	16
mag (obj*Extender)=	63
sec per frame=	0.0333
w(um)=	0.1244
D01(cm^2/sec)=	3.71E-11
Dhop(cm^2/sec)=	6.83E-13

FUNCTION AkiDisp(w,t,D)
multi-expon approx to 1D diff confined in region of width w
re-derived and checked against early Kusumi paper
accurate to 1:1000 @ t=0
w is width of domain (n cells orig)
t is time (i jumps orig)
D is diffusion coeff
IF D=0 THEN 'diffusion for t steps of length 1 with <r2>in steps^2
Tau=(2*w^2)/(pi^2)
ELSE
Tau=w^2/(pi^2*D)'continuous diffusion for a time t with <r2> in cm2

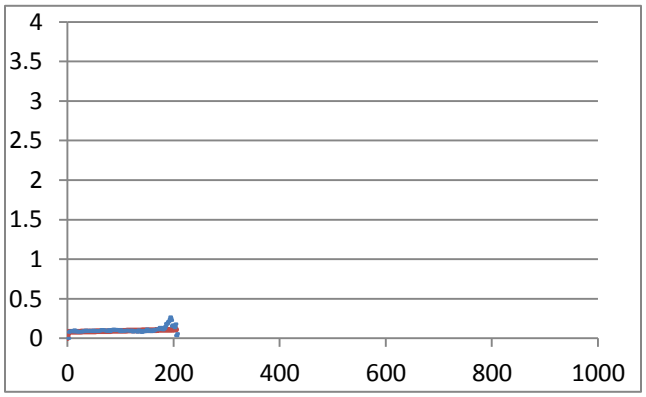

Table A39: Diffusion coefficient of CHO cell coexpressed mutant receptors of FLAG-LHR$^{+hCG/-cAMP}$ and HA-LHR$^{-hCG/+cAMP}$ and treated with 100 nM hCG (p4)

param	value
g Column=	D
iDim=	2
nPts=	305
iFirstRow=	1
iLastRow=	500
sumWts=	46360.0000
sumWtdResid=	585.60
chiSq=	0.012631658
SD=	0.11239065
w (pix)=	1.20E+00
D (pix^2/frame)=	0.058970009
m(pix^2/frame)	3.84624612E-04
um per pixel=	16
mag (obj*Extender)=	63
sec per frame=	0.0333
w(um)=	0.3048
D01(cm^2/sec)=	1.66E-10
Dhop(cm^2/sec)=	7.45E-12

FUNCTION AkiDisp(w,t,D)
multi-expon approx to 1D diff confined in region of width w
re-derived and checked against early Kusumi paper
accurate to 1:1000 @ t=0
w is width of domain (n cells orig)
t is time (i jumps orig)
D is diffusion coeff
IF D=0 THEN 'diffusion for t steps of length 1 with <r2>in steps^2
Tau=(2*w^2)/(pi^2)
ELSE
Tau=w^2/(pi^2*D)'continuous diffusion for a time t with <r2> in cm2

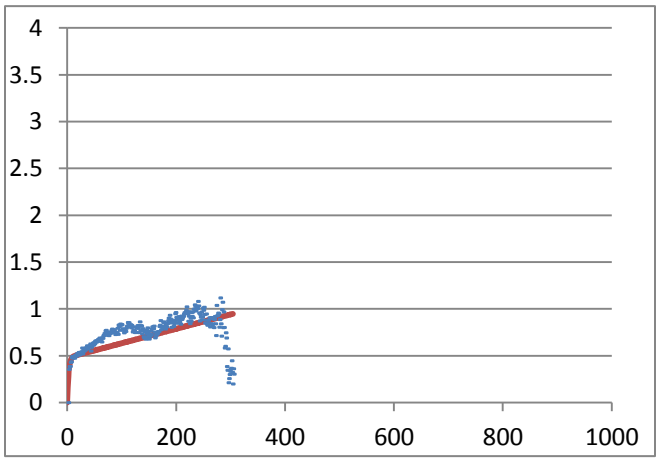

Table A40: Diffusion coefficient of CHO cell coexpressed mutant receptors of FLAG-LHR$^{+hCG/-cAMP}$ and HA-LHR$^{-hCG/+cAMP}$ and treated with 100 nM hCG (p5)

param	value
g Column=	D
iDim=	2
nPts=	565
iFirstRow=	1
iLastRow=	500
sumWts=	157119.0000
sumWtdResid=	2594.22
chiSq=	0.016511155
SD=	0.128495741
w (pix)=	1.00E+00
D (pix^2/frame)=	8.81129E-07
m(pix^2/frame)	9.11639849E-04
um per pixel=	16
mag (obj*Extender)=	63
sec per frame=	0.0333
w(um)=	0.2540
D01(cm^2/sec)=	5.28E-11
Dhop(cm^2/sec)=	1.77E-11

FUNCTION AkiDisp(w,t,D)
multi-expon approx to 1D diff confined in region of width w
re-derived and checked against early Kusumi paper
accurate to 1:1000 @ t=0
w is width of domain (n cells orig)
t is time (i jumps orig)
D is diffusion coeff
IF D=0 THEN 'diffusion for t steps of length 1 with <r2>in steps^2
Tau=(2*w^2)/(pi^2)
ELSE
Tau=w^2/(pi^2*D)'continuous diffusion for a time t with <r2> in cm2

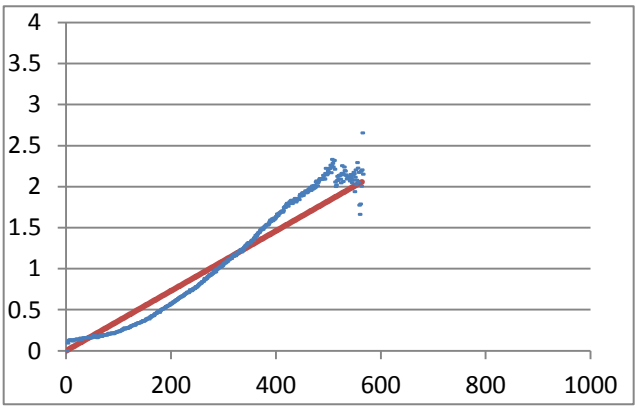

Table A41: Diffusion coefficient of CHO cell coexpressed mutant receptors of FLAG-LHR$^{+hCG/-cAMP}$ and HA-LHR$^{-hCG/+cAMP}$ and treated with 100 nM hCG (p6)

param	value
g Column=	D
iDim=	2
nPts=	569
iFirstRow=	1
iLastRow=	500
sumWts=	159111.0000
sumWtdResid=	7327.22
chiSq=	0.046051023
SD=	0.214595021
w (pix)=	1.90E+00
D (pix^2/frame)=	0.009421452
m(pix^2/frame)	3.69618416E-06
um per pixel=	16
mag (obj*Extender)=	63
sec per frame=	0.0333
w(um)=	0.4825
D01(cm^2/sec)=	1.60E-10
Dhop(cm^2/sec)=	7.16E-14

FUNCTION AkiDisp(w,t,D)
multi-expon approx to 1D diff confined in region of width w
re-derived and checked against early Kusumi paper
accurate to 1:1000 @ t=0
w is width of domain (n cells orig)
t is time (i jumps orig)
D is diffusion coeff
IF D=0 THEN 'diffusion for t steps of length 1 with <r2>in steps^2
Tau=(2*w^2)/(pi^2)
ELSE
Tau=w^2/(pi^2*D)'continuous diffusion for a time t with <r2> in cm2

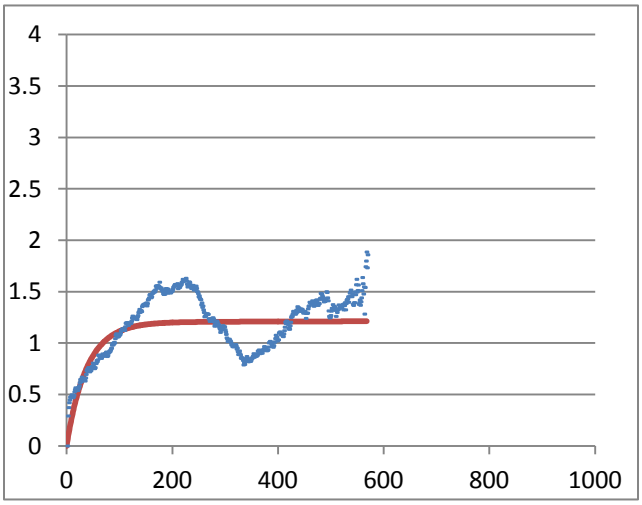

Table A42: Diffusion coefficient of CHO cell coexpressed mutant receptors of FLAG-LHR$^{+hCG/-cAMP}$ and HA-LHR$^{-hCG/+cAMP}$ and treated with 100 nM hCG (p7)

param	value
g Column=	D
iDim=	2
nPts=	778
iFirstRow=	1
iLastRow=	500
sumWts=	263193.0000
sumWtdResid=	621.71
chiSq=	0.002362197
SD=	0.048602443
w (pix)=	3.73E-01
D (pix^2/frame)=	0.499855715
m(pix^2/frame)	3.87332418E-04
um per pixel=	16
mag (obj*Extender)=	63
sec per frame=	0.0333
w(um)=	0.0946
D01(cm^2/sec)=	5.93E-11
Dhop(cm^2/sec)=	7.50E-12

FUNCTION
AkiDisp(w,t,D)
multi-expon approx to 1D diff confined in region of width w
re-derived and checked against early Kusumi paper
accurate to 1:1000 @
t=0
w is width of domain (n cells orig)
t is time (i jumps orig)
D is diffusion coeff
IF D=0 THEN 'diffusion for t steps of length 1 with <r2>in steps^2
Tau=(2*w^2)/(pi^2)
ELSE
Tau=w^2/(pi^2*D)'continuous diffusion for a time t with <r2> in cm2

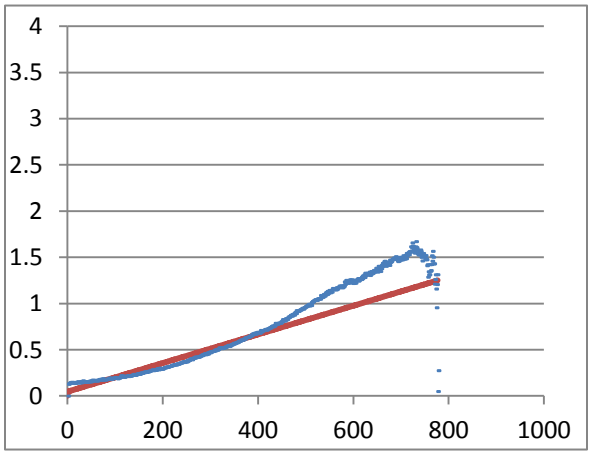

APPENDIX II

Table B1: Homo FRET of untreated CHO cells expressed wild type receptor FLAG-LHR-YFP

T	g	Iv	Ih	Ivbg	Ihbg	Iv-Ivbg	Ih-Ihbg	Ivc	s	r
0	1.41	392.309	362.658	330.564	340.505	61.745	22.153	31.23573	124.2165	0.245614
1	1.41	362.626	347.025	328.209	334.89	34.417	12.135	17.11035	68.6377	0.252145
2	1.41	353.95	342.82	327.693	333.723	26.257	9.097	12.82677	51.91054	0.258719
3	1.41	350.99	341.388	326.943	333.096	24.047	8.292	11.69172	47.43044	0.260493
4	1.41	347.805	339.741	327.219	332.848	20.586	6.893	9.71913	40.02426	0.271507
5	1.41	345.837	339.211	327.211	333.023	18.626	6.188	8.72508	36.07616	0.274445
6	1.41	344.959	338.35	327.025	332.4	17.934	5.95	8.3895	34.713	0.274955
7	1.41	343.915	338.262	327.035	332.644	16.88	5.618	7.92138	32.72276	0.273773
8	1.41	343.339	338.008	327.004	332.47	16.335	5.538	7.80858	31.95216	0.26685
9	1.41	341.197	336.691	326.839	331.842	14.358	4.849	6.83709	28.03218	0.268296
10	1.41	340.253	336.378	326.092	331.717	14.161	4.661	6.57201	27.30502	0.277934
11	1.41	339.289	335.117	325.268	330.514	14.021	4.603	6.49023	27.00146	0.278902
12	1.41	338.373	334.434	324.951	330.215	13.422	4.219	5.94879	25.31958	0.295155
13	1.41	337.694	334.358	324.624	330.156	13.07	4.202	5.92482	24.91964	0.286729
14	1.41	336.444	333.538	324.542	329.92	11.902	3.618	5.10138	22.10476	0.307654
15	1.41	337.084	334.058	325.402	330.487	11.682	3.571	5.03511	21.75222	0.305573

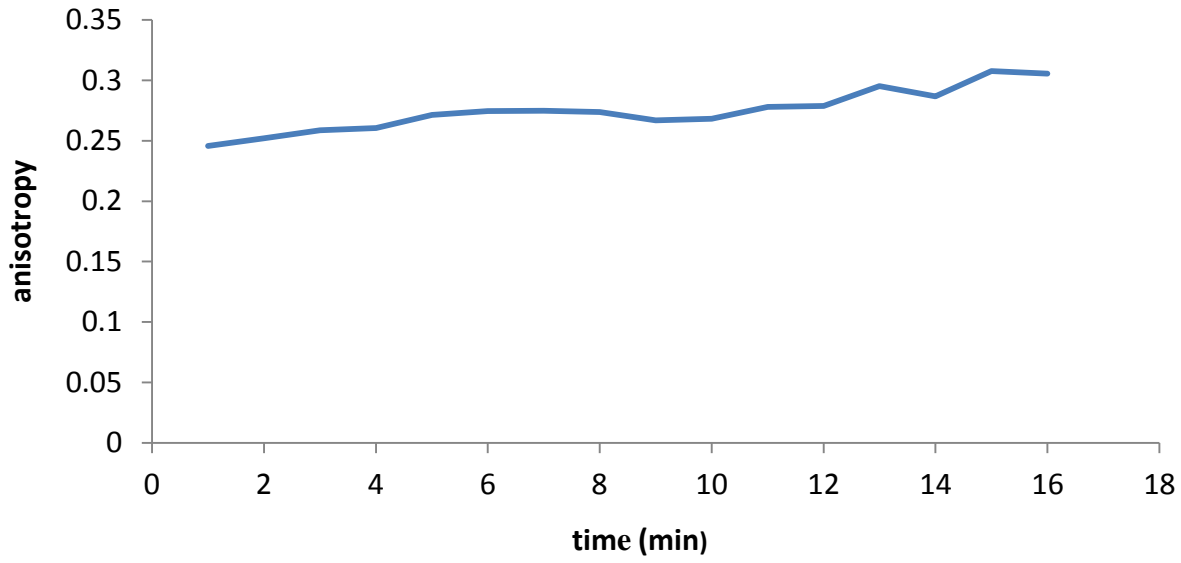

Figure B1: Increasing receptor anisotropy by upon photobleaching of CHO cells expressing FLAG-LHR-YFP wt

Table B2: Homo FRET of CHO cells expressed wild type receptor FLAG-LHR-YFP and treated with 0.1 nM hCG

t min	g	iv	ih	ivbg	ihbg	iv-ivbg	ih-ihbg	ivc	s	r
0	0.8	381.371	380.315	362.984	368.836	18.387	11.479	9.1832	36.7534	0.25042
1	0.8	378.336	376.687	359.475	365.125	18.861	11.562	9.2496	37.3602	0.25726
2	0.8	377.19	375.615	359.77	364.984	17.42	10.631	8.5048	34.4296	0.25894
3	0.8	375.961	374.785	358.08	363.979	17.881	10.806	8.6448	35.1706	0.26261
4	0.8	375.571	374.94	356.903	363.852	18.668	11.088	8.8704	36.4088	0.2691
5	0.8	374.628	374.406	359.607	365.754	15.021	8.652	6.9216	28.8642	0.28060
6	0.8	373.894	373.45	358.295	364.489	15.599	8.961	7.1688	29.9366	0.28160
7	0.8	373.995	373.839	358.377	364.475	15.618	9.364	7.4912	30.6004	0.26557
8	0.8	373.016	373.457	357.328	364.59	15.688	8.867	7.0936	29.8752	0.28767
9	0.8	372.972	373.823	355.361	363.492	17.611	10.331	8.2648	34.1406	0.27375
10	0.8	369.689	366.295	355.738	358.262	13.951	8.033	6.4264	26.8038	0.28072
11	0.8	374.831	377.57	361.508	369.689	13.323	7.881	6.3048	25.9326	0.27063
12	0.8	373.456	375.366	360.639	367.93	12.817	7.436	5.9488	24.7146	0.27790
13	0.8	373.214	375.291	358.262	366.785	14.952	8.506	6.8048	28.5616	0.28525
14	0.8	373.193	374.212	357.393	365.295	15.8	8.917	7.1336	30.0672	0.28823
15	0.8	373.626	375.92	359.115	368.121	14.511	7.799	6.2392	26.9894	0.30648
16	0.8	373.056	375.425	358.885	367.77	14.171	7.655	6.124	26.419	0.30459

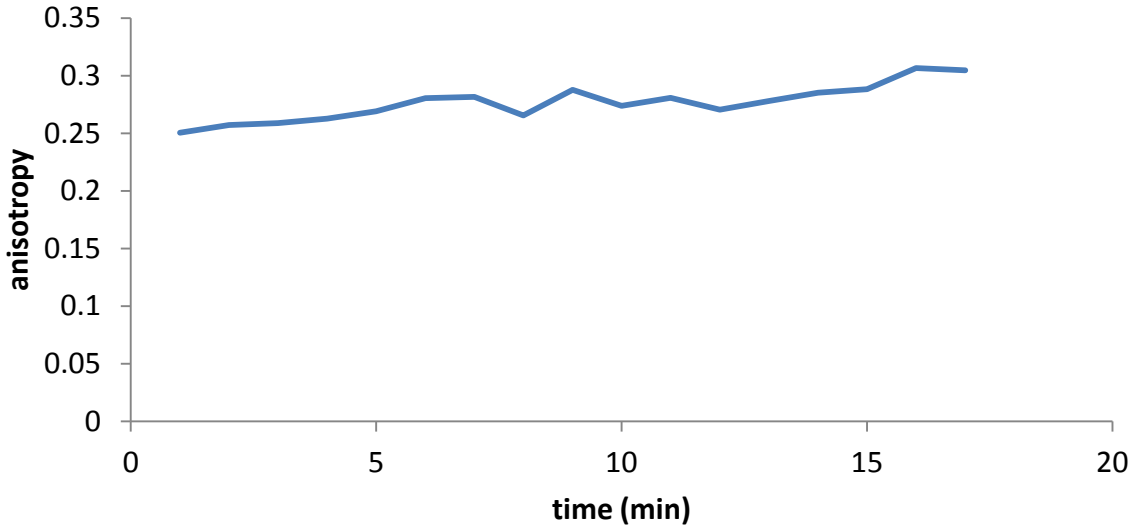

Figure B2: Increasing receptor anisotropy upon photobleaching of CHO cells expressing FLAG-LHR-YFP wt and treated with 0.1 nM hCG

Table B3: Homo FRET of CHO cells expressed wild type receptor FLAG-LHR-YFP and treated with 1 nM hCG

t min	g	iv	ih	ivbg	ihbg	Iv-Ivbg	Ih-Ihbg	Ivc	s	r
0	0.8	429.203	419.322	391.327	393.846	37.876	25.476	20.3808	78.6376	0.22248
1	0.8	423	412.671	387.173	389.327	35.827	23.344	18.6752	73.1774	0.23439
2	0.8	422.615	413.318	387.077	389.318	35.538	24	19.2	73.938	0.22097
3	0.8	422.566	413.451	386.981	389.098	35.585	24.353	19.4824	74.5498	0.21600
4	0.8	421.783	412.626	387.192	388.808	34.591	23.818	19.0544	72.6998	0.21371
5	0.8	423.042	414.654	388.673	391.962	34.369	22.692	18.1536	70.6762	0.22943
6	0.8	420.689	411.164	386.615	388.596	34.074	22.568	18.0544	70.1828	0.22826
7	0.8	421.252	416.014	390.154	395.769	31.098	20.245	16.196	63.49	0.23471
8	0.8	420.052	415.51	386.846	393.865	33.206	21.645	17.316	67.838	0.23423
9	0.8	420.476	414.259	388.154	393.019	32.322	21.24	16.992	66.306	0.23120
10	0.8	416.996	411.192	386.019	391.519	30.977	19.673	15.7384	62.4538	0.24400
11	0.8	420.874	418.538	391.288	399.173	29.586	19.365	15.492	60.57	0.23269
12	0.8	418.937	418.434	390.062	399.935	28.875	18.499	14.7992	58.4734	0.24072
13	0.8	416.066	413.892	386.673	395.712	29.393	18.18	14.544	58.481	0.25391
14	0.8	414.748	413.315	387.212	396.462	27.536	16.853	13.4824	54.5008	0.25786
15	0.8	413.741	414.815	383.404	396.519	30.337	18.296	14.6368	59.6106	0.26338
16	0.8	409.315	407.738	383.327	393.115	25.988	14.623	11.6984	49.3848	0.28935

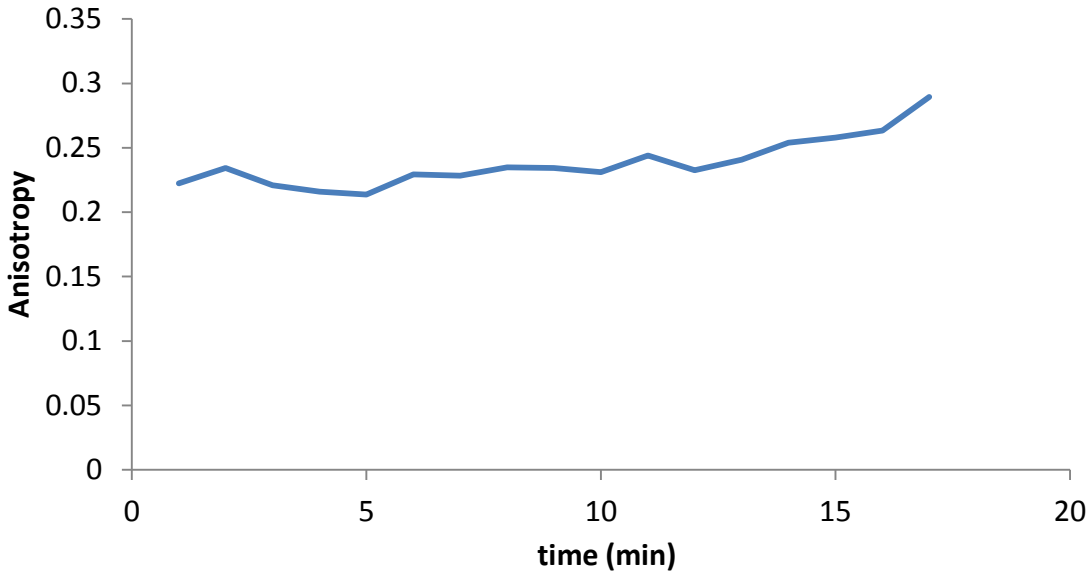

Figure B3: Increasing receptor anisotropy upon photobleaching of CHO cells expressing FLAG-LHR-YFP wt and treated with 1 nM hCG

APPENDIX III

Table C1: CFP/YFPSE ratio of CHO cells expressing FLAG-LHR-YFP +ICUE3 and treated with 0.1 nM hCG

CFP	YFPSE	CFP/YFPSE
2980.599	3484.171	0.855469
2898.839	3390.044	0.855104
2876.596	3365.685	0.854684
2834.741	3328.701	0.851606
2809.798	3289.507	0.85417
2780.082	3254.147	0.85432
2829.33	3319.575	0.852317
2809.813	3302.497	0.850815
2937.168	3409.485	0.86147
2865.713	3324.387	0.862027
2799.397	3250.772	0.861148
2774.06	3219.288	0.8617
2780.023	3215.922	0.864456
2765.303	3165.996	0.873439
2771.363	3203.596	0.865079
2755.116	3202.073	0.860416
2746.289	3181.185	0.863291
2823.724	3298.701	0.856011

/

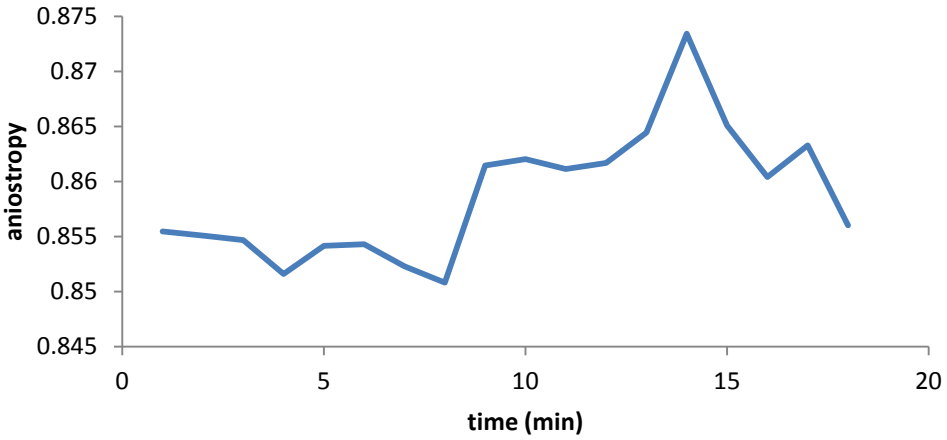

Figure C1: CFP/YFPSE ratio of CHO cells expressed Flag-LHR-YFP +ICUE3 and treated with 0.1 nM hCG

Table C2: CFP/YFPSE ratio of CHO cells expressing FLAG-LHR-YFP +ICUE3 and treated with 1 nM hCG.

CFP	YFPSE	CFP/YFPSE
2315.684	2893.482	0.80031
2321.948	2848.517	0.815143
2285.231	2795.771	0.817388
2404.456	2943.068	0.81699
2272.895	2778.824	0.817934
2259.812	2768.653	0.816214
2365.463	2901.279	0.815317
2219.806	2836.211	0.782666
2344.562	2898.105	0.808998
2281.777	2720.077	0.838865
2326.522	2689.021	0.865193
2374.693	2774.599	0.855869
2311.633	2705.321	0.854476
2307.605	2700.935	0.854373
2303.18	2688.5	0.856678
2222.706	2568.336	0.865426
2194.437	2577.773	0.851292
2167.876	2507.491	0.86456

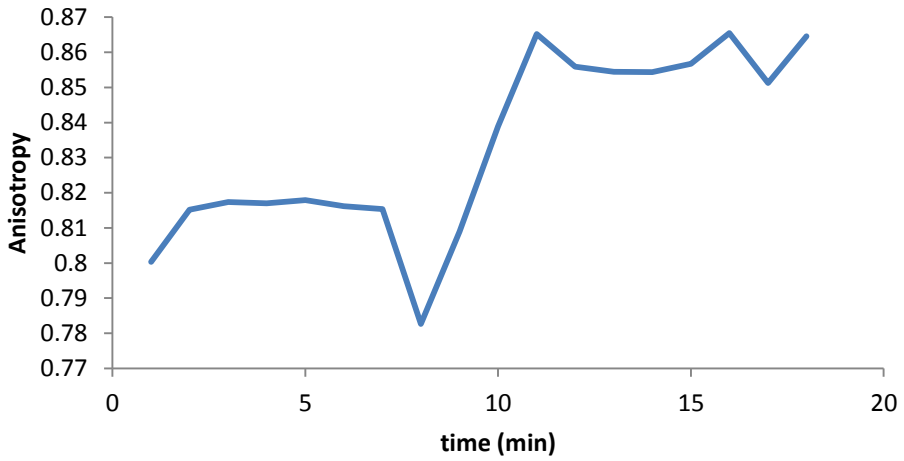

Figure C2: CFP/YFPSE ratio of CHO cells expressing FLAG-LHR-YFP +ICUE3 and treated with 1 nM hCG.

Table C3: CFP/YFPSE ratio of CHO cells expressing FLAG-LHR-YFP +ICUE3 and treated with 100 nM hCG

CFP	YFPSE	CFP/YFPSE
2955.645	3248.04	0.909978
2910.871	3233.263	0.900289
2901.431	3216.342	0.90209
2909.287	3209.06	0.906585
2875.796	3179.016	0.904618
2877.424	3197.218	0.899977
2883.607	3196.069	0.902236
2877.97	3196.804	0.900265
2882.658	3106.938	0.927813
2860.98	3051.747	0.937489
3022.838	3218.379	0.939242
3039.904	3216.39	0.945129
3014.96	3182.215	0.947441
3000.863	3168.443	0.94711
2957.323	3120.036	0.947849
2934.666	3110.903	0.943349
2881.524	3055.406	0.94309
2852.322	3013.238	0.946597

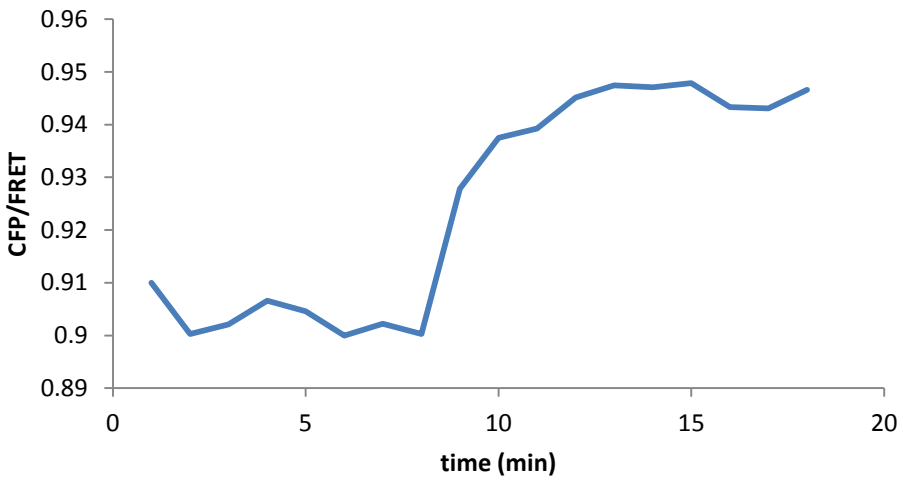

Figure C3: CFP/YFPSE ratio of CHO cells expressing FLAG-LHR-YFP +ICUE3 and treated with 100 nM hCG.

LIST OF ABBREVIATIONS

AC	adenyl cyclase
Asn	asparagin
ATP	adenosine triphosphate
ADP	adenosine diphosphate
BRET	bioluminescence resonance energy transfer
BSA	bovine serum albumin
cm	centimeter
CO2	carbon dioxide
Cys	cysteine
Ca+2	calcium ion
cAMP	cyclic adenosine monophosphate
CFP	cyan fluorescent protein
CHO	Chinese hamster ovary
DMEM	Dulbecco's modified minimum essential medium
D	diffusion coefficient
DAG	diacylglycerol
ECFP	enhanced cyan fluorescent protein
%E	percent energy transfer efficiency
EDTA	ethylenediaminetetraacetic acid
EPAC	exchange protein activated by cAMP
FRAP	fluorescence recovery after photobleaching
FCS	fluorescence correlation spectroscopy
FBS	fetal bovine serum
FITC	fluorescein isothiocyanate
FSH	follicle stimulating hormone
g	g-factor
GFP	green fluorescent protein
GPCR	G protein-coupled receptor
Gs	stimulatory G protein

GDP	guanosine diphosphate
GTP	guanosine triphosphate
hCG	human chorionic gonadotropin
hetero-FRET	hetero-transfer fluorescence resonance energy transfer
homo-FRET	homo-transfer fluorescence resonance energy transfer
I	intensity
IP3	inositol 1,4,5 triphosphate
LRR	leucine rich repeat domain
LH	luteinizing hormone
LHR	luteinizing hormone receptor
LP	lipofectamine
MβCD	methyl-beta-cyclodextrin
µm	micrometer
MEM	modified minimum essential medium
mGlnR	metabotropic glutamate receptor
MSD	mean square displacement
PBS	phosphate buffered saline
PKA	protein kinase A
PKC	protein kinase C
PLC	phospholipase C
PIP2	phosphatidylinositol 4,5-bisphosphate
QD	quantum dots
r	anisotropy
SPT	single particle tracking
sec	seconds
TM	transmembrane
TSH	thyroid stimulating hormone
TrITC	tetramethylrhodamine isothiocyanate
YFP	yellow fluorescent protein
YFPSE	sensitized yellow fluorescent protein